Thermo-chemical characterization of the Italian crust from seismic data and thermodynamic modeling

Ph.D. candidate: Giovanni Diaferia

Supervisor: Fabio Cammarano

University of Roma Tre, Rome (Italy)

Degree of Doctor of Philosophy in Earth Science

November 2018

Contents

Acknowledgments

Dedication, hard work and curiosity are just some of the many ingredients needed for this endeavor, called PhD. It is not an hyperbola if I say that all the people I met during this journey showed these traits and gave me something valuable. I just hope to have given them something back too.

Obviously, most of my gratitude is for my supervisor Fabio. I deeply admired his peculiar mix of contagious curiosity and acute critical thinking. Even in difficult times his support never missed, showing great dedication and deep sense of responsibility. I really appreciated Fabio's equilibrium in supervising, letting the student free to explore new roads, according to his natural inclinations and interests. My thanks also go to Nicola, Ved and Chao. Their contributions were important for this project.

Last bust not least, my gratitude goes to my dear Angela, my family and my grandmother Gianna for her unconditional and warm support.

Preface

The lithosphere and in particular its shallowest part, the crust, largely contributes to all natural processes at the surface, including biological ones. Volcanism, CO_2 degassing, seismic activity and, ultimately, plate tectonics have deeply shaped our planet, allowing the appearance and the evolution of life in its superb and diversified forms. This profound connection with the shallow subsurface is particularly relevant for our species, whose development and sustainability have been relying on, or have been affected by processes occurring within the crust. The exploitation of natural resources fueling two industrial revolutions, the humanitarian disaster following a M=9 earthquake in a highly populated area are just two, non-exhaustive examples of the two-sided connection between the human civilization and the subsurface.

Owing to its importance for human activities and its interaction with the atmosphere and biosphere, the crust has been the target of extensive studies to unravel its structure and chemical composition and to constrain its behavior and role in a variety of disciplines. However, despite its proximity, the crust is largely inaccessible and our knowledge is still limited if compared to its complex heterogeneity, as suggested by geophysical and geological evidence. Lithology, mineralogical associations, preferential mineral arrangement, temperature, pressure, porosity, water content, anisotropy are examples of properties that, with their spatial variations, largely outnumber the data we can collect at surface, resulting in uncertain models of the subsurface or even dissimilar reconstructions of a certain property that still fit the observations equally well.

Temperature is one of the key parameters for characterizing the crustal behavior and its relationship with the underlying mantle and neighboring plates. As an example, the depth of the transition from brittle to ductile behavior affects the seismicity of a certain area and, defining the volume of rock involved in the seismic slip, controls the maximum earthquake magnitude in a certain area. While it is relatively straightforward to infer past crustal and mantle temperature through studies on xenoliths and exhumed portion of deep crustal bodies, the understanding of the present-day thermal structure poses numerous challenges and is only poorly known. In fact, current temperatures at depth are extrapolated through heat flow measurements in boreholes, that are limited and sparse thus unable to capture the likely spatial variability of crustal temperature. Moreover, such an approach requires

the assumption of a conductive heat transfer, strictly valid only in cold, cratonic regions where heat up-flow by advection is assumed to be absent.

Similarly to any material, a varying temperature causes a mineral aggregate to change its stiffness and rigidity, thus varying the velocity of propagation of P-waves and S-waves. Therefore, the anomalies in seismic wave propagation can be exploited for temperature inference. Moreover, since higher temperature causes a faster decay of high-frequency amplitude, the attenuation of seismic waves can be informative on anomalous high temperature at depth. The advantages of using seismic models are rooted in the more homogeneous coverage of the crust and, although the inherent problems of non-uniqueness in the inversion process, the highest resolution images of the subsurface. However, seismic velocities depend on temperature, chemical composition, and pressure through non-linear relationships that must be accurately assessed, as much as the sensitivity of seismic velocities on such variables at crustal conditions. This can be achieved through thermodynamic modeling, by predicting the specific mineralogical aggregate and its seismic features in any conditions of pressure, temperature and chemical composition.

The main motivation of this 3-years long Ph.D. project is assessing and applying an interdisciplinary approach to map the temperature distribution at crustal depth through a combination of seismic data and thermodynamics.

The presented work consists of three main chapters, each one preserving the structure of a stand-alone paper. In **Chapter 1**, we investigate the sensitivity of seismic observables (e.g. shear wave velocities, V_S) to temperature at depth, in comparison to other variables such as lithology and water content. This work represents the experimental basis for further advance in the estimation of crustal temperature from seismic data. We demonstrated that changes in temperature cause the strongest effect of seismic velocities compared to all other variables. In addition, we carefully analyze the temperature-driven transition of quartz from its α to β form, proving that is seismically relevant in regions characterized by hot local conditions and therefore suitable for the estimation of temperature at depth. All results of this chapter have been published on *Tectonics* in 2017. In **Chapter 2**, we apply a joint-inversion of two different and complementary seismic datasets, receiver functions and Rayleigh wave dispersion curves, for the Italian peninsula. The inversion scheme relies on a Bayesian framework that allows a detailed definition of the model uncertainty and does not require any prior parametrization. Building on our previous relationships, we were able to provide a physically meaningful interpretation of the seismic model(s) we inverted. The analysis of our results allows us to identify intra-crustal jumps in V_P/V_S ratio that we interpreted due to the $\alpha-\beta$ quartz transition. We also discuss the possible pitfall of using different datasets in complex areas, proving the importance of a Bayesian inversion scheme like the one we use to avoid misinterpretations. The results presented in this chapter **Chapter 2** have

been submitted for publications to *Journal of Geophysical Research*. Finally, **Chapter 3** deals with the temperature distributions at the Moho for the Italian peninsula that is obtained by applying our thermodynamics-bases relationships to absolute shear wave velocities determined by surface waves in the lower crust. The new thermal map proves the deep crustal origin of several shallow geothermal regions. We obtain indeed a very good agreement with the known geological and tectonic framework of the Italian Peninsula and neighboring regions. Also, we find, for the first time, evidence of a deep thermal source beneath NW Italy, in the Piedmont area. The results of **Chapter 3** show the reliability of our approach to infer crustal temperatures even in complex tectonic regions and have been assembled in a manuscript submitted to *Geophysical Research Letter*.

Chapter 1

Seismic signature of the continental crust: what thermodynamics says. An example from the Italian peninsula

Abstract

Unraveling the temperature distribution and composition of Earth's crust is key for understanding its origin, evolution and mechanical behavior. Models of compressional (V_P) and shear wave (V_S) velocity are obtained from seismological studies and can be interpreted in terms of temperature and composition, using relationship defined through laboratory experiments. These empirical evidences often do not properly account for the effects driven by temperature, pressure, water content and phase change of minerals. In this study, we use thermodynamic modeling to properly investigate the role of these variables in affecting seismic properties, as a tool to guide (joint-) inversion and interpretation of geophysical data. We find that mineralogical phase transitions can be more seismically relevant than a change in chemical composition. In particular, the α-β quartz transition would cause a jump in acoustic impedance and V_P/V_S ratio $>8\%$, occurring in the 15-25 km depth range, depending on the thermal gradient. Moreover, in the case of a cold lower crust, the consumption of plagioclase in favor of high-velocity minerals might represent another relevant seismic discontinuity. Different chemical compositions proposed for the Italian crust would be seismically indistinguishable, since they give overlapping seismic properties. Values of $V_S<3.6$ km/s would imply a strong contribution of sediments and/or partial melt. The V_S/density ratio shows a narrow variability, suggesting that densities at depth can be directly derived in first approximation from V_S.

1 Introduction

The Earth's crust has been largely investigated through geophysical, geochemical and petrological studies. Nonetheless, the origin, composition and thermal structure of the crust remain unclear because of its heterogeneity and complex structure (*Condie*, 2013; *Rudnick and Fountain*, 1995; *Rudnick and Gao*, 2003; *Taylor and McLennan*, 1985; *Windley*, 1996). A better understanding of the crust is fundamental to infer its mechanical behavior, to define its role in plate tectonics and to clarify the origin of magmas. In addition, better constraints on crustal features help to evaluate the contribution of the mantle in geodynamical processes as well as to isolate its signal in geophysical investigations (*Ritsema et al.*, 2009; *Tondi et al.*, 2012). Currently, there is an effort to merge different data and techniques in a multidisciplinary approach to reduce the ambiguities in crustal models. Examples are the joint inversion of receiver functions and surface waves (*Bodin et al.*, 2012, 2016; *Julia et al.*, 2000; *Qashqai et al.*, 2016; *Shen et al.*, 2013), or the simultaneous use of gravity and seismic data (*Kaban et al.*, 2014; *Tesauro et al.*, 2014; *Tiberi et al.*, 2003; *Vernant et al.*, 2002). To fully benefit from the combination of different methods, there is a need to reduce the uncertainty of geophysical models by setting robust and petrologically valid constraints. In order to accomplish this goal, it is essential to evaluate the contribution of each variable (temperature, pressure, composition, water content and possible phase transitions) that affects seismic properties. One of the crustal features that we find not exhaustively explored in existing literature is the role of phase transitions. For example, the α-β quartz transformation (*Shen et al.* 1993) can show a clear signal in geophysical observations. In fact, V_P/V_S anomalies have been recently linked to such transition (*Kuo-Chen et al.*, 2012; *Lowrie and Gussinye*, 2011; *Mainprice and Casey*, 1990; *Mechie et al.* 2004;). However, the quartz structural change is not the only possible cause of variation in V_P/V_S and its relevance compared to other sources of seismic anomalies is not yet fully understood.

A second important point to investigate is whether a mixture of different compositions (as those comprised below the wavelength of any seismic method) have seismic velocities that are equivalent to that of averaged and approximated mineralogical association.

With this work, we attempt to answer the main following questions:

1. Can we detect different chemical compositions within the crust using seismological studies?
2. What are the petrological constraints on the variability of V_P, V_S, density and their relative ratios?
3. How do phase changes affect seismic properties in the crust?

In this study, we investigate the link between geophysical observables and crustal features, using

thermodynamic modeling as a tool for the prediction of seismic properties in a wide range of pressure and temperature. Specifically, (i) we explore to which extent the thermo-chemical characteristics of the crust can be revealed by seismic data, (ii) we determine the role of phase changes and melt, (iii) we quantify their effects on different seismic observables (i.e., Rayleigh-wave dispersion curves and receiver functions). Finally, we detail the implications and pitfalls in the interpretation of seismological data for the crust. In this work we choose the Italian peninsula as a case study, due to the accessibility of several published estimates of its crustal composition , the presence of large temperature variations and locally high thermal gradients as well as abundant and reliable seismological observations covering this area In the following introductory sections, before presenting and discussing our results, we provide an overview of the role of geophysics in the characterization of the crust, discuss possible constraints on crustal composition and present the state of the art on the relationships between seismic observables and material properties.

1.1 Geophysical studies of the crust

Seismic studies and gravimetry have been largely used in the past decades to characterize the crust. Several crustal models have been proposed in terms of seismic velocities and density such as LITHO1.0 (*Pasyanos et al.*, 2014), CRUST 1.0 (*Laske et al.*, 2013), CRUST 2.0 (*Bassin et al.*, 2000) and GEMMA (*Reguzzoni and Sampietro*, 2015). In areas with dense data coverage, models with higher resolution have been provided such as the EPcrust model (*Molinari and Morelli*, 2011) and NACr14 (*Tesauro et al.*, 2014) for the European and North American continent, respectively. The distribution of compressional velocity (V_P) at depth is obtained from the analysis of P-wave arrivals generated by earthquakes worldwide (teleseismic tomography) and/or from local events within the studied area. The obtained tomography images generally show good horizontal resolution on the order of tens of kilometers. For the Italian peninsula, regional, high-resolution tomographic studies have been carried out (Di *Stefano et al.*, 1999, 2009; *Gualtieri et al.*, 2014). In addition, reflection seismic surveys (e.g., CROP project, (*Finetti*, 2005) have provided a relevant insight on the crustal structure of this region. Shear-wave velocities (V_S) at crustal depth are mainly obtained through the analysis of surface waves, either generated from earthquakes or retrieved from ambient-noise interferometry (passive method). The horizontal resolution of the obtained V_S models is generally lower if compared to a V_P tomography. However, the coverage is higher and more homogeneous, especially when using passive approach. Examples of recent crustal models from surface wave analysis are *Molinari et al.* (2015) and *Shen and Ritzwoller* (2016), for the Italian region and North America, respectively. Another geophysical technique employed for crustal studies is based on the analysis of receiver functions (RFs). This method was introduced in the late seventies (*Vinnik*, 1977) and largely developed only in the last decade.

It is based on the analysis of converted P and S phases at seismic discontinuities beneath seismic stations (*Zhu and Kanamori*, 2000). The RFs method is particularly suitable for detecting sharp layer boundaries, such as the Moho. Examples of application of this method for the Italian peninsula have been shown by *Piana Agostinetti and Amato* (2009) and *Bianchi et al.* (2010).

As any geophysical method, the aforementioned techniques require an inversion of data to infer a velocity model of the subsurface. Factors such as noise in the data, the high number of parameters in the inversion problem and uneven illumination of the subsurface require some regularization choices (e.g., smoothing) to help the convergence towards a final solution during the inversion procedure (*Pasyanos and Walter*, 2002; *Vasco et al.*, 2003). As a consequence, the retrieved models might miss sharp discontinuities, even if present. Lastly, the solution to the inversion problem is often non-unique, as several models might explain the observed data equally well.

1.2 Composition of the crust and its determination

Exhumed portions of the crust and xenolith catalogs have been extensively used to infer crustal composition in terms of main oxides and mineralogical associations (*McLennan et al.*, 2005; *Rudnick*, 1992; *Rudnick and Gao*, 2003). It is widely accepted that the average composition of the crust is andesitic (*Rudnick and Gao* 2003, 2014). However, both seismological and geological evidence (e.g., exhumed portion of the crust and xenolits) show a compositional layering (SiO_2 content decreasing with depth while MgO and FeO increasing) suggesting the compositionally distinct upper, middle and lower crust (*Rudnick and Fountain*, 1995; *Taylor and McLennan*, 1985). Considerable uncertainty exists especially regarding the lower crust. As a matter of fact, most of the information about its properties relies on xenolith samples whose depth of origin and representativeness of the lower crust are poorly constrained (*Hacker et al.*, 2015). With respect to the upper and especially middle crust, their thicknesses or even existence are often questioned.

Besides a globally inferred composition of the Earth's crust, average chemical compositions have been also proposed for certain local domains. For this study, we use a range of compositions inferred for the Italian province, but we anticipate that our results might be extended to other areas. A comprehensive summary of the complex geological and geodynamic setting of the Italian region is beyond the scope of this work. Abundant literature is available in this regard and here we only mention some key points of interest in the context of this work. The current geological setting of the Italian region is determined by the Alpine and Apennine orogenesis started in the Cretaceous due to the convergence of the African and European continents (*Carminati et al.*, 2012; *Doglioni et al.*, 1999; *Mantovani et al.*, 2002). The position of the Italian peninsula results from the counter-clockwise rotation of the Apenninic front (15 Ma to present) that led to the opening of the Tyrrhenian Sea basin (*Carminati et*

al., 1998, 2010, 2012; *Doglioni et al.*, 1998, 1999; *Faccenna et al.*, 2001). Diffuse magmatism occurred in the Quaternary and is continuing at the present time (*Carminati et al.*, 2010; *Peccerillo*, 2005). The recent tectonic evolution resulted in the high thermal gradients in the western Apennines (>150 mW/m^2), opposite to the lower values ($\sim$ 30-40 mW/m^2) found in the foreland areas of the Po Plain, Adriatic Coast and the Ionian Sea (*Della Vedova et al.*, 2001). Gravity and seismic data suggest that the crust is mainly continental, with a Moho at 30 km depth on average. The Alpine belt shows a higher crustal thickness (45-50 km) while the Ionian and Tyrrhenian Sea are underlain by a (oceanic) crust around 10 km thick (*Scrocca et al.*, 2003 and references therein). *Sassi* (2003) provides several compositional averages based on extensive sampling of exhumed portion of shallow to deep crust, as in the area of Ivrea Verbano (*Fountain*, 1976). We will thus consider those averages to infer the correspondent seismic properties using thermodynamic modeling.

1.3 Merging composition and geophysical observables

Finding a correlation among chemical composition, petrology and seismic velocities has been a matter of research for decades. Several laboratory experiments explored the change in V_P, V_S and density for several rock types (taken as representative of different portions of the crust) as a function of pressure (P) and temperature (T) (*Birch*, 1961; *Christensen and Mooney*, 1995; *Rudnick and Fountain*, 1995). Empirical relationships have been then derived to associate these variables to V_P, V_S and density (*Brocher*, 2005; *Ludwig et al.*, 1970). However, the simultaneous effects of pressure and temperature are only mildly considered in these studies, albeit P and T show an important role in controlling seismic velocities at depth. In addition, the empirical observations only span a limited temperature and pressure range, while in the crust these can be as high as 2-2.5 GPa and 1500 K, respectively. Therefore, such experimental relationships might not be reliable if applied to the entire crust (*Guerri et al.*, 2015). Finally, the use of the aforementioned empirical relationship neglects the effects of water and/or melt. Some studies (i.e., *Behn and Kelemen*, 2003; *Tassara*, 2006) have proposed empirical formulas to derive major oxides content (e.g. SiO_2, MgO and CaO) from seismic velocities, or vice-versa. However, as already shown in the early studies by *Birch* (1961) and *Christensen and Mooney* (1995), rocks with very different composition and mineralogy show overlapping seismic properties. Thus, if such empirical fits are used, seismic velocities translate in a broad range of SiO_2 (for example if V_P=6.4 km/s, silica content ranges between 53-73 wt% at 20 km, see *Behn and Kelemen*, 2003). Therefore, the use of complementary information (such those on V_S and density) and petrological constraints is fundamental to reduce ambiguities (*Afonso et al.*, 2013). It is worth noting that empirical relations neglect possible phase transformations that might occur at crustal depths (e.g., quartz transition). Also the role of melt, not negligible in zones with high thermal gradients, is not taken into account. Lastly, once

a chemical composition is inferred from observed seismic velocities, its representativeness over the volume of investigation is not fully understood.

In this work, we use thermodynamic modeling to predict seismic properties at crustal conditions. Differently from laboratory experiments, this approach allows to evaluate the simultaneous effects of temperature, pressure, water content, composition and possible phase change. Despite the theoretical nature of the employed method and the obtained results, important observations can be made to enhance our comprehension of the properties of crustal rocks at depth.

2 Data and methods

We used thermodynamic modeling based on Gibbs Free Energy minimization (*Connolly*, 2009), a technique that predicts the stable mineral assemblage given a certain chemical composition and, self-consistently, calculates the seismic velocities and density of each mineral, for any point in the P-T space. The seismic properties of the (synthetic) bulk rock are then obtained by averaging schemes such as Voigt-Reuss-Hill (*Hill*, 1952). We used the thermodynamic database from *Holland and Powell* (1998) with the shear and bulk moduli of minerals from *Hacker and Abers* (2004). The database includes the experimental results from *Ohno et al.* (2006) that accounts for the anomalous elastic behavior of quartz at the α-β transition, useful for our specific intent to model crustal, quartz-bearing rocks. *Abers and Hacker* (2016) already implemented the peculiar properties of quartz in a thermodynamic framework, but their approach is not self-consistent since the equilibrium of mineral species is not assured for the ranges of P and T considered in their work. It must be pointed out that our method is also not internally consistent since the bulk and shear moduli are experimentally determined and not calculated as derivatives of the Gibbs free energy. While loosing consistency, such approach is more flexible and allows the incorporation of experimental information of elastic properties of minerals that are key to explore the relationships between different physical properties (e.g. seismic velocities and density) of crustal rocks.

To quantify the role of chemical composition in affecting seismic properties, we considered eight chemical averages proposed for the Italian province (*Sassi*, 2003). These compositions refer to different geological domains (Figure 1) where crustal rocks are sufficiently exposed to provide a meaningful mean composition for the upper, middle and lower crust. Locations include the Alpine Orogen, the Calabrian and Sicilian Arc, with lithologies including granitoids, sedimentary and metamorphic rocks. All compositions include the most abundant seven oxides, representing >99% of the whole chemical composition (Table 1). For the sake of comparison, we also consider the mean global composition of the crust proposed by *Rudnick and Gao* (2003).

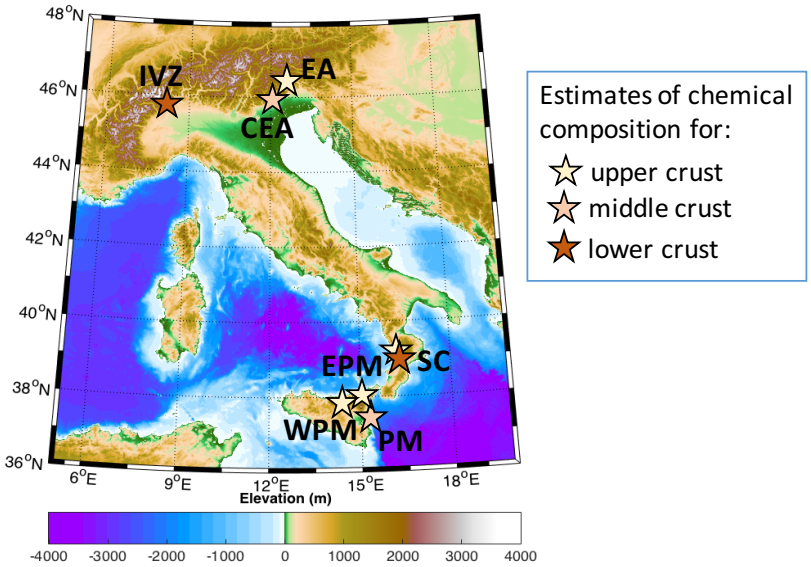

Figure 1: Locations of the considered average chemical compositions of the continental crust proposed for the Italian Province (listed in Table 1). Data is from *Sassi* (2003).

For each considered composition we use thermodynamic modeling to retrieve i) the mineralogical association stable at any crustal P and T condition ii) the seismic properties and density of the bulk rock. The same procedure above was applied considering the addition of 0.25 wt% of H_2O, to allow the formation of melt at temperature above solidus. Using thermodynamic modeling the migration of melt is not accounted for, as it is considered in equilibrium with the restitic fraction. This permits to evaluate the contribution of melt in changing the seismic properties of the bulk rock. We decided to not consider the case of higher water content. Figure 2 shows V_S as function of temperature at 4 kbar, for an anhydrous and two wet compositions (0.25 and 1.0 wt% H_2O, respectively). At sub-solidus conditions, a water content higher than 0.25 wt% does not result in appreciable changes in seismic velocities, albeit giving petrologically different rocks. When the temperature is above the solidus, melt forms and V_S drastically decreases by the same amount for the two hydrous compositions. This experiment illustrates that melts exert a dominant influence on seismic velocities, more than water content itself. Therefore, we opted for a minimum end-member in water content, set to 0.25 wt% in our thermodynamic modeling. A more detailed analysis of water-driven (second-order) effects on seismic velocities in the crust can be found in *Guerri et al.* (2015). The seismic properties obtained from our modeling are presented in boxplots, one for each rock composition (Figure 3). Each rectangular box contains 50% of the data, within the 1st (25%) and 3rd (75%) quartiles of the cumulative distribution, in the temperature range of 400-1000 K and for portions of the upper, middle and lower crust.

Our synthetic seismic velocities are compared with those from two seismological models covering the area of interest. These are the EPcrust model (*Molinari and Morelli*, 2011) and the one from

Molinari et al.(2015), MB from now on. The first is derived from the combination (i.e. weighted average, see reference for more details) of previous models covering the European continent. It is relevant to note that the V_S and density of EPcrust are calculated through the empirical formulas of *Brocher* (2005) from the V_P. The latter is a shear-wave velocity model derived from ambient-noise tomography from surface waves. The model is parameterized in upper and lower crust, provides also V_P (obtained from inversion) and density (fixed at 2.75 and 2.9 g/cm^3 for the upper and lower crust, respectively).

We also modeled the V_P/V_S ratio and acoustic impedances to highlight the role of phase transitions and/or compositional changes as possible seismic discontinuities. Finally, we constructed a whole synthetic crust parameterized in upper, middle and lower crust, computed the synthetic receiver functions (RFs) and Rayleigh wave dispersion curves along three geothermal gradients, in order to directly quantify the effects of the considered variables on seismic observables.

Location	**Composition**	**SiO_2**	**Al_2O_3**	**FeO**	**MgO**	**CaO**	**Na_2O**	**K_2O**
upper crust								
Eastern Peloritani Mountains	EPM	66,5	17,6	6,1	2,3	1,9	2,9	2,8
Serre Calabre	SC	68	16,2	5,4	1,5	3,4	2,9	3,6
Western Peloritani Mountains	WPM	66,4	18,1	6,3	2,4	1,7	1,9	3,4
Eastern Alps	EA	68,8	16,8	5,1	1,6	1,5	2,6	3,7
Rudnick and Gao (2003)	RG	66,6	15,4	5	2,5	3,6	3,3	2,8
middle crust								
Central Eastern Alps	CEA	65,9	18,8	7,3	2,1	1,2	1,8	3
Peloritani Mountain	PM	65,3	19,9	8,1	1,8	0,4	1,2	3,3
Rudnick and Gao (2003)	RG	63,5	15	6	3,6	5,3	3,4	2,3
lower crust								
Ivrea Verbano Zone	IVZ	54,9	18,2	9,8	6,2	7,6	2,1	1,5
Serre Calabre	SC	61,8	18,8	8,4	3,4	3,6	2,1	2
Rudnick and Gao (2003)	RG	53,4	16,9	8,6	7,2	9,6	2,7	0,6
Note: Arbitrary toponyms are given for each composition								

Table 1: Chemical compositions used to model the seismic properties of the upper, middle, and lower crusts

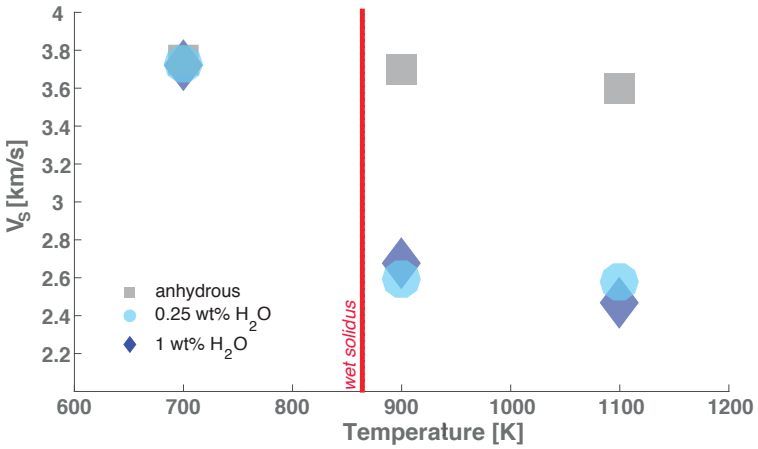

Figure 2: Shear-wave velocity as a function of temperature at 4 kbar for dry composition and with the addition of 0.25 and 1 wt % H_2O. In all cases, chemical composition is that of *Rudnick and Gao* (2003) for the middle crust. The presence of melt in the bulk rock is the major player affecting seismic velocity.

3 Results

3.1 Shear Velocity (V_S)

V_S at crustal depths (upper, middle and lower crust) varies between 3.6 and 4.5 km/s when compositions are anhydrous (Figure 3, left panels). A strong variation with temperature, evidenced by larger 'boxes' in Figure 3, is observed, especially in the upper crust. At relatively shallow depths, adding water causes the formation of melt at high temperature with the consequent reduction of velocities (Figure 3, upper left panel). In the middle and lower crust, the influence of water is remarkably less important, leading to overlapping V_S ranges. The MB model shows a wider distribution of V_S in the upper crust. This is probably caused by the presence of sediments in the area covered by model, while we consider only a crystalline crust. The variability of V_S becomes smaller at increasing depth and V_S are lower than those determined from thermodynamic modeling. For the lower crust, the V_S range from the MB model is close to those predicted for a hydrated composition. The EPcrust shear velocities are systematically lower compared to those from thermodynamic modeling. Note that EPcrust is almost entirely based on V_P, while the V_S values are empirically derived from Brocher's relationship (*Brocher*, 2005). This suggests that the empirical fit might not be able to capture the variability of V_S within the crust.

3.2 Compressional velocity (V_P)

Results for V_P are not shown as due to their similarity to those for V_S. Compressional wave velocity changes as a function of temperature exclusively for wet composition, and only in the upper crust.

The effect of water becomes negligible in the middle and lower crust (where melt conditions are not reached) and V_P exhibits similar average values and distributions, regardless of the composition. For an anhydrous crust, V_P is bounded between 6 and 7.7 km/s, in the 5-30 km depth interval: the lowest value is reached at shallow depth (<15 km) for high temperature (1000 K), while the highest value corresponds to the base of the crust at a temperature <500 K. In the upper crust, V_P values of EPcrust are similar to those modelled for wet compositions. In the middle crust, EPcrust has V_P that are close to those we model for the lower crust. The MB model shows substantially higher V_P than those derived from thermodynamic modeling, especially in the upper and middle crust. This discrepancy is likely due to the poor capability of surface waves in retrieving P-wave velocities at depth, as discussed later (see Discussion section).

3.3 $\mathbf{V}_S$/density

The highest variability of V_S/density ratio is seen mostly in the upper crust and for hydrated compositions (Figure 3, right panel). Here the ratio ranges from 1 to 1.5. In the middle and lower crust, the V_S/density ratio varies within a small range, roughly between 1.29 and 1.39, regardless the variable temperature and composition. The V_S/density obtained from the EPcrust model has also a narrow distribution, bounded in the same range we find from thermodynamic modeling. A significant discrepancy exists between the V_S/density estimated by MB and those we modelled. This is likely due to the assumption of fixed densities in the upper and lower crust.

3.4 $\mathbf{V}_P/\mathbf{V}_S$

The middle panel in Figure 3 is about the V_P/V_S ratio. The lowest values are reached in the upper crust, comprised between 1.6 and 1.7. An increasing variability and higher values (up to 1.8) are observed deeper. For wet compositions, the formation of melt above the solidus (T>800 K) yields values of about 2. However, at larger depths, both the effects of temperature and water become negligible and the medians of V_P/V_S ratio stabilize between 1.65-1.75. EPcrust shows a narrow range of V_P/V_S, and its medians mostly overlap with those obtained from thermodynamic modeling. This is consistent with the fact the VV_S of EPcrust has been empirically derived from V_P. MB shows particularly high V_P/V_S. We explain this with the inability of data used to derive this model, to provide plausible V_P at depth. We highlight the effect of quartz transition on the V_P/V_S ratio in Figure 4. We consider here an anhydrous, simplified crust with the composition for the upper, middle and lower crust as in *Rudnick and Gao* (2003). The crust is 35 km thick and it has the compositional boundaries between upper-middle and middle-lower crust at 15 and 25 km, respectively. We show the

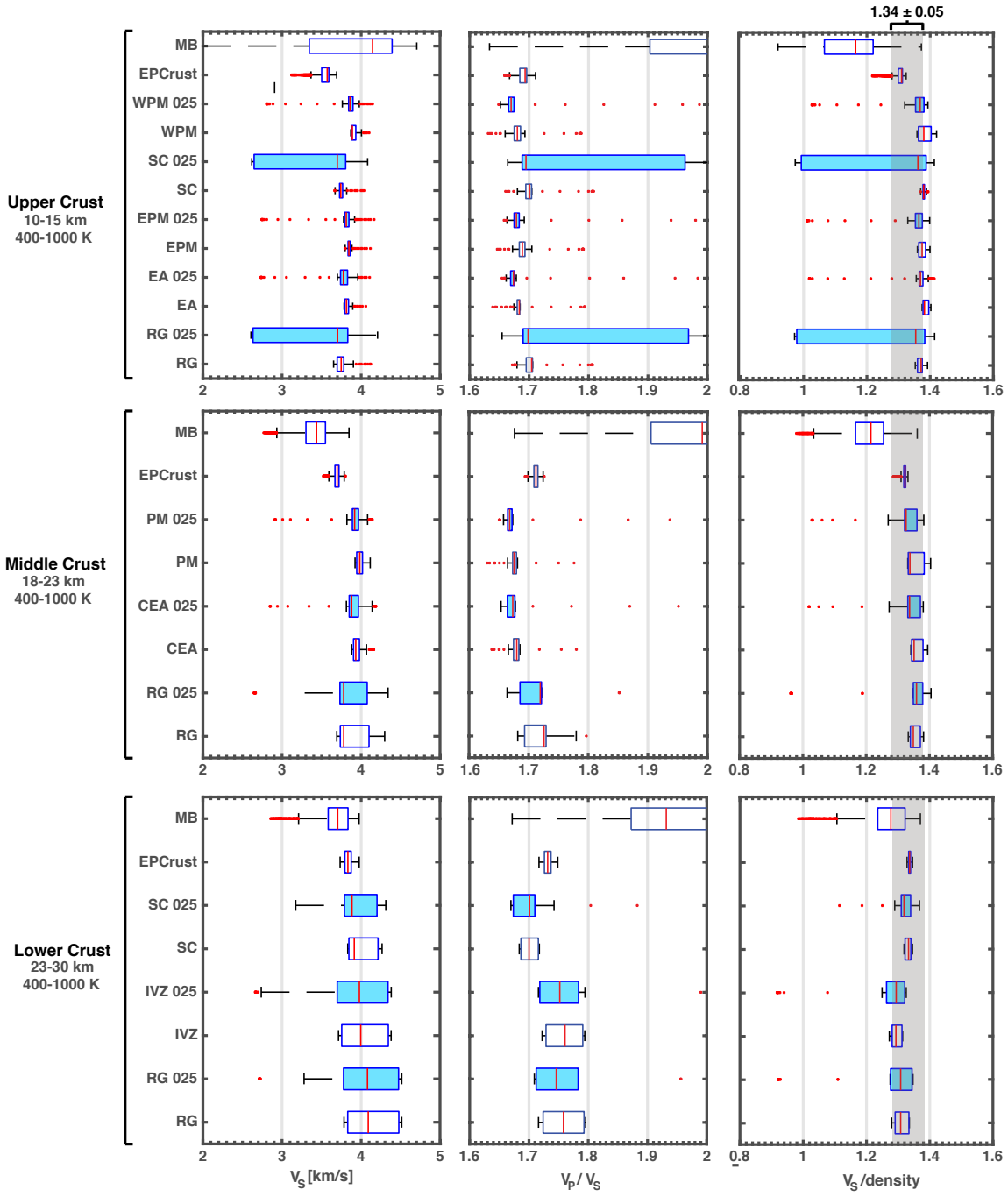

Figure 3: Boxplots showing the variation of V_S, V_P/V_S, and the V_S/density at temperature between 400 and 1.000 K for portions of the upper, middle, and lower crusts. Compositions labeled with "025" (identified with a blue-filled bar) contain H_2O at 0.25 wt%. The box includes 50% of the data within the first (25%) and third (75%) quartiles of the cumulative distribution. The black whiskers contain the majority of the data (∼99%), and the red dots are the outliers of the distribution. The median is represented by a red line.

variation of V_P/V_S along three linear geothermal gradients of 10, 30 and 40 K/km. A sharp decrease followed by an increase of V_P/V_S is observed around 15 km depth for the highest thermal gradient (i.e. 40 K/km). The same feature occurs at 23 km depth for an average thermal gradient (30 K/km). An inspection on the mineral association that is stable at these pressures and temperatures confirms

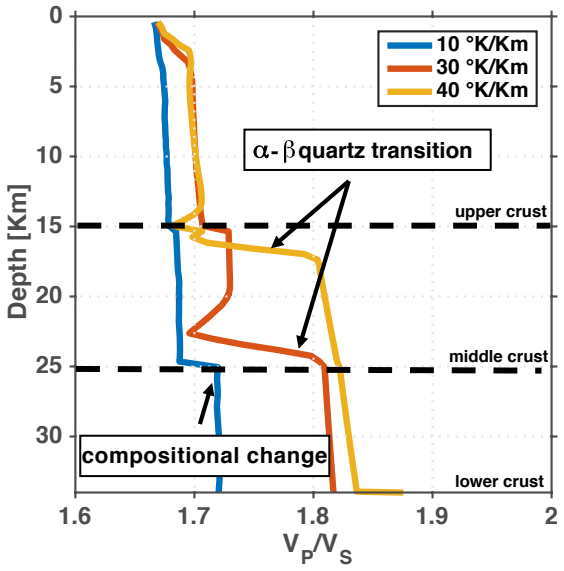

Figure 4: Variation of the V_P/V_S ratio as a function of depth and thermal gradient. The compositions of the upper, middle, and lower crusts are from *Rudnick and Gao* (2003). For an average and high gradient, the sharp jump at 15 and 23 km is due to the transformation of α-quartz in β-quartz occurring at T = 900-1.000 K. The effect of quartz transformation masks the one induced by the compositional change at boundaries.

that the change in V_P/V_S is due to α-β quartz transformation. As shown by experiments in *Ohno* (1995), this phase transformation first induces a decrease in compressibility, resulting in a decrease of V_P/V_S, then is characterized by a rapid increase in V_P/V_S (here up to 1.8) when the transformation is completed and quartz structure is stable in the stiffer and denser β form. We observe that the jump in V_P/V_S due to the α-β quartz transition is higher than the jump caused by the varying composition between layer boundaries, which is visible in Figure 4 for the lowest thermal gradient (10 K/km).

3.5 Seismic properties of a mixed chemical composition

Seismic tomography has a notoriously limited resolution, implying that observed seismic velocities are an average over volumes that include different crustal compositions and lithologies. Therefore, it is important to test whether an average composition in chemical equilibrium (that could be derived from a seismic model) would exhibit similar seismic properties and density of a mechanical mixture of different compositions. To address this point, we consider the compositions of Ivrea-Verbano Zone and Serre Calabre (here IVZ and SR, respectively) as end-members for the lower crust. We chose them as they show the highest relative difference in SiO_2, CaO and MgO contents (see Table 1). In our test, we consider the V_S/density ratio, as this is the parameter that is possibly more sensitive to composition and less to pressure and temperature (see Section 3.3). We computed the V_S/density ratio of a 1:1 compositional mixture of the chosen end-members, as a function of temperature (Figure 5, black line). We compare this with the behavior of a mechanical mixture, represented by the average

V_S/density between the end-members (dashed line in Figure 5). In both cases, the V_S/density ratio change non-linearly with temperature and, more importantly, are completely overlapping. This simple test shows that an average chemical composition has seismic properties that are indeed approximately equal to the average seismic features of the end-members.

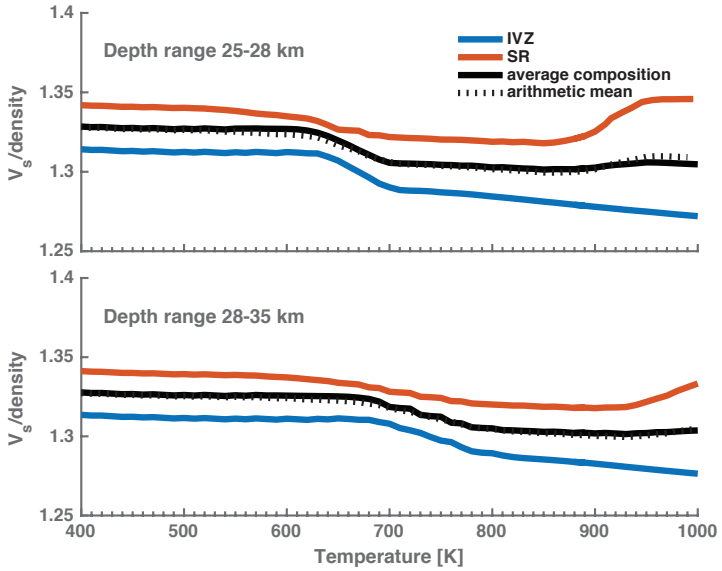

Figure 5: V_S/density ratio as a function of temperature for two anhy- drous compositions, Ivrea-Verbano Zone (IVZ) and Serre Calabre (SR), and for their 1:1 mixture (black). The dotted line represents the arithmetic mean between the V_S/density ratio of two compositional end-members.

3.6 Acoustic impedance (AI)

In order to show the presence of possible seismic discontinuities, we plot the acoustic impedance, defined as AI = V_P × density, in a depth-temperature domain (Figure 6). We considered a 35 km-thick crust with the upper-middle and middle-lower crust transitions at 15 and 25 km, respectively, and using the compositions given by *Rudnick and Gao* (2003). The modeled layered crust enables us to compare the effects of compositional changes vs. phase transitions as possible sources of seismic discontinuities.

An AI jump is clearly visible in the upper and middle crust, at a temperature between 850 and 950 K depending on depth. This is due to the quartz transition in the upper and middle crust, already mentioned for causing an increase in V_P/V_S ratio (see section 3.4). In Figure 6, the dashed black line indicates the transition temperature that has a gradient of 0.0256 K/bar as defined by *Shen et al.* (1993). The higher quartz content in the upper crust (> 20 wt%) produces here a more pronounced jump in AI, compared to that of the middle and lower crust where quartz is less abundant. Interestingly, Figure 6 shows that compositional changes at the layer boundaries produce a relatively mild jump in AI at the upper-middle crust boundary.

In conditions of high pressure and low temperature at mid-crustal depth, a sharp increase in AI is observed. Inspecting the mineral phases that are stable under these conditions (reported in Table 2), we note that the AI increase is caused by the consumption of plagioclase in favor of clino-pyroxene and kyanite, both having remarkably high seismic velocities ($V_P > 8$ km/s). Table 2 also shows that the presence of water is responsible for the formation of hydrous, high-velocity mineral phases (i.e., epidote and amphibole), causing a jump in AI that is 0.1% higher than the anhydrous case. At greater crustal depths, not modelled in this study, the breakdown of plagioclase would favor the formation of typical high-pressure mineral species, such as garnet (*Behn and Kelemen*, 2003).

	anhydrous		**0.25 w% H_2O**	
Temperature (K)	600			
Pressure (kbar)	4.2	5.7	4.2	5.7
Depth (km)	17	23	17	2
Acoustic impedance (AI)	18.5	19.7	18.2	19.4
AI jump (%)	6.7		6.8	
quartz	16.3	21	15.4	18.2
ortho-pyroxene	13.5	11.2	9.6	10.1
K-feldspar	15.5	16.3	15.4	15.6
plagioclase	**49.3**	**12.8**	**48.9**	**32.1**
clino-pyroxene	5.5	18.16	-	9.9
kyanite	0	21	-	2.7
epidote	-	-	-	4.4
amphibole	-	-	10.1	6.7
TOT	100.1	100.5	99.4	99.7

Table 2: Stable mineral phases and their abundances (% vol) at 600 K and 4.2-5.7 kbar (middle crust), obtained by thermodynamic modeling. *Note*: The used chemical composition is from Rudnick and Gao (2003). The jump in acoustic impedance (AI) is due to the consumption of plagioclase, driven by the increasing pressure in isothermal condition at mid-crustal depth. In bold: P-T condition used for thermodynamic modeling. In italic: stable minerals composing the bulk rock

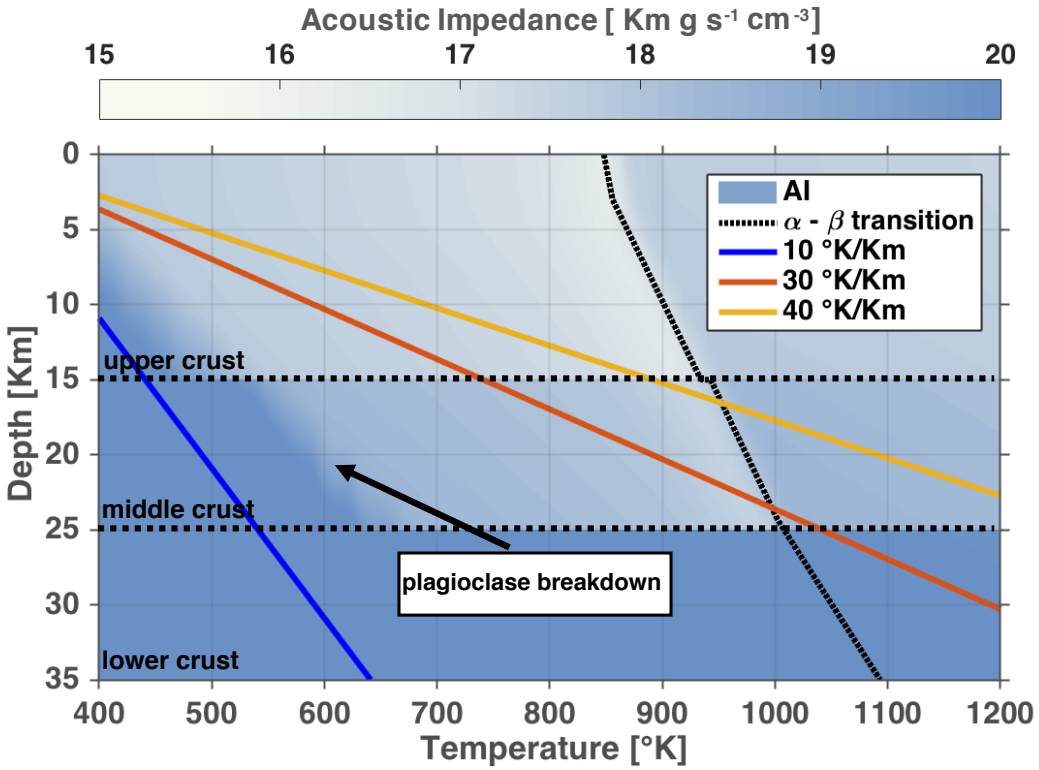

Figure 6: Acoustic impedance (VP $*$ density) as a function of temperature and depth in a three-layers, 35 km thick crust with compositions from *Rudnick and Gao* (2003). The black dotted curve indicates the temperature α-α quartz transformation temperature from *Shen et al.* (1993). This phase transition produces a jump in AI in the upper crust (due to its higher content in quartz), less pronounced in the middle and lower crusts. Another AI increase occurs at high pressure and low temperature due to the breakdown of plagioclase

4 Discussion

4.1 Constraints on V_P, V_S and density

Based on thermodynamic modeling, we explored the variability of V_P, V_S and density as a function of temperature, pressure, composition and water content. Our investigation aims to clarify the relative weight of these variables in controlling seismic velocities and density.

We found that the possibility of discriminating between different compositions within the same crustal layer is prevented by the overlapping values of V_P and V_S. Our results confirm previous works in literature (see Introduction). For example, *Behn and Kelemen* (2003) drew the same conclusion using an analogous thermodynamic approach. Despite the conclusion that different rocks have similar seismic properties, they proposed experimental fits to obtain chemical composition from observed V_P. This leads to wide ranges of oxide content that can fit the same value of seismic velocity equally well. A problem with their approach is the assumption of no water and melt. We believe that this simplification might hamper the application of such formulas in certain crustal domains. *Behn and Kelemen* (2006) also used a thermodynamic approach, now implementing the role of melt and water.

Our findings are not totally consistent with this study, in terms of modeled seismic velocities and mineralogical assemblages. The reason may be due to the different compositions and thermodynamic database used for calculations. For example, in our database we account for the anomalous behavior of quartz, that may show an important role in controlling seismic velocities within the crust, as will be discussed later. We show that the seismic properties of the local compositions proposed for the Italian crust closely overlap to those of *Rudnick and Gao* (2003). This result suggests that an average global composition can be a reasonable approximation, also at local scale. Indeed, the error made by assuming a global composition is lower than the uncertainty arising from variations in temperature and melt, usually unknown at depth and poorly constrained by seismic methods. An additional uncertainty is due to the limited resolution of any seismic tomography. Any compositional change within the crust is likely smaller than the wavelength of propagating P- and S-wave. We showed that it would be impossible to distinguish between a 1:1 mechanical mixture of two rock types and their compositional average. Thus, when the chemical composition is assumed to be an average of two end-members, its seismic properties are also the average of the end-members. Observed seismic wave velocities at depth thus represent an average value over a certain volume, and can be used to infer the average chemical composition over that volume. Lithological and compositional heterogeneities considered in this study might be beyond the resolution of any geophysical method. Temperature and/or phase transitions might play the dominant effect. The unawareness of the limits of geophysical models can be the principle reason for several misunderstandings between different communities in geosciences.

Among all factors, temperature is the most dominant in affecting V_P and even more V_S, especially if water is present. We found that V_S values as low as 3.6 km/s can occur for a hydrated (crystalline) crust, above solidus temperature (900 K). Therefore, crustal domains with such low V_S might be likely associated with the presence of partial melt. Low V_P and V_S are typical of sediments (which are common in the upper crust) and meta-sediments (at lower depth), that are neglected in this study. Their effects would give rise to distinctive anisotropies that would be visible both in surface-wave tomography and in receiver function studies. An example is reported in *Hacker et al.* (2014) where the low V_S ($<$3.4 km/s) encountered in a certain portion of the Tibetan crust and the observed 6-7% radial anisotropy are interpreted as the combined effect of melt and horizontally oriented micas. For the case of the Italian peninsula, *Okeler et al.* (2009) pointed out a strong anisotropy ($>$10%) in the Southern Apennines as result of a partially melted crust. The role of temperature must be taken into account especially in areas with high thermal gradients that can enhance the velocity reduction. It is the case of the Italian peninsula where anomalous thermal gradients are observed in areas of relevant magmatism (i.e., southern Tuscany, Tyrrhenian Sea, Aeolian Islands). In Italy, the role of sediments

can also be relevant. Examples are the basin area of the Po Plain where they reach a thickness of 15 km (*Molinari et al.*, 2015), and the foreland of the Apulian Platform characterized by a 6-7 km thick carbonatic sequence that then dips under the southern Apennine fold-and-trust belt (*Mariotti and Doglioni*, 2000). Note that in our work we did not account for anelasticity, a phenomenon that could enhance the role of high temperatures in producing low seismic velocities (*Karato*, 1993; *Watanabe*, 1993). We are aware that also porosity might play a role in decreasing low seismic velocities, especially in the top portion of the crust (*Guerri et al.*, 2015).

We found that the V_S/density ratio takes a rather constant value around 1.34 km cm^3 s^{-1} g^{-1}, despite the variable temperature, water content and composition. In contrast with our result, *Brocher* (2005) found a non-linear, fifth-order polynomial fit between V_S and bulk density. The relation was derived from laboratory experiments based on a variety of rock types, but neglecting the simultaneous effect of pressure, temperature, water content, melt and phase changes. On the contrary, in our thermodynamic approach, we account for these variables at once. *Levandowski et al.* (2015, 2016) proposed a correction to the Brocher's polynomial fit to account for temperature, assuming a constant thermal conductivity for the whole crust. In regions where conduction is not the only mechanism of heat transport, such as in zones characterized by large fluid circulation (a common case for the Italian province), this assumption might be too stringent. On the contrary, the substantial linear dependency between V_S and density that we have derived, accounts in first approximation for the possible role of temperature, water and composition. It means that crustal densities might be firstly derived from a shear-wave velocity model. Of course, the use of gravity data would be necessary to validate and possibly improve the density model. We acknowledge that a possible reason for the narrow range of our modelled V_S/density ratio can be related to the thermodynamic database used in this study. In fact, for some minerals the shear modulus is not available experimentally and their properties are approximated to those of known minerals with similar structure (*Hacker and Abers*, 2004). A comprehensive discussion of the uncertainty of thermodynamic properties of major minerals can be found in *Hacker et al.* (2003). However, data do exist for most important crustal minerals, such as ortho-pyroxene, clino-pyroxene and quartz (*Anderson et al.*, 1992; *Bina and Helffrich*, 1992; *Ohno et al.*, 2006). Better constraints on the mechanical behavior of minerals will hopefully give more reliable predictions on the characteristics of the crust.

The importance of using correct seismic constraints is demonstrated by the comparison of our thermodynamic data with two seismic models covering the Italian region. We observed that if seismic properties are empirically inferred, assumed or poorly constrained, these are inconsistent with what thermodynamics suggests. A convincing example is given by the V_P/V_S in the MB model. It ranges from 1.65 to 2.3, whereas both the EPcrust model and our modeled data show a much narrower range,

centered around 1.7. MB is constructed from surface waves and thus is poorly sensitive to V_P. The absence of an adequate a-priori constraint during the inversion stage produces unrealistic values of V_P in the final model. In summary, we suggest that either (i) poorly constrained parameters should not be presented in the published model because its interpretation (from those unaware of this critical issue) can translate in wrong conclusions and, (ii) petrologically valid constraints should be used to narrow the variability of such parameters. Thermodynamic modeling can give a valuable insight in this regard.

Finally, we stress that our method and results might be hardly applicable to the uppermost crust where the influence of pore and sediments might be dominant. In this work we simulated a crystalline, isotropic, pore-free mineral aggregate. Moreover, we did not take anisotropy into account, an important feature for seismic data if sediments or meta-sediments are present at depth. More complex thermodynamic modeling tools have been developed (e.g., HeFESTo from *Stixrude and Lithgow-Bertelloni*, 2011) to account for the full elastic tensor, but, as discussed earlier, there is a lack of experimental data in current databases even for isotropic properties.

4.2 Phase-changes as seismic discontinuities

Our results suggest that the α-β quartz transition has a considerable effect on the bulk properties of a crustal rock. We found that when the transition temperature (ranging from 850 to 950 K, depending on pressure) is approached, the V_P/V_S ratio first decreases (<5%) and then increases up to a value of 1.8 or more. The depth of the quartz transformation is governed by the thermal gradient. Figure 7 (left panel) clarifies the role of temperature gradient on V_P/V_S when the transition of quartz occurs. A gradient between from 28 to 40 K/km results in a quartz transition in the middle crust (15-25 km depth). Importantly, we show that the increase in V_P/V_S due to this transition is higher than that driven by the compositional layering of the crust. If the thermal gradient is lower than 28 K/km, the quartz transition would occur in the lower crust. Its mild effect (mild because of the low quartz content) is masked by an increase in V_P/V_S due to the compositional change at the middle-lower crust boundary. *Mechie et al.* (2004) interpreted the high V_P/V_S anomalies observed in Tibetan crust as evidence of the α-β quartz transition at around 20 km depth. Their interpretation assumes that the involved crustal rocks have a quartz content that is high enough (>30 % vol) to yield a significant V_P/V_S anomaly, as shown in *Le Maitre* (1976). In contrast, our thermodynamic modeling shows that a significant change in V_P/V_S due to the quartz transition already occurs with less quartz content (<20% vol).

Even if seismically relevant, the quartz transition is probably difficult to detect. Being not sharp

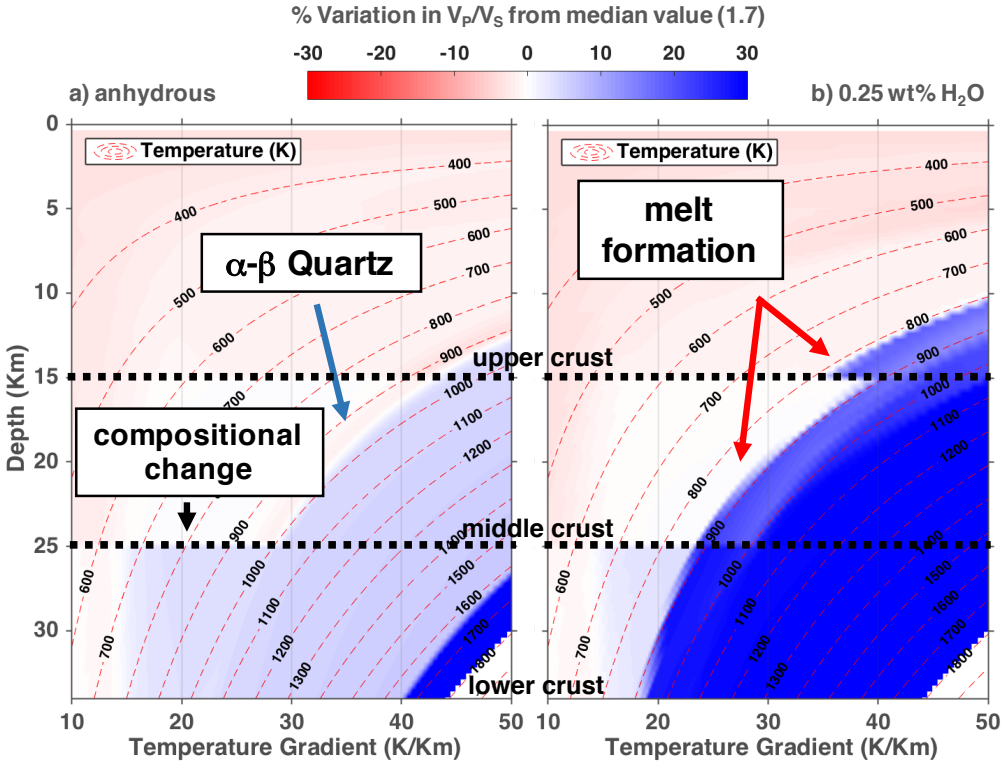

Figure 7: Relative change of V_P/V_S in % from a value of 1.7 (median in the P-T space), as a function of depth and temperature gradient. Crust is 35 km thick with composition from *Rudnick and Gao* (2003). (a) Case of an anhydrous crust where the transformation of quartz is the major cause of the change of V_P/V_S. (b) Case of a wet crust where the formation of melt significantly increases V_P/V_S above the solidus temperature, masking the α-β quartz transition.

(it occurs over a depth range of 3-5 km, see Figure 4), seismic methods with low vertical resolution (i.e., surface wave tomography) might not be able to resolve it. However, we think that the use of receiver functions would be beneficial for the detection the α-β transition. A promising outlook is the use of this phase change as possible geo-thermometer, as firstly proposed by *Mechie et al.*, (2004). The detection of this transition can also have major implications to determine crustal rheology at depth. In fact, close to the transition temperature, the Young's modulus of quartz decreases by $\sim 30\%$ (*Peng and Redfern*, 2013). Therefore, if stress is applied, a quartz-bearing rock might undergo a relevant mechanical weakening near the transition temperature, favoring strain accumulation. An additional parameter that is affected at quartz transition is thermal conductivity. *Gibert and Mainprice* (2009) reported a minimum value of thermal conductivity of quartz at the α-β transition. If confirmed, this peculiarity would affect the geothermal gradient at the depth of the phase transition. Moreover, the latent heat absorbed for the transformation could decrease the thermal gradient even more, thickening the depth interval where the transformation occurs.

The increase in V_P/V_S within the crust cannot be univocally interpreted as the α-β quartz transition. Temperature above solidus in a wet crust induces the formation of partial melt, causing a strong

decrease in V_S and thus an increase in V_P/V_S ratio. Figure 7 (right panel) shows the relative change in V_P/V_S as a function of depth and temperature gradient in a wet crust. The raise in V_P/V_S is caused by the presence of melt ($\sim$ 1% vol in our thermodynamic calculation) at depths and temperature that are close to those of the α-β transition. Hence, only considering the V_P/V_S ratio can lead to a wrong interpretation. Both V_P and V_S datasets must be thus taken into account when interpreting variations in V_P/V_S. Note that the calculated seismic properties are reliable also at solidus and sub-solidus conditions. Our thermodynamic computations make use of the comprehensive and extensively used database from *Ghiorso et al.* (2002) for phase relations between mineral aggregate and silicate melts. In contrast, we point out that our modeled V_P/V_S are not reliable for temperatures that are too high above the solidus. This condition favors the production of large quantity of melt (> 1-2% vol), causing excessively low V_P/V_S in the bulk rock, as those seen in Figure 7 at T>900° C. The assumption made in our thermodynamic modeling that melt is in equilibrium with the mineral aggregate is not realistic in this case. Large amount of melt is unstable and tend to migrate from the restitic fraction.

Beside the quartz transition, we showed that the breakdown of plagioclase can also affect seismic velocities. Figure 6 and Figure 7 (left panel) shows that it occurs at low temperatures (500- 800 K) in the lower crust and mildly in the middle crust, causing an increase in acoustic impedance (>10%) and V_P/V_S(7%). Here plagioclase is consumed in favor of dense, high-velocity minerals (e.g., clino-pyroxene). Interestingly, the associated sharp contrast in AI would exceed the effect of a chemical change at the middle-lower crust boundary. This implies that an observed sharp increase in seismic velocities is not necessarily associated with a change in chemical composition and/or the formation of garnet (that we find stable at higher pressures than those presented in our study). We conclude that the breakdown of plagioclase could play a significant role as seismic discontinuity. It could be even more relevant for anhydrous compositions, as suggested in *Guerri et al.* (2015).

4.3 Effects on seismic observables

Can we detect different compositions within the crust? And how do phase-changes affect its seismic properties? To address these questions, we compute synthetic Rayleigh-wave dispersion curves and receiver functions using the V_P, V_S and density profiles obtained through thermodynamic modeling. Surface waves are sensitive to the V_S profile at depth. For forward computation, we use a code based on *Hisada* (1994), *Lai* (1998) and *Lai and Rix* (1999) that retrieves the Green's function for a vertically layered heterogeneous medium. On the other hand, receiver functions are sensitive to seismic discontinuities underneath seismic stations. We compute RFs using a Thomson-Haskell propagator matrix for layered media. Figure 8 (b) shows the dispersion curves along three different thermal

gradients (10, 30 and 40 K/km), for a 35 km-thick crust with composition from *Rudnick and Gao* (2003), as so far. The average and high thermal gradients produce almost overlapping dispersion curves, due to the similar V_S structure at depth regardless the different thermal gradients considered. Indeed, the V_S profiles in the two cases are almost identical (Figure 8, panel c). On the contrary, a low gradient of 10 K/km is associated with values of Rayleigh phase velocities that are remarkably higher, especially in the 15-25 s range.

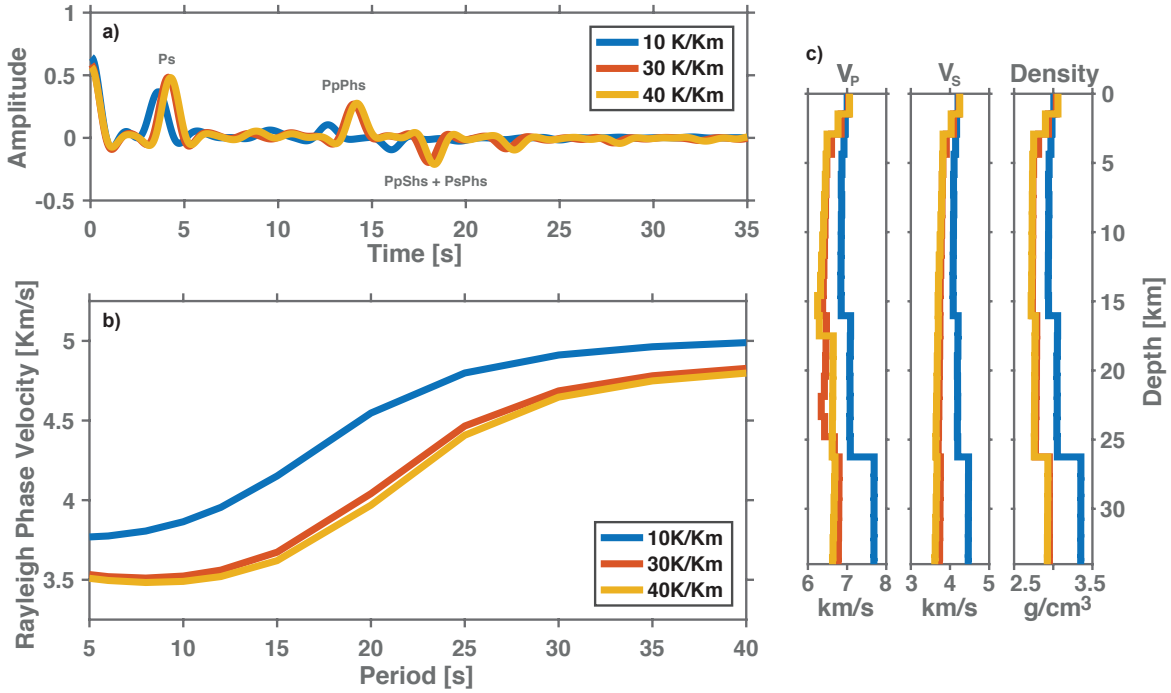

Figure 8: Synthetic observables calculated for the same crustal composition (Rudnick & Gao, 2003), along different thermal gradients. (a) Synthetic receiver functions (RFs). (b) Synthetic dispersion curves of Rayleigh waves phase velocity. (c) V_P, V_S, and density profiles obtained from thermodynamic modeling used for the computation of the seismic observables.

The key role of quartz transformation emerges when computing synthetic RFs. The average and high gradients give similar RFs waveforms, both in amplitude and phase. More importantly, these waveforms are dominated by the quartz transformation that affects both the V_P and V_P/V_S. If such similar RFs are observed, they would lead to almost identical velocity profile after inversion. The difference with the case of a cold gradient (10 K/km) is significant. The arrivals are earlier (e.g., up to 2s for the PpShs+PsPhs phase) with respect to the "warm" waveforms. This is due to the higher V_P and V_S along the depth profile (see Figure 8, panel c). Moreover, amplitudes of phases in the "cold" RF are lower, due to the small jump in AI and V_P/V_S occurring at the compositional transitions.
Far from being an exhaustive example, this exercise shows that temperature largely influences seismic velocities. Same chemical compositions exhibit diverse velocity profiles that are controlled by the temperature distribution at depth. Temperature defines the seismic properties of minerals, their

stability and controls mineralogical transformation. Therefore, independent information on the local temperature gradient is fundamental for an improved and reliable interpretation of seismological data of the crust.

5 Limitation and conclusions

In spite of abundant data, the formation, evolution, structure and composition of the crust are still unclear and matter of debate. Geophysical methods provide biased information because of the strong non-uniqueness of the retrieved models, model assumptions and non-linearity of relations used to tie physical and seismic properties. In order to improve the interpretation of geophysical data in a multi-disciplinary framework, we analyzed the effects of temperature, pressure, composition and water content on the seismic properties of the crust in a thermodynamically consistent approach. Our major findings are:

1. Different dry compositions, typical of crystalline crust (note that we do not consider in this study a variety of sedimentary rocks that can characterize the top portion of the crust) can be seismically undistinguishable. The variation induced by a different composition is always lower than that caused by temperature and water content. The global chemical composition of the crust proposed by *Rudnick and Gao* (2003) provides similar seismic properties as those determined at a regional scale. Therefore, it can be used as a reasonable approximation for the chemical composition also for local studies.

2. In order to infer temperature and/or composition of the crust, it is necessary to use complementary geophysical datasets and thermodynamic constraints.

3. The V_S/density has an almost constant value around 1.34 for variable temperatures (400-1000 K), pressure, dry composition and water content. In absence of better constraints, this ratio could be used in joint-inversion of gravity and seismic data assuming a crystalline, pore-free rock.

4. The α-β quartz transition might represent an important seismic discontinuity in the middle crust (15-25 km). It is marked by an increase in V_P and V_P/V_S, both larger than those generated by compositional changes at the upper-middle, middle-lower crust boundaries.

5. The increase in V_P/V_S cannot be univocally referred to the quartz transition. In a wet crust, the formation of melt causes also a highV_P/V_S, due to the decrease in V_S. Therefore, a correct interpretation of seismological data must be based also on the joint interpretation of independent V_P and V_S data to discriminate between the two cases.

6. In the presence of a localized pressure gradient and temperature between 500 and 800 K, the plagioclase breakdown can produce an increase of acoustic impedance and V_P/V_S in the lower

crust. The change in seismic properties, also in this case, is higher than that caused by a chemical transition at the boundary between middle and lower crust.

The use of thermodynamic modeling in this work required some simplifications. Firstly, seismic properties were modelled assuming the thermodynamic equilibrium of all phases for any pressure and temperature while, in reality, crustal rocks can be in a metastable condition. Secondly, our modeling assumes an isotropic and pore-free bulk rock. This simplification might not be valid in the shallowest crust where mineral might still preserve a preferential orientation and porosity can significantly decrease seismic velocities. In addition, temperature-induced anelasticity is not accounted for, and, as already mentioned, we did not thoroughly assess the effects of sedimentary rocks on seismic velocities, that might not be negligible in the upper crust. The considerations of these effects would be a matter of further investigation, for a better understanding of crust in terms of its thermo-chemical characteristics.

Acknowledgments

We thank V. Lekic for making available the code for RFs and dispersion curves computation. We kindly thank A. Stallone and S. Speziale for the effort dedicated to the review of this article. Furthermore, we thank the four anonymous reviewers and the Associate Editor for their comments and suggestions that largely contributed to the improvement of the manuscript. Data are freely available and published under the CC BY 4.0 license, https://doi.org/10.6084/m9.figshare.5217205.

Bibliography

Afonso, J. C., Fullea, J., Griffin, W. L., Yang, Y., Jones, A. G., D Connolly, J. A., & O'Reilly, S. Y. (2013). 3-D multiobservable probabilistic inversion for the compositional and thermal structure of the lithosphere and upper mantle. I: A priori petrological information and geophysical observables. *Journal of Geophysical Research: Solid Earth*, *118*(5), 2586-2617. https://doi.org/10.1002/jgrb.50124

Anderson, O. L., Isaak, D., & Oda, H. (1992). High-temperature elastic constant data on minerals relevant to geophysics. *Reviews of Geophysics*, *30*(1), 57-90. https://doi.org/10.1029/91RG02810

Abers, G. A., & Hacker, B. R. (2016). A MATLAB toolbox and Excel workbook for calculating the densities, seismic wave speeds, and major element composition of minerals and rocks at pressure and temperature. *Geochemistry, Geophysics, Geosystems*, *17*(2), 616-624. https://doi.org/10.1002/2015GC006171

Bassin, C., G. Laske, and G. Masters (2000). The current limits of resolution for surface wave tomography in North America. *Eos Trans. AGU*, *81*(48), Fall Meet. Suppl., Abstract S12A - 03.

Behn, M. D., & Kelemen, P. B. (2003). Relationship between seismic P-wave velocity and the composition of anhydrous igneous and meta-igneous rocks. *Geochemistry, Geophysics, Geosystems*, *4*(5). https://doi.org/10.1029/2002GC000393

Behn, M. D., & Kelemen, P. B. (2006). Stability of arc lower crust: Insights from the Talkeetna arc section, south central Alaska, and the seismic structure of modern arcs. *Journal of Geophysical Research: Solid Earth*, *111*(B11). https://doi.org/10.1029/2006JB004327

Bianchi, I., Park, J., Piana Agostinetti, N., & Levin, V. (2010). Mapping seismic anisotropy using harmonic decomposition of receiver functions: An application to Northern Apennines, Italy. *Journal of Geophysical Research: Solid Earth*, *115*(B12). https://doi.org/10.1029/2009JB007061

Bina, C. R., & Helffrich, G. R. (1992). Calculation of elastic properties from thermodynamic equation of state principles. *Annual Review of Earth and Planetary Sciences*, *20*(1), 527-552. https://doi.org/10.1146/annurev.ea.20.050192.002523

Birch, F. (1961). The velocity of compressional waves in rocks to 10 kilobars: 2. *Journal of Geophysical Research*, *66*(7), 2199-2224. https://doi.org/10.1029/JZ066i007p02199

Bodin, T., Sambridge, M., Tkalčič, H., Arroucau, P., Gallagher, K., & Rawlinson, N. (2012). Transdimensional inversion of receiver functions and surface wave dispersion. *Journal of Geophysical Research: Solid Earth*, *117*(B2). https://doi.org/10.1029/2011JB008560

Bodin, T., Leiva, J., Romanowicz, B., Maupin, V., & Yuan, H. (2016). Imaging anisotropic layering with Bayesian inversion of multiple data types. *Geophysical Journal International*, *206*(1), 605-629. https://doi.org/10.1093/gji/ggw124

Brocher, T. M. (2005). Empirical relations between elastic wavespeeds and density in the Earth's crust. *Bulletin of the Seismological Society of America*, *95*(6), 2081-2092. https://doi.org/10.1785/0120050077

Carminati, E., Wortel, M. J. R., Spakman, W., & Sabadini, R. (1998). The role of slab detachment processes in the opening of the western-central Mediterranean basins: some geological and geophysical evidence. *Earth and Planetary Science Letters*, *160*(3), 651-665. https://doi.org/10.1016/S0012-821X(98)00118-6

Carminati, E., Lustrino, M., Cuffaro, M., & Doglioni, C. (2010). Tectonics, magmatism and geodynamics of Italy: what we know and what we imagine. *Journal of the Virtual Explorer*, *36*(8). https://doi.org/10.3809/jvirtex.2010.00226

Carminati, E., Lustrino, M., & Doglioni, C. (2012). Geodynamic evolution of the central and

western Mediterranean: Tectonics vs. igneous petrology constraints. *Tectonophysics*, *579*, 173-192. https://doi.org/10.1016/j.tecto.2012.01.026

Christensen, N. I., & Mooney, W. D. (1995). Seismic velocity structure and composition of the continental crust: A global view. *Journal of Geophysical Research: Solid Earth*, *100*(B6), 9761-9788. https://doi.org/10.1029/95JB00259

Connolly, J. A. D. (2009). The geodynamic equation of state: what and how. *Geochemistry, Geophysics, Geosystems*, *10*(10). https://doi.org/10.1029/2009GC002540

Condie, K. C. (2013). Plate tectonics & crustal evolution. Elsevier.

Della Vedova, B., Bellani, S., Pellis, G., & Squarci, P. (2001). Deep temperatures and surface heat flow distribution. In *Anatomy of an orogen: the Apennines and adjacent Mediterranean basins* (pp. 65-76). Springer Netherlands. https://doi.org/10.1007/978-94-015-9829-3_7

Di Stefano, R., Chiarabba, C., Lucente, F., & Amato, A. (1999). Crustal and uppermost mantle structure in Italy from the inversion of P-wave arrival times: geodynamic implications. *Geophysical Journal International*, *139*(2), 483-498. https://doi.org/10.1046/j.1365-246x.1999.00952.x

Di Stefano, R., Kissling, E., Chiarabba, C., Amato, A., & Giardini, D. (2009). Shallow subduction beneath Italy: Three-dimensional images of the Adriatic-European-Tyrrhenian lithosphere system based on high-quality P wave arrival times. *Journal of Geophysical Research: Solid Earth*, *114*(B5). https://doi.org/10.1029/2008JB005641

Doglioni, C., Mongelli, F., & Pialli, G. (1998). Boudinage of the Alpine belt in the Apenninic back-arc. *Mem. Soc. Geol. It*, *52*, 457-468.

Doglioni, C., Harabaglia, P., Merlini, S., Mongelli, F., Peccerillo, A. T., & Piromallo, C. (1999). Orogens and slabs vs. their direction of subduction. *Earth-Science Reviews*, *45*(3), 167-208. https://doi.org/10.1016/S0012-8252(98)00045-2

Faccenna, C., Becker, T. W., Lucente, F. P., Jolivet, L., & Rossetti, F. (2001). History of subduction and back arc extension in the Central Mediterranean. *Geophysical Journal International*, *145*(3),

809-820. https://doi.org/0.1046/j.0956-540x.2001.01435.x

Finetti, I. R. (2005). CROP project: deep seismic exploration of the central Mediterranean and Italy (Vol 1). Elsevier.

Fountain, D. M. (1976). The Ivrea-Verbano and Strona-Ceneri Zones, Northern Italy: A cross-section of the continental crust-New evidence from seismic velocities of rock samples. *Tectonophysics*, *33*(1-2), 145-165. https://doi.org/10.1016/0040-1951(76)90054-8

Ghiorso, M. S., Hirschmann, M. M., Reiners, P. W., & Kress, V. C. (2002). The pMELTS: A revision of MELTS for improved calculation of phase relations and major element partitioning related to partial melting of the mantle to 3 GPa. *Geochemistry, Geophysics, Geosystems*, *3*(5), 1-35. https://doi.org/10.1029/2001GC000217

Gibert, B., & Mainprice, D. (2009). Effect of crystal preferred orientations on the thermal diffusivity of quartz polycrystalline aggregates at high temperature. *Tectonophysics*, *465*(1), 150-163. https://doi.org/10.1016/j.tecto.2008.11.006

Gualtieri, L., Serretti, P., & Morelli, A. (2014). Finite-difference p wave travel time seismic tomography of the crust and uppermost mantle in the Italian region. *Geochemistry, Geophysics, Geosystems*, *15*(1), 69-88. https://doi.org/10.1002/2013GC004988

Guerri, M., Cammarano, F., & Connolly, J. A. (2015). Effects of chemical composition, water and temperature on physical properties of continental crust. *Geochemistry, Geophysics, Geosystems*, *16*(7), 2431-2449. https://doi.org/10.1002/2015GC005819

Guerri, M., Cammarano, F., & Tackley, P. J. (2016). Modeling Earth's surface topography: Decomposition of the static and dynamic components. *Physics of the Earth and Planetary Interiors*, *261*, 172-186. https://doi.org/10.1016/j.pepi.2016.10.009

Hacker, B. R., Abers, G. A., & Peacock, S. M. (2003). Subduction factory 1. Theoretical mineralogy, densities, seismic wave speeds, and H2O contents. *Journal of Geophysical Research*: Solid Earth, *108*(B1). https://doi.org/10.1029/2001JB001127

Hacker, B. R., & Abers, G. A. (2004). Subduction Factory 3: An Excel worksheet and macro for calculating the densities, seismic wave speeds, and H2O contents of minerals and rocks at pressure and temperature. *Geochemistry, Geophysics, Geosystems*, *5*(1). https://doi.org/10.1029/2003GC000614

Hacker, B. R., Ritzwoller, M. H., & Xie, J. (2014). Partially melted, mica-bearing crust in Central Tibet. *Tectonics*, *33*(7), 1408-1424. https://doi.org/10.1002/2014TC003545

Hacker, B. R., Kelemen, P. B., & Behn, M. D. (2015). Continental lower crust. *Annual Review of Earth and Planetary Sciences*, *43*, 167-205.

Hill, R. (1952). The elastic behaviour of a crystalline aggregate. *Proceedings of the Physical Society. Section A*, *65*(5), 349. https://doi.org/10.1088/0370-1298/65/5/307

Hisada, Y. (1994). An efficient method for computing Green's functions for a layered half-space with sources and receivers at close depths. *Bulletin of the Seismological Society of America*, *84*(5), 1456-1472.

Holland, T. J. B., and R. Powell (1998). An internally consistent thermodynamic data set for phases of petrological interest*, J. Metamorph. Geol.*, *16*, 309-343. https://doi.org/10.1111/j.1525-1314.1998.00140.x

Julia, J., Ammon, C. J., Herrmann, R. B., & Correig, A. M. (2000). Joint inversion of receiver function and surface wave dispersion observations. *Geophysical Journal International*, *143*(1), 99-112. https://doi.org/10.1046/j.1365-246x.2000.00217.x

Kaban, M. K., Tesauro, M., Mooney, W. D., & Cloetingh, S. A. (2014). Density, temperature, and composition of the North American lithosphere-New insights from a joint analysis of seismic, gravity, and mineral physics data: 1. Density structure of the crust and upper mantle. *Geochemistry, Geophysics, Geosystems*, *15*(12), 4781-4807. https://doi.org/10.1002/2014GC005483

Karato, S. I. (1993). Importance of anelasticity in the interpretation of seismic tomography. *Geophysical Research Letters*, *20*(15), 1623-1626. https://doi.org/10.1029/93GL01767

Kuo-Chen, H., Wu, F. T., Jenkins, D. M., Mechie, J., Roecker, S. W., Wang, C. Y., & Huang, B. S. (2012). Seismic evidence for the α -β quartz transition beneath Taiwan from Vp/Vs tomography. *Geophysical Research Letters*, *39*(22). https://doi.org/10.1029/2012GL053649

Lai, C.G. (1998). *Simultaneous Inversion of Rayleigh Phase Velocity and Attenuation for Near-Surface Site Characterization,* (Ph.D. Thesis). Atlanta, US: Georgia Institute of Technology.

Lai, C. & Rix, G.J. (1999). Inversion of multi-mode effective dispersion curves. In M. Jamiolkowski, R. Lancellotta, & D. Lo Presti (eds.*), Pre-failure Deformation Characteristics of Geomaterials.* 411-418. Rotterdam: Balkema.

Laske, G., Masters, G., Ma, Z., & Pasyanos, M. (2013). Update on CRUST1.0 - A 1-degree global model of Earth's crust *In Geophys. Res. Abstr* (Vol 15, p. 2658).

Le Maitre, R. W. (1976). The chemical variability of some common igneous rocks. *Journal of petrology*, *17*(4), 589-598. https://doi.org/10.1093/petrology/17.4.589

Levandowski, W., Boyd, O. S., Briggs, R. W., & Gold, R. D. (2015). A random-walk algorithm for modeling lithospheric density and the role of body forces in the evolution of the Midcontinent Rift. *Geochemistry, Geophysics, Geosystems*, *16*(12), 4084-4107. https://doi.org/10.1002/2015GC005961

Levandowski, W., Boyd, O. S., & Ramirez-GuzmÃ¡n, L. (2016). Dense lower crust elevates long-term earthquake rates in the New Madrid seismic zone. *Geophysical Research Letters*, *43*(16), 8499-8510. https://doi.org/10.1002/2016GL070175

Lowry, A. R., & PÃ©rez-GussinyÃ©, M. (2011). The role of crustal quartz in controlling Cordilleran deformation. *Nature*, *471*(7338), 353-357. https://doi.org/10.1038/nature09912

Ludwig, W. J., Nafe, J. E., & Drake, C. L. (1970). Seismic refraction. *The sea* (Vol 4, pp. 53-84).

Mainprice, D., & Casey, M. (1990). The calculated seismic properties of quartz mylonites with typical fabrics: relationship to kinematics and temperature. *Geophysical Journal International*, *103*(3), 599-608. https://doi.org/10.1111/j.1365-246X.1990.tb05674.x

Mantovani, E., Albarello, D., Babbucci, D., Tamburelli, C., & Viti, M. (2002). Trench-Arc-BackArc systems in the Mediterranean area: examples of extrusion tectonics. *Journal of the Virtual Explorer*, *8*, 131-147.

Mariotti, G., & Doglioni, C. (2000). The dip of the foreland monocline in the Alps and Apennines. *Earth and Planetary Science Letters*, *181*(1), 191-202. https://doi.org/10.1016/S0012-821X(00)00192-8

McLennan, S.M., Taylor, S.R., Heming, S.R. (2005). Composition, differentiation, and evolution of continental crust: constraints from sedimentary rocks and heatflow. In M. Brown, T. Rushmer (Eds.), *Evolution and Differentiation of the Continental crust*, (pp. 92-134). Cambridge, UK: Cambridge Univ. Press

Mechie, J., Sobolev, S. V., Ratschbacher, L., Babeyko, A. Y., Bock, G., Jones, A. G. & Zhao, W. (2004). Precise temperature estimation in the Tibetan crust from seismic detection of the α -β quartz transition. *Geology*, *32*(7), 601-604. https://doi.org//10.1130/G20367.1

Molinari, I., & Morelli, A. (2011). EPcrust: a reference crustal model for the European Plate. *Geophysical Journal International*, *185*(1), 352-364. https://doi.org/10.1111/j.1365-246X.2011.04940.x

Molinari, I., Argnani, A., Morelli, A., & Basini, P. (2015). Development and testing of a 3D seismic velocity model of the Po Plain sedimentary basin, Italy. *Bulletin of the Seismological Society of America*, *105*(2A), 753-764. https://doi.org/10.1785/0120140204

Molinari, I., Verbeke, J., Boschi, L., Kissling, E., & Morelli, A. (2015). Italian and Alpine three-dimensional crustal structure imaged by ambient-noise surface-wave dispersion. *Geochemistry, Geophysics, Geosystems*, *16*(12), 4405-4421. https://doi.org/10.1002/2015GC006176

Ohno, I. (1995). Temperature Variation of Elastic Properties of -quartz up to the to transition. *Journal of Physics of the Earth*, *43*(2), 157-169.

Ohno, I., Harada, K., & Yoshitomi, C. (2006). Temperature variation of elastic constants of quartz

across the α -β transition. *Physics and Chemistry of Minerals*, *33*(1), 1-9. https://doi.org//10.1007/s00269-005-0008-3

Ökeler, A., Gu, Y. J., Lerner-Lam, A., & Steckler, M. S. (2009). Seismic structure of the southern Apennines as revealed by waveform modelling of regional surface waves *Geophysical Journal International*, *178*(3), 1473-1492. https://doi.org/10.1111/j.1365-246X.2009.04229.x

Pasyanos, M. E., & Walter, W. R. (2002). Crust and upper-mantle structure of North Africa, Europe and the Middle East from inversion of surface waves. *Geophysical Journal International*, *149*(2), 463-481. https://doi.org//10.1046/j.1365-246X.2002.01663.x

Pasyanos, M. E., Masters, T. G., Laske, G., & Ma, Z. (2014). LITHO1. 0: An updated crust and lithospheric model of the Earth. *Journal of Geophysical Research: Solid Earth*, *119*(3), 2153-2173. https://doi.org/10.1002/2013JB010626

Peng, Z., & Redfern, S. A. (2013). Mechanical properties of quartz at the α -β phase transition: Implications for tectonic and seismic anomalies. *Geochemistry, Geophysics, Geosystems*, *14*(1), 18-28. https://doi.org/10.1029/2012GC004482

Peccerillo, A. 2005. Plio-Quaternary Volcanism in Italy. *Petrology, Geochemistry, Geodynamics.* Springer, Heidelberg. https://doi.org/10.1007/3-540-29092-3

Piana Agostinetti, N., & Amato, A. (2009). Moho depth and Vp/Vs ratio in peninsular Italy from teleseismic receiver functions. *Journal of Geophysical Research: Solid Earth*, *114*(B6). https://doi.org/10.1029/2008JB005899

Qashqai, M., Carlos Afonso, J., & Yang, Y. (2016). The crustal structure of the Arizona Transition Zone and southern Colorado Plateau from multiobservable probabilistic inversion. *Geochemistry, Geophysics, Geosystems*, *17*(11), 4308-4332. https://doi.org/10.1002/2016GC006463

Reguzzoni, M., & Sampietro, D. (2015). GEMMA: An Earth crustal model based on GOCE satellite data. *International Journal of Applied Earth Observation and Geoinformation*, *35*, 31-43. https://doi.org/10.1016/j.jag.2014.04.002

Ritsema, J., Van Heijst, H. J., Woodhouse, J. H., & Deuss, A. (2009). Long-period body wave traveltimes through the crust: implication for crustal corrections and seismic tomography. *Geophysical Journal International*, *179*(2), 1255-1261. https://doi.org/10.1111/j.1365-246X.2009.04365.x

Rudnick, R. L. (1992). Xenoliths-samples of the lower continental crust. *Continental lower crust, 23*, 269-316.

Rudnick, R. L., & Fountain, D. M. (1995). Nature and composition of the continental crust: a lower crustal perspective. *Reviews of geophysics*, *33*(3), 267-309. https://doi.org/10.1029/95RG01302

Rudnick, R. L., & Gao, S. (2003). Composition of the continental crust. *Treatise on geochemistry*, *3*, 659. https://doi.org/10.1016/B0-08-043751-6/03016-4

Sassi, F. P. (2003). The abundance of 55 elements and petrovolumetric models of the crust in 9 type areas from the crystalline basements of Italy, with some Geophysical and petrophysical data. *Scritti e Documenti. Accademia Nazionale delle Scienze detta dei XL* (Vol 32).

Scrocca, D., Doglioni, C., & Innocenti, F. (2003). Constraints for an interpretation of the Italian geodynamics: a review. *Memorie Descrittive della Carta Geologica d'Italia*, *62*, 15-46.

Shen, A. H., W. A. Bassett, and I.-M. Chou (1993). The α -β quartz transition at high temperatures and pressures in a diamond-anvil cell by laser interferometry. *Am. Mineral.*, *78*, 694-698.

Shen, W., Ritzwoller, M. H., & Schulte-Pelkum, V. (2013). A 3-D model of the crust and uppermost mantle beneath the Central and Western US by joint inversion of receiver functions and surface wave dispersion. *Journal of Geophysical Research: Solid Earth*, *118*(1), 262-276. https://doi.org/10.1029/2012JB009602

Shen, W., & Ritzwoller, M. H. (2016). Crustal and uppermost mantle structure beneath the United States. *Journal of Geophysical Research: Solid Earth*, *121*(6), 4306-4342. https://doi.org/10.1002/2016JB012887

Stixrude, L., & Lithgow-Bertelloni, C. (2011). Thermodynamics of mantle minerals-II. Phase equilibria. *Geophysical Journal International*, *184*(3), 1180-1213. https://doi.org/10.1111/j.

1365-246X.2010.04890.x

Tassara, A. (2006). Factors controlling the crustal density structure underneath active continental margins with implications for their evolution. *Geochemistry, Geophysics, Geosystems*, *7*(1). https://doi.org/10.1029/2005GC001040

TaylorSR, M. (1985). The continental crust: its composition and evolution. United States: Blackwell Scientific Publications. https://doi.org/10.1017/S0016756800032167

Tesauro, M., Kaban, M. K., Mooney, W. D., & Cloetingh, S. (2014). NACr14: A 3D model for the crustal structure of the North American Continent. *Tectonophysics*, *631*, 65-86. https://doi.org/10.1016/j.tecto.2014.04.016

Tesauro, M., Kaban, M. K., Mooney, W. D., & Cloetingh, S. A. (2014). Density, temperature, and composition of the North American lithosphere-new insights from a joint analysis of seismic, gravity, and mineral physics data: 2. Thermal and compositional model of the upper mantle. *Geochemistry, Geophysics, Geosystems*, *15*(12), 4808-4830. https://doi.org/10.1002/2014GC005484

Tiberi, C., Diament, M., DÃ©verchÃ¨re, J., Petit-Mariani, C., Mikhailov, V., Tikhotsky, S., & Achauer, U. (2003). Deep structure of the Baikal rift zone revealed by joint inversion of gravity and seismology. *Journal of Geophysical Research: Solid Earth*, *108*(B3). https://doi.org/10.1029/2002JB001880

Tondi, R., Schivardi, R., Molinari, I., & Morelli, A. (2012). Upper mantle structure below the European continent: Constraints from surface-wave tomography and GRACE satellite gravity data. *Journal of Geophysical Research: Solid Earth*, *117*(B9). https://doi.org/10.1029/2012JB009149

Vasco, D. W., Johnson, L. R., & Marques, O. (2003). Resolution, uncertainty, and whole Earth tomography. *Journal of Geophysical Research: Solid Earth*, *108*(B1). https://doi.org/10.1029/2001JB000412

Vernant, P., Masson, F., Bayer, R., & Paul, A. (2002). Sequential inversion of local earthquake traveltimes and gravity anomaly-The example of the western Alps. *Geophysical Journal International*, *150*(1), 79-90. https://doi.org/10.1046/j.1365-246X.2002.01694.x

Vinnik, L. P. (1977). Detection of waves converted from P to SV in the mantle. *Physics of the Earth and planetary interiors*, *15*(1), 39-45. https://doi.org/10.1016/0031-9201(77)90008-5

Watanabe, T. (1993). Effects of water and melt on seismic velocities and their application to characterization of seismic reflectors. *Geophysical Research Letters*, *20*(24), 2933-2936. https://doi.org/10.1029/93GL03170

Windley, B. F. (1996). The evolving continents. *Oceanographic Literature Review*, *8*(43), 785.

Zhu, L., Kanamori, H. (2000). Moho depth variation in southern California from teleseismic receiver function. *J. Geophys. Res. 105*, 2969-2980. https://doi.org/10.1029/1999JB900322

Chapter 2

Seismic constraints on the crustal thermal structure of the Italian Peninsula

Abstract

Temperature distribution at depth is of key importance to characterize the crust, defining its role and behavior in relation to neighboring plates and the mantle underneath. Temperature can be retrieved by heat flow measurements in boreholes, but data are sparse and shallow and do not provide the necessary coverage and reliability, especially in active and geologically recent areas. Laboratory data and thermodynamic modeling demonstrate that temperature exerts a strong control on the seismic properties of rocks, supporting the hypothesis that seismic data can be used to unravel the crustal thermal structure. We use Rayleigh wave dispersion curves (SWD) and receiver functions (RFs), jointly inverted with a trans-dimensional Monte Carlo Markov Chain algorithm, to retrieve the V_S and V_P/V_S at crustal depth for the Italian peninsula. Except for the areas where the geological complexities have hampered the retrieval of a satisfactory model, the obtained subsurface models are exploited for the crustal characterization. The high values (> 1.9) of V_P/V_S suggest a relevant role of filled-fluid cracks in the middle and lower crust. Intra-crustal discontinuities associated with large values of V_P/V_S are interpreted as the $\alpha - \beta$ quartz transition and used for the estimation of geothermal gradients. The use of thermodynamics to translate shear-wave velocities into temperature leads to similar estimates, in agreement with the known tectonic and geodynamic setting of the Italian Peninsula. Seismological data are therefore a viable alternative to heat flow measurements for the thermal characterization of the crust.

1 Introduction

Unraveling the thermo-chemical structure of the crust is fundamental for the understanding of its tectonic, magmatic and geodynamical processes, both at local and global scales. With its rheological behavior, the crust has a direct implication on the type of interaction between plates, the storage of mechanical stress, and, consequently, overall seismicity. Moreover, the crust has effects on magmatic processes, controlling their spatial and temporal evolution, the chemical signature of magmas, their emplacement and erupting style.

Temperature is a key parameters for the characterization of the crust. It controls the depth of the brittle-to-ductile transition (BDT, *Rutter* (1986)), marking the change from an elastic behavior (causing earthquakes) to the plastic one. On larger time scales than fault rupture, temperature is the key factor affecting the viscosity and flow of the lower, ductile portion of the crust, with direct implications on processes such as exhumation and delamination (*Ranalli*, 2000). Our understanding of the respective contribution of crust and mantle on isostatic adjustments (i.e. uplift and subsidence on regional scale) is bounded by the definition of the thermal structure at depth (*Lachenbruch et al.*, 1997). Moreover, temperature is directly indicative of the enrichment in radiogenic isotopes, the up-welling (or percolation) of fluids through fault systems, as well as of deep-mantle heat source or accumulation of partial melts. Despite its importance, temperature is only poorly known at depth and is inferred through heat flow measurements in boreholes, assuming a purely conductive heat transfer mechanism. For these reasons, heat flow data is scarce, has poor spatial representativeness and suffers from systematic errors due to the measurement technique employed in borehole(*Stein*, 1995). Particularly for active regions, a purely conductive heat transfer is unrealistic because the generally high values of heat flow suggest a relevant role of fluid up-welling (*advection*) as an important, or probably major, mechanism for heat transfer.

To overcome the limitations of heat flow measurements, a more accurate and spatially representative method is desirable for temperature estimation, possibly based on observed seismic velocities that offer better coverage and less uncertainty. In this direction, an attempt is represented by *Schutt et al.* (2018), based on anomalies of refracted Pn waves for the retrieval of temperature at Moho in Western Unites States. With this work, we integrate two different seismic datasets and thermodynamics, as equations of state in a mineral aggregate are the link between observed seismic velocities (*Diaferia and Cammarano*, 2017) and temperature. Specifically, we jointly invert dispersion curves of Rayleigh surface waves (SWD) and receiver functions (RFs) using a reversible-jump Markov Chain Monte Carlo. The inversion method does not require strong prior information on the geometry of the subsurface structure. Specifically, the number of model parameters is considered as an unknown in

the inversion. The Bayesian nature of the inversion also allows the estimates of the model parameter uncertainties. We retrieve temperatures at depth by (i) using thermodynamic modeling, assuming a crustal composition as in *Rudnick and Gao* (2003) and (ii) detecting the seismic signature of the quartz transition, since this mineralogical transformation is mostly temperature-driven and can be used as geo-thermometer.

The target of our study is the Italian peninsula that, with its recent tectonic history and relevant seismic and magmatic activity, is one of the key spots to understand the evolution of the Mediterranean. Its formation is the result of the Alpine and Apennine orogenic events, due to the collision of the African and European plates since the Cretaceous. In the past 15 Ma, the Italian Peninsula rotated counterclockwise, causing the opening of the Tyrrhenian Sea basin. A relevant volcano-magmatic activity started in the Quaternary and still continues, as testified by the diffuse volcanism and the high heat flow measured at the surface in certain areas. For imaging its structure at depth, and thus better understand its tectonic and geodynamic setting, the Italian Peninsula has been the target of a wealth of studies based on seismological investigations. Examples of investigations with seismic reflection and refraction are found in *Waldhauser et al.* (2014) and *Bruckl et al.* (2007), tomographic images based on P-waves arrivals are provided by *Chiarabba and Amato* (1996), *Piromallo and Morelli* (2003), *Serretti and Morelli* (2011), *Gualtieri et al.* (2014). *Diehl et al.* (2009) and *Di Stefano et al.* (2009) are examples of high-resolution, local earthquake tomographies, *Piana Agostinetti et al.* (2002),*Piana Agostinetti and Amato* (2009) and *Bianchi et al.* (2010) employed receiver functions. An integration of different seismological methods is attempted in *Spada et al.* (2013) to define the depth and geometry of the Moho. The CROP project (*Finetti*, 2005) shed light on intra-crustal features through through deep seismic reflection. While these studies have mainly characterized the crust in terms of compressional-wave velocities, *Verbeke et al.* (2012),*Molinari et al.* (2015) and *Kästle et al.* (2018) used ambient noise to obtain the shear-velocity distribution at depth. Despite the abundance of data, their interpretation is often difficult due to uneven coverage, varying resolution and sensitivity of each method. In addition, the conversion of seismic velocities into parameters such as water content, temperature and lithology is a difficult task.

2 Data and method

Among the wealth of seismic data available for the Italian peninsula, we rely on the Rayleigh phase velocity used in *Molinari et al.* (2015). These are retrieved from ambient noise (more details in the following section), assuring a large coverage across the Italian peninsula and sensitivity to crustal

depth. To recover the V_P/V_S at depth and increase the resolution of the ambient noise data, we integrate it with receiver functions. RFs provide information on possible sharp seismic discontinuities at depth. We jointly invert the two datasets using a reversible-jump Markov chain Monte Carlo (rj-MCMC) that does not require any prior discretization of the subsurface model. Specifically, the number of layers is an unknown itself and, theoretically, is only constrained by the data if the prior information do not provide any restriction (*Bodin and Sambridge*, 2009; *Gao and Lekiˆc*, 2018). The depth of the seismic discontinuities is provided as posterior probability density function, providing an indication of their strength and uncertainty. Finally, we use the inverted shear-wave velocities profile for i) detecting the quartz transformation ii) and converting of such velocities into absolute temperature through thermodynamics.

2.1 Receiver Functions

The teleseismic data, recorded in the last 10-12 years by 50 both permanent and temporary stations from the Istituto Nazionale di Geofisica e Vulcanologica (INGV, Italy), have been used to construct the RF data-sets. All considered seismic events have at least MW >=5.5, with an epicentral distance between 30°and 100°. Seismic station with more than two years of data have been considered, to obtain a good back-azimuthal coverage. For each event, we deconvolve in the frequency domain the vertical and radial components of the incoming wavefield with a Gaussian filter resulting in a central frequency of 1 Hz (*Di Bona*, 1998). Following *Bianchi et al.* (2010), we extracted back-azimuthal harmonics from each data-set, to obtain a single RF (the first angular harmonics, k=0) that represents the 1-D, horizontally layered, isotropic structure beneath the seismic section (*Park and Levin*, 2016) . The uncertainty on each k=0 harmonics is estimated by bootstrap re-sampling, while data correlation along each RF is obtained by deconvolution of the vertical component with itself. Those two information, uncertainty on k=0 harmonics and correlation function, are used to build the Covariance matrix of the RF data, used to compute the likelihood between data and model predictions (*Piana Agostinetti and Malinverno*, 2018). The 50 locations are those that provide the best error-statistics and the least uncertainty on the receiver function waveform. The forward solver used in the inversion routine is based on the Thomson-Haskell propagator matrix (*Thomson*, 1950; *Haskell*, 1953) for isotropic and vertically layered media.

2.2 Dispersion curves

We use ambient-noise recordings with a data coverage that is not dependent on earthquakes distribution. The dispersion curves of Rayleigh phase velocities are computed by *Molinari et al.* (2015) from

the passive, 1-year long recordings (2008) of *Verbeke et al.* (2012) that cover the Alpine area as well as the majority of the Italian peninsula. Phase velocities are given in the period range of 5-45 s, on a evenly spaced 0.25° x 0.25° grid. These periods provide a good sensitivity from the upper to lower crust and beyond. At the location for which RFs are available, we interpolate the phase velocities at each frequency to obtain the dispersion curves to be used in the joint-inversion.

2.3 The joint-inversion strategy

For the retrieval of the subsurface model from observed data, we use a model-space sampling strategy based on Bayes' theorem. Our approach allows a proper and effective sampling of the multivariate space that constitutes the final model. This is in the form of an ensemble solution and its wideness is directly indicative of its uncertainty. In comparison with a classical approach based on linearized inversion, our approach has the advantage of not being trapped in local minima and of providing estimate of the model uncertainties.

The rj-MCMC algorithm

Owing to our need to invert simultaneously two different datasets, we opt for the approach presented in *Bodin et al.* (2012). The method we adopt employs a reversible jump, Monte Carlo Markov chain scheme (rj-MCMC) for the joint-inversion of a RF and dispersion curve. The inversion problem is formulated with a Bayesian framework, where the final solution is represented by a posterior probability density function and is sampled through a trans-dimensional approach (*Maliverno*, 2002), i.e. the number of model unknowns (e.g. the number of layers) is itself unknown. This approach avoids the requirement of any subjective a-priori discretization of the solution (*Piana Agostinetti and Maliverno*, 2010). The rationale of the method is to sample the posterior density function, combining our a-priori knowledge of the subsurface and updating it with the information provided by the data. Formally, this is expressed by the Bayes theorem (*Bayes and Price*, 1763):

$$p(\mathbf{m}|\mathbf{d}_{obs}) \propto p(\mathbf{d}_{obs}|\mathbf{m}) \times p(\mathbf{m}) \tag{1}$$

where $p(\mathbf{m}|\mathbf{d}_{obs})$ is the posterior density function (expressed as the probability of having the model parameters in $\mathbf{m}$, given the observed data); $p(\mathbf{d}_{obs}|\mathbf{m})$ is the likelihood (the probability of observing the data, given the model); $p(\mathbf{m})$ is the prior, the information we have about the model in terms of probabilities, before observing the data. The likelihood is expressed as:

$$p(\mathbf{d}_{obs}|\mathbf{m}) = \frac{1}{\sqrt{|\mathbf{C}|(2\pi)^n}} \exp\left\{\frac{-\phi(\mathbf{m})}{2}\right\}. \tag{2}$$

$\mathbf{C}$ is the co-variance matrix of the data vector (since the error in a RF is strongly correlated, *Di Bona* (1998)) and $\phi(\mathbf{m})$ is the misfit between the vector of observed data $\mathbf{d}_{obs}$ and forward estimation $g(\mathbf{m})$ from the model, expressed as the Mahalanobis distance: (*Mahalanobis*, 1936)

$$\phi(\mathbf{m}) = (g(\mathbf{m}) - \mathbf{d}_{obs})^T \mathbf{C}^{-1} (g(\mathbf{m}) - \mathbf{d}_{obs}) \tag{3}$$

The posterior density $p(\mathbf{m}|\mathbf{d}_{obs})$ cannot be directly computed, hence it is sampled iteratively. At each step, the current model is randomly perturbed (the Monte Carlo approach) to generate a candidate model that can be accepted or rejected. Thus, the resulting chain of models (the Markov Chain), if sufficiently long, will provide a reliable estimation of the posterior density. The Metropolis-Hasting criterion (*Metropolis et al.*, 1953; *Hastings*, 1970) is used to decide on the retention of a candidate model for the i^{th} iteration favoring the proposed model if it leads to a decrease of the misfit with the observed data.

The perturbation of the current model occurs by randomly choosing among four options: change the velocity of a layer, change the thickness of a layer, add a layer and propose its velocity, remove a layer. For every option, the new velocity (and/or layer depth) is drawn from a Gaussian distribution centered on the current value. In Table 1 we show the (uniform) probability function used as prior for each of the variables we invert for and their allowed perturbation in terms of standard deviation. The possibility that the number of layers can indeed vary along the chain expresses the trans-dimensionality of the inversion algorithm.

With respect to *Bodin et al.* (2012), we employ the rj-MCMC algorithm strategy with some modifications, motivated by our specific needs and observations. *Bodin et al.* (2012) keep the ratio V_P/V_S fixed for decreasing the computational cost of the inversion. Following *Gao and Lekić* (2018), we decide to leave V_P/V_S as a variable that can be randomly perturbed along the chain. As a matter of fact, both laboratory experiments (*Ohno et al.*, 2006; *Peng and Redfern*, 2013) and thermodynamic modeling (*Diaferia and Cammarano*, 2017) suggest that V_P/V_S can strongly vary at crustal depth as result of the phase transition of quartz from its α- to β-form. Therefore, given the scope of this study, we find that fixing V_P/V_S at a (arbitrary) value will hamper a correct interpretation.

The algorithm in *Bodin et al.* (2012) is hierarchical, meaning that data error of both RFs and dispersion curves is itself unknown and estimated by the inversion procedure. It is not the case for our algorithm: this allows us to decrease the computational demand. The decision relies on the good estimates of data variance for both the RFs and dispersion curves. The average standard deviation on the RFs waveform is 0.010, that is $\sim$10% of first arrival with the lowest amplitude and $\sim$3% with respect to the highest one. The uncertainty on the phase velocity of dispersion curves is estimated to

$\sim$0.03 km/s (Molinari - personal communication).

For a proper sampling of the posterior density function for a given location, tens (or hundreds) of independent chains are run simultaneously, in parallel on a large multi-core computer cluster. In our case, we have a dataset of more than 50 RFs and dispersion curves, which require a prohibitive computational cost if we want to follow the procedure of *Bodin et al.* (2012), where the joint-inversion is carried out for only one location. For this study, we looked for an optimal trade-off between a satisfactory sampling of the posterior density and the required computational cost by means of a series of tests for a sample station.

First, we modify the approach proposed in *Bodin et al.* (2012) so that models that are implausible (i.e. the shallowest layer faster and/or denser than the deepest) are rejected before computing their forward response. Thus, only models that are geologically meaningful are actually compared against the data, improving the convergence of the inversion. Second, through dedicated tests, we find the values of the perturbation that maximize the efficiency of the algorithm (shown in Table 1). Smaller perturbations would require many iterations for convergence, whereas large perturbations inhibit the converge itself (the algorithm reaches and leaves the high-likelihood region of the model space). The amount of perturbation allowed on the different model parameters are realistic and comparable to the uncertainties over the measurements and result in an overall model acceptance rate around 33%. For each location, we run ten independent chains, with 500,000 iterations each, on the DT2 supercomputer from the University of Maryland. For the first 90.000 iterations, models are not retained for the posterior ("burn-in phase"). Along the remaining iterations, the misfit stabilizes at a sufficiently low plateau, implying that the high-likelihood region of the model space is reached. The inversion converges with these settings because the results were substantially similar to those obtained in a test with more (30) and longer chains(1.5e6 iterations). Adding more and longer chains does not result in a significant gain in terms of sampling of the posterior density.

	Prior (uniform probability)	**Perturbation** (st. dev.)
$\mathbf{V_S}$ (km/s)	1.5 - 4.7	0.12
$\mathbf{V_P/V_S}$	1.6 - 2.1	0.10
density (g/cm^3)	2.4 - 3.1	0.003
layer depth (km)	-	0.6

Table 1: Prior density distribution and standard deviation of the perturbation allowed in each iteration of the rj-MCMC inversion algorithm

2.4 Thermodynamics

We use thermodynamic modeling to predict the absolute temperatures at depth from seismic velocities. We employ the code `Perple_X` (*Connoly*, 2009), an algorithm that is based on Gibbs Free energy minimization for the calculation of i) the stable mineral association at any P-T, given a certain chemical composition, ii) the density and seismic velocities of the resulting mineralogical aggregate. We assume the model of *Rudnick and Gao* (2003) as crustal composition, parametrized in upper, middle and lower continental crust. Originally, the crustal composition from *Rudnick and Gao* (2003) is provided as dry. We add 1% of H_2O, thus allowing the modeling of hydrated mineralogical phases (e.g. amphibole) for a more realistic representation of the actual crust. The assessment of the main parameters, i.e. water and composition in addition to temperature and pressure, has been carried out by *Guerri et al.* (2015) and *Diaferia and Cammarano* (2017).

We correct the observed V_S to account for porosity. In doing this, we increase the seismic velocities as if the rock was a pore-free mineralogical aggregate, that is the approximation made in thermodynamic modeling. Porosity as a function of depth is estimated with the empirical, quadratic formula in *Vitovtova et al.* (2014):

$$log\phi = -0.65 - 0.16h + 0.0019h^2 \tag{4}$$

where ϕ is the porosity and h the depth in km. Known the porosity at depth, we compensate the effect of porosity on the shear wave velocities using the empirical relation $V_{Scorr} = V_S + 7.07\phi$ in *Castagna et al.* (1985). After such correction, the observed velocities can be matched to those modeled through thermodynamics for temperature inferences.

3 Results

In order to estimate the crustal temperature from our seismic observations, we need to accurately characterize the shear wave velocities and V_P/V_S ratio of the subsurface. Therefore, it is important to first analyze the performance of the Bayesian inversion in fitting the observed data. The misfit between observed data and forward response of the inverted model is not homogeneous across locations. In several cases, it is rather difficult to retrieve a subsurface model that reconciles sufficiently well both receiver functions and surface-wave dispersion. In the discussion, we provide a possible explanation for these observations.

In order to compare the ability to fit the different datasets, we normalize the misfit of RFs, SWD and their sum with respect to the highest misfit recorded. Results are shown in Figure 1. The RFs

fit (Figure1, left panel) is particularly good in the south-eastern part of the peninsula (see station MRVN in Figure 1) and in specific locations of the eastern and western Apennines. In the rest of the Peninsula, the RFs are very complex and more difficult to fit. The SWD data misfit is generally very low for all stations. However, looking at the normalized misfit (Figure 1, right panel), it emerges that the area in the Northern Apennines has the worse fit, especially at longer periods (e.g., see the small panel for the station PARC in Figure 1). Interestingly, this is the area where also the RFs fit is rather poor. *Qashqai et al.* (2018) have pointed out similar difficulties in jointly fitting dispersion curves and RFs for certain locations in the Central-Western United States where,supposedly, major structural complexities are expected.

We use the normalized sum of the RFs and SWD misfit as a guide for the evaluation of the performance of the joint-inversion across locations (Figure 1, right panel). We select 19 locations having normalized misfit <0.3 where, therefore, the models are able to reconcile both RFs and SWD. We argue that the interpretation of the obtained inverted models in these stations can lead to a more reliable interpretation of the complex variability of seismic velocities within the crust.

The inverted V_S for all the 19 stations shows a bi-modal distribution with distinct peaks at 3.3 and 4.3 km/s (see Figure 2, left panel), reflecting the sensitivity of the data to both crustal and mantle depths. The V_P/V_S ratios show a more uni-modal pattern with its peak of 1.76 (Figure 2, right panel), though higher values between 1.85 - 1.95 are also frequent. The posterior probability density function of V_S indicates the presence of three to five major layers in most of the locations. The increase of V_S

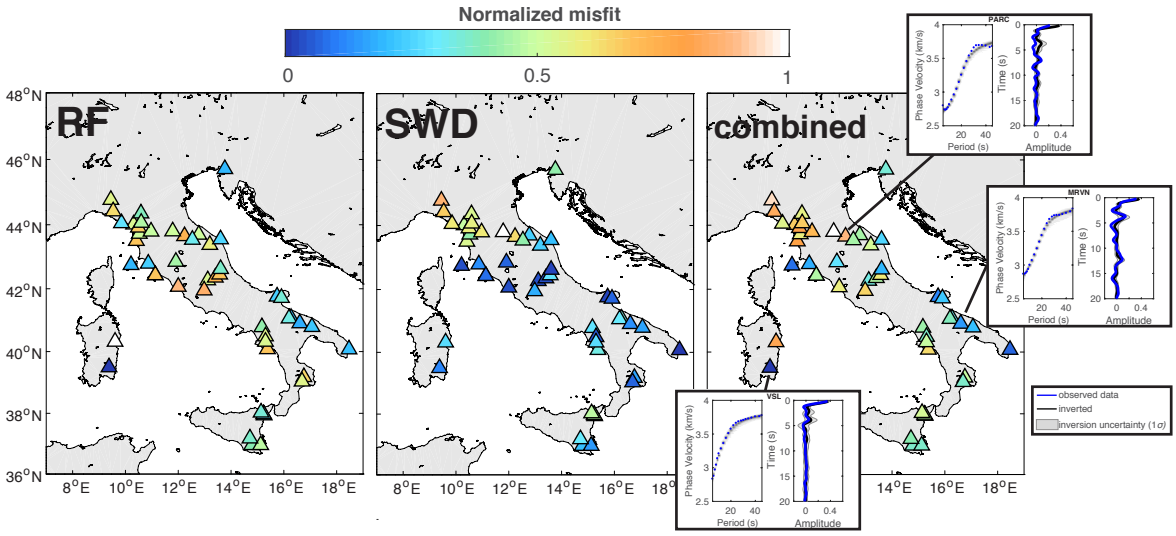

Figure 1: Misfit between the observed data and forward response of the mean model after inversion, for receiver functions (left), surface waves dispersion curves (centre) and combination of both (left). The normalization is carried out with respect to the location with the maximum misfit. The RFs in the central and northern part of the Apennines are systematically more difficult to fit than in the rest of the peninsula. Here, also the misfit with the dispersion curves is higher (especially at longer periods), though generally good for the whole dataset. Considering the combined misfit of both RF and SWD, we decide to retain the first best 20 locations (normalized misfit < 0.3) to allow a reliable interpretation of the subsurface model.

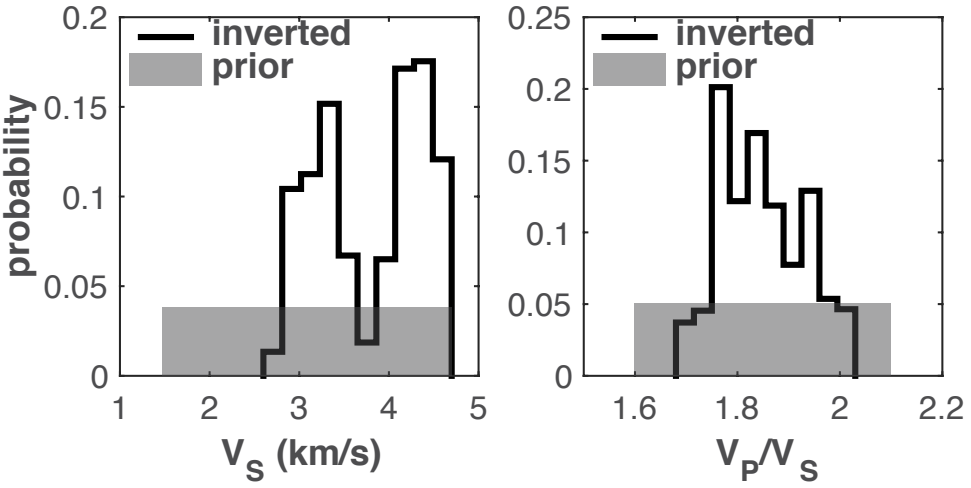

Figure 2: Histograms of the V_S and V_P/V_S retrieved after rj-MCMC inversion of surface waves data and receiver functions. The shaded areas are the uniform prior distributions for the two variables (see Table 1)

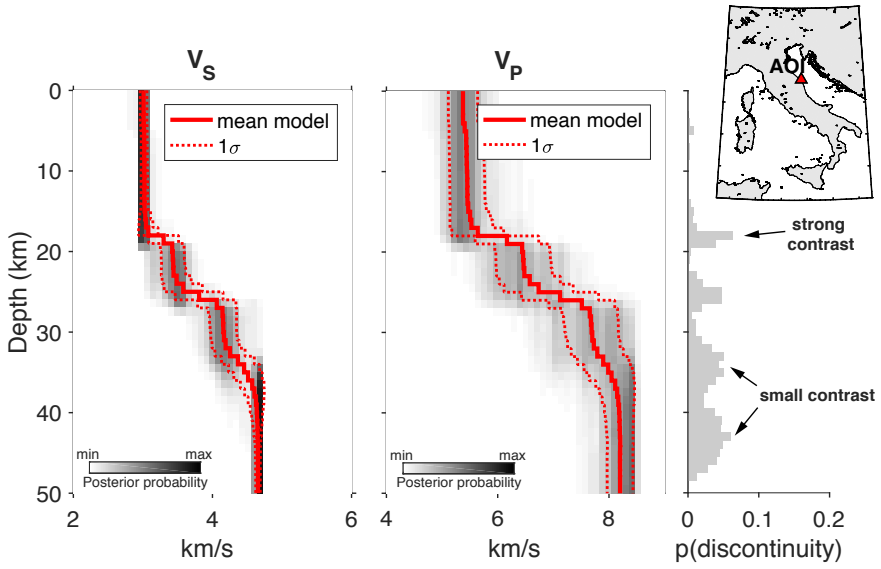

Figure 3: Station AOI, western Apennines. Ensemble solution in terms of posterior probability density function for V_S, V_P (with 1σ uncertainty) and discontinuity, as a function of depth. The velocity jump at 19 km is well constrained as confirmed by the sharp increase in probability of an interface. On the contrary, the deeper jumps in velocity are more gradual and their depths show higher uncertainty, confirmed by the smearing of the discontinuity probability over a large depth interval.

at the Moho is not always sharp but often gradual on a 3-5 km depth range.

An example of the inversion outcome is shown in Figure 3 for the station AOI, situated in the eastern Apennines. The panels on the left-hand side and in the center represent the posterior probabilities for V_S and V_P, respectively. The solid line indicates the mean model of the ensemble solution and the dashed line is its uncertainty in terms of units of σ. On the right, the panel shows p(discontinuity), the posterior probability of having an interface. The jump in V_S and V_P at 19 km and the narrow peak in the discontinuity probability suggests a sharp interface that is well constrained by the data. Around 27 km depth V_S reaches typical mantle velocities. Here the smeared p(discontinuity) over the

5 km suggest a transitional Moho rather than a sharp interface.Other probable discontinuities, albeit with a weak impedance contrast, occur deeper, around 35 and 45 km depth.

For the best 19 stations, we plot all the inverted values of V_P/V_S against V_S and their depth (Figure 4). Three main regions can be easily recognized and they roughly correspond to the shallow crust, middle and lower crust and mantle domains. To better image these regions, we use k-means cluster analysis for setting their boundaries and centroids (respectively the dashed lines and crosses in Figure 5). The shallow crust shows the higher variability for V_P/V_S, having values from 1.68 and (rarely) as high as 1.95-2. Considering their centroids, shallow crust and mantle have similar mean values of V_P/V_S, around 1.8. Interestingly, the mean V_P/V_S for the mantle is in perfect agreement with the global averages at these depths from the PREM (*Dziewonski and Anderson*, 1981) and IASPEI91 (*Kennett*, 1991) models.

The rest of the crust shows a rather distinct behavior. V_P/V_S shows here remarkably higher values, bounded in the 1.85-2.05 range (Figure 4). Such high values are clearly anomalous compared to expectations. For example, as a comparison, we plot the V_P/V_S and V_S as in EPcrust (from *Molinari and Morelli* (2011)). In this model of the European crust, velocities at depth are mainly retrieved from P-wave tomography and then converted to V_S by 4^{th}-degree polynomial fit proposed by *Brocher* (2005). The poor misfit between our results and those obtained in (*Molinari and Morelli*, 2011) is indicative of the geological heterogeneity of the subsurface, which translates into complex and non-linear

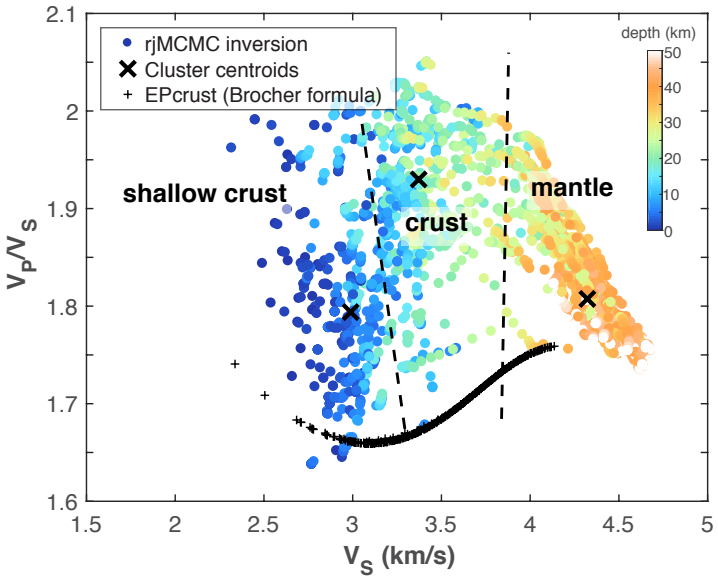

Figure 4: V_P/V_S against V_S at depth (see color-scale) after inversion for all the locations. Three main regions are easily recognized, as also identified by cluster analysis (crosses are the cluster centroids, dashed lines indicates the clusters boundaries). The shallow crust shows high variability of V_P/V_S ratio, with an average value that is comparable to that at mantle depth. The rest of the crust shows systematically higher values of V_P/V_S, in the range 1.9-2. For the sake of comparison, the V_P/V_S and V_S from EPcrust are reported: they follow the 4th degree polynomial formula from *Brocher* (2005) used in EPcrust (*Molinari and Morelli*, 2011) to convert V_P to V_S

relationships between geophysical variables (here V_P/V_S ratio and V_S). The amount of complexity is well imaged by the dispersion of our data, see Figure 4, and it results from the integration of different geophysical methods, but cannot be retrieved if an empirical formula is used.

The use of RFs allows to better constrain the depth of sharp velocity transitions. We explore the characteristics of the observed seismic discontinuities in terms of change in V_S and V_P/V_S (Figure 5). On the left panel, we show the depth of the major discontinuities and the V_S underneath. The color scale is according to the "discontinuity factor", a quantity that we introduce to measure the strength and the uncertainty of the interface in our posterior solution. It is the product of the of p(discontinuity) and the corresponding V_S jump in a depth interval of 2 km around the interface. Thus, a gradual and/or poorly constrained interface scores a low "discontinuity factor". The interfaces between 10 and 30 km depth with $V_S < 3.8$ km/s show the highest discontinuity factor, suggesting strong and well constrained seismic interfaces within the crust. Contrarily, low values of discontinuity factor are found at shallow depth, at and below the Moho indicating less abrupt changes in seismic velocity. In Figure 5, right panel, the detected discontinuities are shown according to their V_P/V_S. The velocity jumps within the crust are systematically associated to high V_P/V_S (up to 2), whereas those referred to the mantle and the shallow crust have values around 1.8.

Our data suggests that the Italian crust has rather distinct seismic properties that we can exploit for its characterization. In particular, we select all the locations where such discontinuities are the strongest and well imaged i) at a depth of at least 10 km, ii) with V_S smaller than 3.8 km and iii) V_P/V_S greater than 1.8. For nine stations over 19, we find a crustal interface that satisfies these criteria. We assume these seismic discontinuities as caused by the transition of quartz from the α to β phase. We discuss this further in section 4.3.

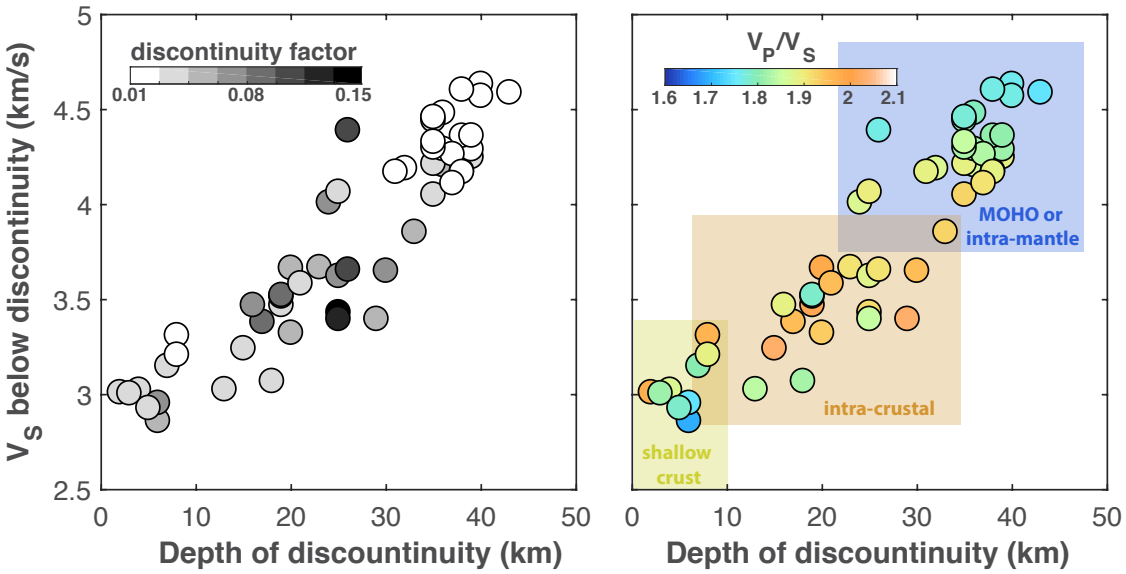

Figure 5: Left: The V_S underneath a discontinuity are reported as a function of the depth of the seismic interface for all inverted location. The 'discontinuity factor' is the product of the discontinuity probability (see Figure 3, left panel) and the velocity jump in a depth interval of 2 km around the interface. Therefore, the discontinuity factor is a measure of the strength of the velocity jump and its constraint by data inversion. The discontinuities at intra-crustal depths (10-30 km) are well constrained, as opposed to those of the mantle and shallow crust. In both cases the velocity jump is lower and/or its depth is more uncertain. The seismic interfaces at intra-crustal depth shows also the higher V_P/V_S (see right panel). These are possibly indicative of the phase transition of quartz and used for the estimation of the geothermal gradient

4 Discussion

Seismic constraints are necessary to infer subsurface temperatures. Our combination of receiver functions and dispersion curves of Rayleigh waves in a Bayesian inversion framework provides information on V_S structure, V_P/V_S ratio and the possibility of having intra-crustal discontinuities within the crust. This information, jointly used with an accurate relationship between temperature and seismic velocities, which do account for mineralogical phase transitions as well, is able, in principle, to get a new insight on the thermal structure of the Italian crust.

Our approach potentially allows an even coverage of the studied region, as opposed to temperature estimates from classical heat flow measurements that are spatially limited, often uncertain and unreliable especially in geologically active areas.

4.1 Data integration: pros and cons

Our attempt to integrate two seismological datasets has lead to important observations on both the potential and drawbacks of such an approach. For about half of our locations, the Bayesian inversion method provided a model of the subsurface that fits well both the RFs and SWD data. Considering

all the stations, the normalization of the total misfit reveals a clear spatial pattern in the data fit (see Figure 1). For SWD data alone (Figure 1, center), our models show an overall good concordance with observed data at all stations. Stations in the Northern Apennines (NA) represent the only exception due to their relatively higher misfit, especially in the 30-40 s period range. Here, also the combined misfit with RFs is among the highest, suggesting that our inversion algorithm did not provide a model that reconciles both the RF and SWD data sufficiently well. We speculate that the reason can be found in the complexity of the geological and tectonic setting of this area, at the transition between the Apenninic and Alpine orogen (*Vignaroli et al.*, 2014). The NA represent the active front of the NW-SE trending fold-and-thrust where the compressive seismicity suggests the ongoing, steep, subduction of the Adriatic slab. Particularly, the retrieval of RFs from converted P-to-S waves is based on the assumption that model interfaces are flat, and this assumption might fail in this environment. Anisotropy is another element that may affect both the observed Rayleigh wave phase velocities and RFs but is not accounted for. For this area, the harmonic decomposition of the transverse component of RFs over the entire azimuthal range (*Bianchi et al.*, 2010) revealed a NE-SW trending symmetry axis. Moreover, *Plomerova et al.* (2006) pointed out a complex anisotropy pattern from SKS splitting that can affect the arrival used to calculate RF waveforms. In conclusion, the thick and tectonized accretionary prism in the North Apenninic front and the anisotropic crust and mantle underneath may hinder the retrieval of a satisfactory model from RFs (that encode only the 1-D isotropic approximation of the actual structure at depth) and jointly fitting a complementary observable, SWD in this case.

The thick sedimentary layer of the Po Plain that overlays the North Apenninic thrust represents another element of complexity. Arrivals recorded at the edge of such sedimentary basin (that is the case for our stations in the NA) can be contaminated by reverberations that mask the P-to-S conversions at the Moho and intra-crustal discontinuities. More specifically, the reverberations would have different amplitude depending on the direction of the seismic wave arrival, due to the abrupt change in thickness of the sedimentary pile at the basin edge (*Yu et al.*, 2015). Only the use of ad-hoc resonance filter prior the stacking of RFs over the azimuthal range may mitigate the effect of such reverberation. We learn from such findings and our study that, while data integration must be encouraged (as experiments on synthetics are often promising), the inherent complexities of the subsurface limit our capability to image them. This conclusion has also been drawn by *Eilon et al.* (2018) and *Qashqai et al.* (2018) when attempting to combine different dataset in complex areas.

If the integration of RFs and SWD has been particularly challenging in specific, geologically complex areas in the Italian peninsula, several locations are clearly on the other side of the spectrum. In fact, our Bayesian approach performed particularly well in the Apulian platform as well as in several

coastal areas in the western and eastern side of the Apenninic orogen. Here, our successful integration of such different but complementary datasets might be the consequence of a simpler geological setting. For example, all stations located in the Apulian platform (in the south est of the Italian peninsula) score the lowest misfit. As a matter of fact, this area is a geologically stable, undeformed foreland consisting of a thick, horizontally layered carbonate succession from the Meso-Cenozoic (*Mariotti and Doglioni*, 2000). In literature, there are no indications of seismic anisostropy that might complicate seismic wave propagation and the low angle/horizontal layering of the carbonate succession as well as the rather regular Moho represent an ideal case for the retrieval and use of RFs.

4.2 V_P/V_S ratio within the crust

For our interpretation, we select 19 stations where the low total misfit indicates a good agreement with both the RFs and SWD. While the mean values of V_P/V_S and V_S for the mantle are in agreement with those of global models, the crust appears rather peculiar and heterogeneous, with well distinct seismic domains. We speculate that varying mineralogical assemblages can be the reason of such distinct seismic patterns. The low V_P/V_S we observe in the shallow crust can be indicative of higher quartz content (*Birch*, 1966; *Christensen*, 1982), a scenario that fits with a chemical stratification of the crust. Higher V_P/V_S at deeper depth is coherent with less abundant quartz but more plagioclase *Kern and Schenk* (1991). However, the anomalous high values we observe within the crust must invoke a further mechanism. In *Wang et al.* (2014) numerical modeling and laboratory experiments on granite specimen suggest that high V_P/V_S (>1.9) can be reached at seismic frequencies if the rock has saturated, randomly oriented, elongated cracks. High crack density, reaching 0.2-0.3, can explain even higher values of V_P/V_S (>2). To sustain crack openings at middle-lower crustal depths, a high pore-pressure is necessary, thus suggesting an important role of fluids within the Italian crust. This would be a scenario supported by our seismic evidence and deep magnetotellurics sounding at both global and local scale. *Simpson* (1999)(and references therein) reports several examples of low resistivities (10-20 Ωm) in the middle and lower crust, implying the presence of fluids in an otherwise highly resistive medium. In Italy, *Patella et al.* (2005) observed highly conductive bodies (<10 Ωm) at depth >15 km in the Southern Apennines. Here, both the high flux in CO_2 and the abundant mantle ^{3}He are consistent with the hypothesis of a pervasive presence of fluid, possibly fed by mantle sources (*Italiano et al.*, 2000). Interestingly, *Becken et al.* (2008) and *Ogawa et al.* (2001) have observed that seismicity clusters at the transition between highly saturated geological bodies and less permeable ones, indicating a direct involvement of fluid migration in the nucleation of earthquakes. We discard the hypothesis of high V_P/V_S caused by partial melts in middle and lower portions of the crust. In fact, we do not usually observe any major decrease in V_S as an indication of shear softening due to

partial melting.

4.3 Temperature at depth

We have observed that the seismic discontinuities comprised between 10 km and the Moho are the sharpest that we observe in the region of interest, and are well constrained by our inversion. Moreover, these are associated with high V_P/V_S ratio. Both laboratory experiments on single mineral and rock aggregates(*Shen et al.*, 1993; *Peng and Redfern*, 2013) and thermodynamic modeling (*Diaferia and Cammarano*, 2017) suggest that the $\alpha - \beta$ quartz transition is the major, seismically relevant phase change that can occur within the crust. The transition temperature is $T_q = 575°C$ at ambient pressure and varies with a gradient of 0.0256°C/bar (for example T_q = 702°C at 20 km and 777°C at 30 km), according to the laboratory experiments of *Shen et al.* (1993). Since quartz is stiffer in its β-form, the transition is seismically marked by an increase in V_P/V_S (>1.8 in a porous-free rock aggregate, *Diaferia and Cammarano* (2017)) and in both V_P and V_S. For nine locations, the strongest seismic discontinuity that we observe at crustal depth can be reasonably associated with the quartz transition. Knowing the transition temperature, we calculate the geothermal gradient at these locations, see Figure 6 (y-axis). The width of the posterior p(discontinuity) at the discontinuity is used to evaluate the uncertainty on the gradient estimation. Since each peak of p(discontinuity) has an approximate Gaussian shape, we take the standard deviation of the best fitting Gaussian distribution as a measure of the uncertainty on the depth of the interpreted quartz transition. Here the rather sharp posteriors translate in small errors in the estimation of geothermal gradient in most of the locations (σ <1°C/km). Interestingly, we derive high thermal gradients, between 30 and 40°C/km, for stations located within the Tuscan magmatic province. Here, an "orogenic" magmatism took place in the last 8.5 Ma, related to the westward subduction of the Adriatic plate and formation of the Apenninic orogen (*Peccerillo and Frezzotti*, 2015). The chemical signatures of both intrusive and extrusive magmatic products indicate heterogeneous mantle sources with the contamination of crustal melts and fractional crystallization within the crust. Currently, the substantial geothermal activity and the high heat flow (>100 mW/m^2, *Della Vedova et al.* (2001)) suggest a pervasive partial melt at crustal depth as residual phase of the past magmatism.

A high geothermal gradient (34°C/km) is also observed at the station MMME. Interestingly, this station is located 25 km NE of Mt. Etna, a currently active strato-volcano in the contest of the Sicilian magmatic province. The so-called European Asthenospheric Reservoir (EAR, *Lustrino and Wilson* (2007)) is believed to be the deep mantle source (>400 km) causing a typical "anorogenic" magmatism (*Peccerillo and Frezzotti*, 2015) that is poorly affected by the nearby subduction of the Ionian slab. Such deep source is compatible with the heat flow at surface 50-60 mW/m^2, *Della Vedova*

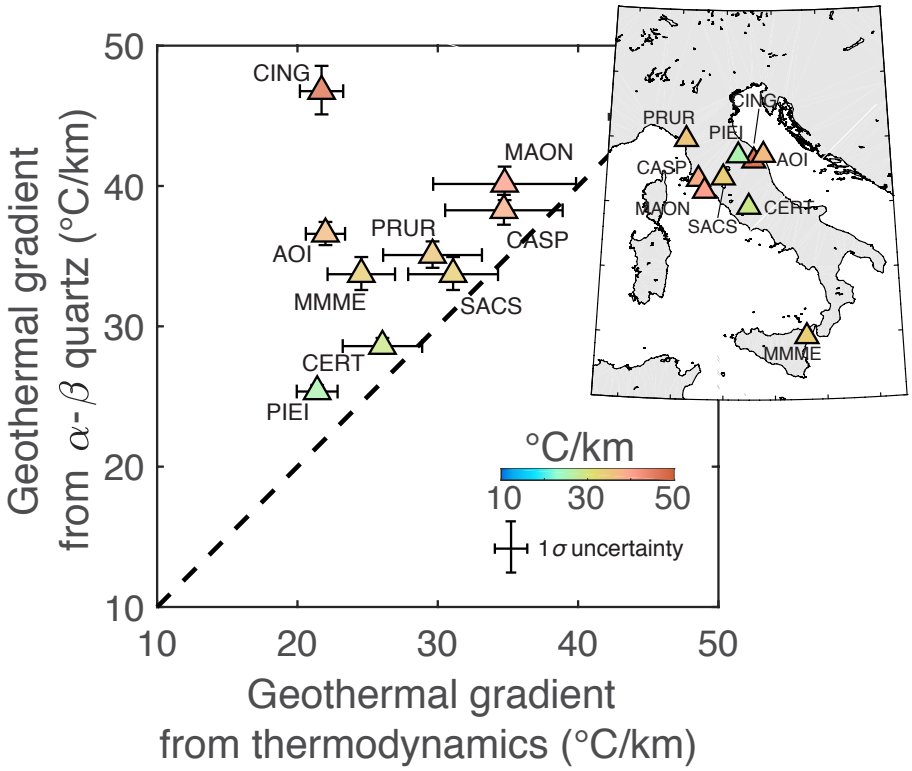

Figure 6: Assuming that discontinuities at 9 locations are caused by the transition of quartz, known their depth and the temperature of transition at such depth, the geothermal gradient is estimated (y-axis). Such values are compared against those obtained with an alternative method based on thermodynamic modeling (x-axis): shear wave velocities in the lower crust are translated into temperatures assuming a wet (1 wt%) chemical composition from Rudnick and Gao (2003) and fitted with a robust, weighted linear model. Except for the stations CING and AOI, the two approaches provide similar, highly correlated values.

et al. (2001)), as compared to the Tuscan magmatic province.

At stations PIEI and CERT we find the lowest values of geothermal gradient, 25 and 29°C/km respectively. PIEI is located on the Apennines orogen where the high crustal thickness (35-38 km, *Piana Agostinetti and Amato* (2009)) is compatible with the low geothermal gradient we calculate. CERT is in the Roman magmatic province, characterized by rare and explosive volcanic activity in the past 1 Ma and a current, diffuse CO_2 degassing. This is the results of the reaction of carbonate-contaminated, poorly mobile partial melts in the upper mantle that rarely reach the shallow subsurface(*Frezzotti et al.*, 2010; *Chiodini et al.*, 2013), as confirmed by the moderate heat flow (*Della Vedova et al.*, 2001). For the stations CING and AOI we calculate very high geothermal gradients. Considering AOI as an example (Figure 3), the cause of the seismic discontinuity at 20 km is probably other than the assumed quartz transition (e.g. a strong lithological change). In fact, both AOI and the nearby CING are located in the front of the strongly tectonized, Apenninic wedge where the seismic signature of the quartz transition might be obliterated by the likely strong lithological heterogeneity occurring at depth.

The reliability of our approach based on the $\alpha - \beta$ as geo-thermometer is tested through a comparison

with an alternative method. We take the V_S model of *Molinari et al.* (2015) for the lower crust, correct for the porosity contribution and estimate temperatures at depth through thermodynamic modeling, assuming a hydrous chemical composition from *Rudnick and Gao* (2003). Figure 6 (x-axis) indicates the geothermal gradients obtained by a robust, weighted linear fit of the lower crustal temperature. The error on the gradient estimation is evaluated considering the 68.3% (1σ) confidence interval of the angular coefficient (i.e. the geothermal gradient) of the best fitting line. Though the higher uncertainty on the estimation made through thermodynamics, the similarity between the two independent methods is remarkable, as indicated by the vicinity of the estimated geothermal gradients to the line of perfect resemblance. Interestingly, with thermodynamics we find gradients at stations CING and AOI that now closely resemble the value at the nearby PIEI, as one would expect, as opposed to the case when the quartz transition is used. This result strengthens the hypothesis that at stations CING and AOI the $\alpha - \beta$ transition has led to wrong temperature estimation.

The two alternative methods provide highly correlated results (r=0.98, if CING and AOI are excluded). However, estimates from the $\alpha - \beta$ transition are systematically higher of 3-5°C/km compared to thermodynamics, translating in 90-150°C temperature difference at 30 km depth. However, deciding which approach is superior in terms of reliability is challenging. The discrepancy we observe can be alternatively interpreted as an overestimation of temperature if the $\alpha - \beta$ transition is used, or an underestimation by thermodynamics. Both methods rely on seismic observables but are based on different, peculiar assumptions. Thus, their performance can differ depending on the area of study and the validity of such assumptions. The detection of the $\alpha - \beta$ transition requires profiles of V_S and V_P/V_S with sufficient high-resolution. The transition of quartz is only temperature dependent and implies the assumption of sufficient modal quartz in the bulk rock. In *Diaferia and Cammarano* (2017) we demonstrated that a quartz content below <20% vol is already sufficient to produce an appreciable increase in V_P/V_S at the transition, suggesting that especially within the upper and middle crust the detection of the quartz transition might be seismically relevant. However, caution is necessary in geologically complex areas with expected structural and lithological heterogeneity that can undermine the reliability of RFs (from which V_P/V_S are derived) due to the presence of dipping interfaces and anisotropies. Moreover, a strong lithological change at depth can be misinterpreted as the quartz transition, leading to erroneous estimation of temperature gradients. Concerning the use of thermodynamics, we assume a unique crustal composition for the lower crust, whilst its actual composition and water content can be spatially heterogeneous. However, the assumption of a rather uniform lower crust is reasonable for the sake of temperature inference, as suggested by the fact that the geothermal gradients we obtain for the Italian magmatic provinces and at the front of the Apenninic orogen are plausible and in agreement with the known geological setting.

Either based on thermodynamics or on the quartz transition, we believe that the use of seismic velocities is a viable alternative to the thermal characterization of the crust through heat flow measurements. Heat flow is obtained through temperature measurements in geothermal and exploration boreholes during the drilling process, mostly assuming the thermal conductivity of the drilled rock (*Stein*, 1995). This method suffers from a series of critical issues: i) boreholes are scarce and represent punctual information with a limited spatial representativeness, ii) the majority of boreholes do not exceed a few hundred meter depths, where rocks might still record the seasonal and secular fluctuations of temperature at surface, undermining the reliability of the temperature measures, iii) mud circulation during the drilling process obliterates the geothermal profile, requiring a certain time for it to be restored. Temperature is extrapolated beyond the borehole depth applying a steady-state heat conduction equation (*Chapman*, 1986). This approach, diffusely used in literature neglects other mechanisms of heat transport, such as advection, that might be relevant especially in the upper crust. Here the local geothermal gradient can be increased by hot fluid up-welling or flattened by meteoric percolation. As a consequence, in active areas with relevant geothermal potential (e.g. Tuscan province), the extrapolated temperature within the crust would be too high if heat flow and conduction equation are used. On the other hand, areas affected by fluid down-welling, favored by the local lithological and topographic setting, would result in a relevant underestimation of the geothermal gradients and temperature at depths. Other sources of uncertainty arise from the required assumptions on the heat produced by radioactive isotopes and the thermal conductivity of crustal rocks.

Our method exploits the abundance of seismic data and their large coverage to assess temperature distribution at depth. Temperature is a major parameter in seismically active regions where it controls the brittle-to-ductile transition (BDT, *Rutter* (1986)), which marks the transition from an elastic behavior (prone to cause earthquakes) to the plastic one. Locating the depth of the BDT is vital to estimate the crustal volumes involved in co-seismic slip, allowing the evaluation of the maximum expected earthquake magnitude in a certain area (*Doglioni et al.*, 2011). A correct assessment of the BDT is also fundamental for understanding the mechanics of crustal deformation (*Kusznir and Park*, 1986), especially for what concerns fold-and-thrust belts (*Carminati and Siletto*, 1997).

5 Limitations

We have observed that the geological complexities and the intrinsic limitations of the employed inversion strategy strongly control the possibility of fitting, simultaneously, two distinct seismic datasets. For future research, it is worthwhile to assess whether accounting for seismic anisotropies and dipping interfaces can better reconcile different RFs and SWD in complex areas.

In order to recover crustal temperatures from our seismic model, we employ a number of assumptions. Regarding the quartz transition as current geo-thermometer, it must be used with caution because, though supported by laboratory experiments and thermodynamic modeling, the interpretation of a strong, intra-crustal discontinuity as the quartz transition is doubtful. It remains impossible to discern with certainty between this mineralogical transformation and changes in lithology or chemical composition. As a result, misinterpreting a lithological change as the quartz transition can lead to erroneous estimates of geothermal gradients.

Alternatively, the temperature can be calculated through thermodynamics. Our assumption regards the homogeneous, hydrated lower crust that might not be representative of the actual vertical and lateral variation in chemical composition. However, we recover geothermal gradients that are in agreement with the quartz geo-thermometer and that are plausible at locations where the latter failed.

6 Conclusions

The thermal characterization of the Italian crust is of key importance for a better understanding of its current geological setting and evolution. However, it is challenging due to the sparsity of heat flow data, their uncertainty and the strong underlying assumptions.

We attempted an alternative approach based on the combination of two distinct seismic datasets (RFs and SWD), jointly inverted in Bayesian framework to retrieve the V_S and V_P/V_S at depth.

1. Geological complexities have hampered the recovery of a satisfactory subsurface model that fits both RFs and SWD data. Conversely, in stable or less tectonized areas the integration of these data has been successful.

2. The middle and lower crust exhibit high values of V_P/V_S ratio that we interpret as the evidence of pervasive fluid-filled cracks. This supports the observed low-resistivities in deep magnetotellurics soundings both, at global and local scales.

3. Our inversion has imaged strong and well constrained intra-crustal discontinuities. These are used for the detection of the transition from α to β quartz and calculation of the local geothermal gradients. These are in agreement with the known geological contest and comparable to the gradients obtained through thermodynamics.

4. Despite the different assumptions and approximations required by each of the approaches for temperature estimation, these provide comparable results. This demonstrates that the use of seismic data to obtain crustal temperature is a viable alternative to heat flow measurements and

steady-state conduction equation that are affected by limited applicability, data scarcity and high uncertainty.

Bibliography

Mr. Bayes, & Price, M. (1763). An essay towards solving a problem in the doctrine of chances. by the late rev. mr. bayes, frs communicated by mr. price, in a letter to john canton, amfrs.*Philosophical Transactions (1683-1775)*, 370-418.

Becken, M., Ritter, O., Park, S. K., Bedrosian, P. A., Weckmann, U., & Weber, M. (2008). A deep crustal fluid channel into the San Andreas Fault system near Parkfield, California. *Geophysical Journal International, 173*(2), 718-732.

Bianchi, I., Park, J., Piana Agostinetti, N., & Levin, V. (2010). Mapping seismic anisotropy using harmonic decomposition of receiver functions: An application to Northern Apennines, Italy. *Journal of Geophysical Research: Solid Earth, 115*(B12).

Birch, F. (1966). Compressibility; elastic constants. *Handbook of physical constants*, 97-173.

Bodin, T., Sambridge, M., Tkalcic, H., Arroucau, P., Gallagher, K., & Rawlinson, N. (2012). Transdimensional inversion of receiver functions and surface wave dispersion. *Journal of Geophysical Research: Solid Earth, 117*(B2).

Bodin, T., & Sambridge, M. (2009). Seismic tomography with the reversible jump algorithm. *Geophysical Journal International, 178*(3), 1411-1436.

Brocher, T. M. (2005). Empirical relations between elastic wavespeeds and density in the Earth's crust. *Bulletin of the seismological Society of America, 95*(6), 2081-2092.

Brückl, E., Bleibinhaus, F., Gosar, A., Grad, M., Guterch, A., HrubcovÃ¡, P., & Yliniemi, J. (2007). Crustal structure due to collisional and escape tectonics in the Eastern Alps region based on profiles Alp01 and Alp02 from the ALP 2002 seismic experiment. *Journal of Geophysical Research: Solid Earth, 112*(B6).

Carminati, E., & Siletto, G. B. (1997). The effects of brittle-plastic transitions in basement-involved foreland belts: the Central Southern Alps case (N Italy). *Tectonophysics, 280*(1-2), 107-123.

Castagna, J. P., Batzle, M. L., & Eastwood, R. L. (1985). Relationships between compressional-wave and shear-wave velocities in clastic silicate rocks *Geophysics, 50*(4), 571-581.

Chapman, D. S. (1986). Thermal gradients in the continental crust. *Geological Society, London, Special Publications, 24*(1), 63-70.

Chiarabba, C., and A. Amato (1996), Crustal velocity structure of the Apennines (Italy) from P-wave travel time tomography, *Ann. Geophys.,XXXIX*(6), 1133-1148.

Chiodini, G., Cardellini, C., Caliro, S., Chiarabba, C., & Frondini, F. (2013). Advective heat transport associated with regional Earth degassing in central Apennine (Italy).*Earth and Planetary Science Letters, 373*, 65-74.

Christensen, N. I. (1982). Seismic velocities. *Handbook of physical properties of rocks*, 1-228.

Connolly, J. A. D. (2009). The geodynamic equation of state: what and how. *Geochemistry, Geophysics, Geosystems, 10*(10).

Della Vedova, B., Bellani, S., Pellis, G., & Squarci, P. (2001). Deep temperatures and surface heat flow distribution. In *Anatomy of an orogen: the Apennines and adjacent Mediterranean basins* (pp. 65-76). Springer, Dordrecht.

Bona, M. (1998). Variance estimate in frequency-domain deconvolution for teleseismic receiver function computation. *Geophysical Journal International, 134*(2), 634-646.

Di Stefano, R., E. Kissling, C. Chiarabba, A. Amato, and D. Giardini (2009), Shallow subduction beneath Italy: Three-dimensional images of the Adriatic-European-Tyrrhenian lithosphere system based on high-quality P wave arrival times, *J. Geophys. Res., 114*, B05305, doi: 10.1029/2008JB005641.

Diaferia, G., & Cammarano, F. (2017). Seismic signature of the continental crust: What thermodynamics says. An example from the Italian peninsula. *Tectonics*, 36, 3192-3208. https://doi.org/10.1002/2016TC004405

Diehl, T., Husen, S., Kissling, E., & Deichmann, N. (2009). High-resolution 3-D P-wave model of the Alpine crust. *Geophysical Journal International, 179*(2), 1133-1147.

Doglioni, C., Barba, S., Carminati, E., & Riguzzi, F. (2011). Role of the brittle-ductile transition on fault activation. *Physics of the Earth and Planetary Interiors, 184*(3-4), 160-171.

Dziewonski, A. M., & Anderson, D. L. (1981). Preliminary reference Earth model. *Physics of the earth and planetary interiors, 25*(4), 297-356. https://doi.org/10.1016/0031-9201(81)90046-7

Eilon, Z., Fischer, K. M., & Dalton, C. A. (2018). An adaptive Bayesian inversion for upper-mantle structure using surface waves and scattered body waves. *Geophysical Journal International, 214*(1), 232-253.

Finetti, I. R. (2005). CROP project: Deep seismic exploration of the Central Mediterranean and Italy, *Atlases of Geoscience* (Vol. 1, 785 pp.). Amsterdam: Elsevier

Frezzotti, M.L., Peccerillo, A. & Panza, G. (2010). Earth's CO2 degassing in Italy. *Journal of the Virtual Explorer*, 36, paper 18, http://dx.doi.org/10.3809/jvir- tex.2010.00227.

Gao, C.,& Lekiċ, V. (2018). Consequences of parametrization choices in surface wave inversion: insights from transdimensional Bayesian methods. *Geophysical Journal International, 215*(2), 1037-1063.

Guerri, M., Cammarano, F., & Connolly, J. A. (2015). Effects of chemical composition, water and temperature on physical properties of continental crust. *Geochemistry, Geophysics, Geosystems, 16*(7), 2431-2449. https://doi.org/10.1002/2015GC005819

Gualtieri, L., P. Serretti, and A. Morelli (2014), Finite-difference p wave travel time seismic tomography of the crust and uppermost mantle in the Italian region, *Geochem. Geophys. Geosyst., 15*, 69-88, doi:10.1002/2013GC00498

Haskell, N. A. (1953). The dispersion of surface waves on multilayered media. *Bulletin of the seismological Society of America, 43*(1), 17-34.

Hastings, W. K. (1970). Monte Carlo sampling methods using Markov chains and their applications. *Biometrika, 57*(1), 97-109.

Italiano, F., Martelli, M., Martinelli, G., & Nuccio, P. M. (2000). Geochemical evidence of melt intrusions along lithospheric faults of the Southern Apennines, Italy: geodynamic and seismogenic implications. *Journal of Geophysical Research: Solid Earth, 105*(B6), 13569-13578.

Kästle, E. D., El-Sharkawy, A., Boschi, L., Meier, T., Rosenberg, C., Bellahsen, N., & Weidle, C. (2018). Surface Wave Tomography of the Alps Using Ambient-Noise and Earthquake Phase Velocity Measurements. *Journal of Geophysical Research: Solid Earth, 123*(2), 1770-1792.

Kennett, B. L. N. (1991). IASPEI 1991 seismological tables. *Terra Nova, 3*(2), 122-122.

Kern, H., & Schenk, V. (1988). A model of velocity structure beneath Calabria, southern Italy, based on laboratory data. Earth and Planetary Science Letters, 87(3), 325-337.

Kusznir, N. J., & Park, R. G. (1986). Continental lithosphere strength: the critical role of lower crustal deformation. *Geological Society, London, Special Publications, 24*, 79-93.

Lachenbruch, A. H., & Morgan, P. (1990). Continental extension, magmatism and elevation; formal relations and rules of thumb. *Tectonophysics, 174*(1-2), 39-62.

Lustrino, M., & Wilson, M. (2007). The circum-Mediterranean anorogenic Cenozoic igneous province. *Earth-Science Reviews, 81(1)*, 1-65.

Mahalanobis, P. C. (1936). On the generalized distance in statistics. National Institute of Science of India.

Malinverno, A. (2002). Parsimonious Bayesian Markov chain Monte Carlo inversion in a nonlinear geophysical problem. . *Geophysical Journal International, 151(3)*, 675-688.

Mariotti, G., & Doglioni, C. (2000). The dip of the foreland monocline in the Alps and Apennines. *Earth and Planetary Science Letters 181*(1-2), 191-202. https://doi.org/10.1016/S0012-821X(00)00192-8

Metropolis, N., Rosenbluth, A. W., Rosenbluth, M. N., Teller, A. H., & Teller, E. (1953). Equation of state calculations by fast computing machines. *The journal of chemical physics, 21*(6), 1087-1092.

Molinari, I., & Morelli, A. (2011). EPcrust: a reference crustal model for the European Plate. *Geophysical Journal International, 185*(1), 352-364.

Molinari, I., Verbeke, J., Boschi, L., Kissling, E., & Morelli, A. (2015). Italian and Alpine three-dimensional crustal structure imaged by ambient-noise surface-wave dispersion. *Geochemistry, Geophysics, Geosystems, 16*(12), 4405-4421.

Ogawa, Y., Mishina, M., Goto, T., Satoh, H., Oshiman, N., Kasaya, T., & Takahashi, Y. (2001). Magnetotelluric imaging of fluids in intraplate earthquake zones, NE Japan back arc. *Geophysical research letters, 28*(19), 3741-3744.

Ohno, I., Harada, K., & Yoshitomi, C. (2006). Temperature variation of elastic constants of quartz across the alpha-beta transition. *Physics and Chemistry of Minerals, 33*(1), 1-9.

Park, J., and V. Levin, 2016a, Anisotropic shear zones revealed by backa- zimuthal harmonics of teleseismic receiver functions: *Geophysical Journal International, 207*, 1216-1243, doi: 10.1093/gji/ggw323.

Patella, D., Petrillo, Z., Siniscalchi, A., Improta, L., & Di Fiore, B. (2005). Magnetotelluric profiling along the CROP-04 section in the Southern Apennines. *CROP PROJECT: Deep Seismic Exploration of the CENTRAL Mediterranean and Italy*, 263-280.

Peccerillo, A., & Frezzotti, M. L. (2015). Magmatism, mantle evolution and geodynamics at the converging plate margins of Italy. *Journal of the Geological Society, 172*(4), 407-427.

Peng, Z., & Redfern, S. A. (2013). Mechanical properties of quartz at the $\alpha - \beta$ phase transition: Implications for tectonic and seismic anomalies. *Geochemistry, Geophysics, Geosystems, 14*(1), 18-28.

Piana Agostinetti, N. P., & Malinverno, A. (2010). Receiver function inversion by trans-dimensional Monte Carlo sampling. *Geophysical Journal International, 181*(2), 858-872.

Piana Agostinetti, N. P., Lucente, F. P., Selvaggi, G., & Di Bona, M. (2002). Crustal structure and Moho geometry beneath the Northern Apennines (Italy). *Geophysical Research Letters, 29*(20), 60-1.

Piana Agostinetti, N., & Amato, A. (2009). Moho depth and Vp/Vs ratio in peninsular Italy from teleseismic receiver functions. *Journal of Geophysical Research: Solid Earth, 114*(B6).

Piana Agostinetti, N., & Malinverno, A. (2018). Assessing uncertainties in high-resolution, multifrequency receiver-function inversion: A comparison with borehole data. *Geophysics, 83*(3), KS11-KS22.

Piromallo, C., & Morelli, A. (2003). P wave tomography of the mantle under the Alpine-Mediterranean area. Journal of Geophysical Research: Solid Earth, 108(B2). doi:10.1029/2002JB001757.

Plomerova, J., Margheriti, L., Park, J., Babuska, V., Pondrelli, S., Vecsey, L., & Salimbeni, S. (2006). Seismic anisotropy beneath the Northern Apennines (Italy): Mantle flow or lithosphere fabric?. *Earth and Planetary Science Letters, 247*(1-2), 157-170.

Qashqai, M. T., Afonso, J. C., & Yang, Y. Physical State and Structure of the Crust Beneath the Western-Central United States From Multiobservable Probabilistic Inversion. *Tectonics*.

Ranalli, G. (2000). Rheology of the crust and its role in tectonic reactivation. *Journal of geodynamics, 30*(1-2), 3-15.

Rudnick, R. L., & Gao, S. (2003). Composition of the continental crust. *Treatise on geochemistry, 3*, 659.

Rutter, E. H. (1986). On the nomenclature of mode of failure transitions in rocks. *Tectonophysics, 122*(3-4), 381-387.

Serretti, P., & Morelli, A. (2011). Seismic rays and traveltime tomography of strongly heterogeneous mantle structure: application to the Central Mediterranean. *Geophysical Journal International, 187*(3), 1708-1724.

Schutt, D. L., Lowry, A. R., & Buehler, J. S. (2018). Moho temperature and mobility of lower crust in the western United States. *Geology, 46*(3), 219-222.

Shen, A. H., Bassett, W. A., & Chou, I. M. (1993). The alpha-beta quartz transition at high temperatures and pressures in a diamond-anvil cell by laser interferometry. *American Mineralogist, 78*(7-8), 694-698.

Simpson, F. (1999). Stress and seismicity in the lower continental crust: A challenge to simple ductility and implications for electrical conductivity mechanisms. *Surveys in Geophysics, 20*(3-4), 201-227.

Spada, M., Bianchi, I., Kissling, E., Agostinetti, N. P., & Wiemer, S. (2013). Combining controlled-source seismology and receiver function information to derive 3-D Moho topography for Italy. textitGeophysical Journal International, 194(2), 1050-1068.

Stein, C. A. (1995). Heat flow of the Earth. *Global earth physics: a handbook of physical constants, 1*, 144-158.

Thomson, W. T. (1950). Transmission of elastic waves through a stratified solid medium. *Journal of applied Physics, 21*(2), 89-93.

Verbeke, J., Boschi, L., Stehly, L., Kissling, E., & Michelini, A. (2012). High-resolution Rayleigh-wave velocity maps of central Europe from a dense ambient-noise data set. *Geophysical Journal International, 188*(3), 1173-1187.

Vignaroli, G., Faccenna, C., Jolivet, L., Piromallo, C., & Rossetti, F. (2008). Subduction polarity reversal at the junction between the Western Alps and the Northern Apennines, Italy. *Tectonophysics, 450*(1-4), 34-50. https://doi.org/10.1016/j.tecto.2007.12.012

Vitovtova, V. M., Shmonov, V. M., & Zharikov, A. V. (2014). The porosity trend and pore sizes of the rocks in the continental crust of the earth: Evidence from experimental data on permeability. Izvestiya, *Physics of the Solid Earth, 50*(5), 593-602.

Waldhauser, F., Kissling, E., Ansorge, J., & Mueller, S. (1998). Three dimensional interface modelling with two-dimensional seismic data: the Alpine crust-mantle boundary. *Geophysical Journal International, 135*(1), 264-278.

Wang, X. Q., Schubnel, A., Fortin, J., David, E. C., GuÃ©guen, Y., & Ge, H. K. (2012). High Vp/Vs ratio: Saturated cracks or anisotropy effects? *Geophysical Research Letters, 39*(11).

Yu, Y., Song, J., Liu, K. H., & Gao, S. S. (2015). Determining crustal structure beneath seismic stations overlying a low-velocity sedimentary layer using receiver functions. *Journal of Geophysical Research: Solid Earth, 120*(5), 3208-3218. http://doi.org/10.1002/2014JB011610

Chapter 3

Thermal structure of a vanishing subduction system. An example of seismically-derived crustal temperature in the Italian peninsula.

Abstract

We determine the thermal structure of the crust beneath the Italian peninsula combining the shear velocity model of *Molinari et al.* (2015) with thermodynamic modeling, assuming a global average crustal composition with no lateral variations. Our model, presented in terms of Moho temperature and crustal thermal gradients, shows a very good agreement with the known thermal anomalies associated with the back-arc spreading during the Apennine subduction. In addition, we envisage anomalously high temperatures at the Moho in NW Italy (T>800°C at 30 km), at the transition between the Alps and Apennine orogens. The lowest temperatures (corresponding to geothermal gradients <19°C/km) are obtained in the still active but slow-convergent portion of the northern Apennine. The Moho increase its temperature moving southwards along the Apennine chain, consistently with the evidence of a ceased subduction and consequent rebalancing of the once depressed isotherms along the slab.

1 Introduction

The temperature of the crust and lithospheric mantle at a convergent margin is complex, being altered by the down-welling of cold lithosphere material into the mantle. As such, the thermal field is depressed in the subduction zone and upraise in the back-arc regions (*Currie and Hyndman*, 2006). Subduction velocity, shear stress along plate contact (*Peacock*, 1996), delamination of the lithospheric mantle from the crust (*Bird*, 1979) and by their 3-D settings (*Kincaid and Griffiths*, 2003) are all parameters that may influence the temperature field. Moreover, this can be function of the specific stage of convergence process, controlling the rheological behavior of the involved plates as well as the amount and spatio-temporal evolution of seismicity at depth.

In literature, the inference of lithospheric temperature relied on heat flow measurements only or together with complementary data, such as gravity and seismic velocities (*Zeyen et al.*, 1994; *Sobolev et al.*, 1997; *Fullea et al.*, 2009; *Simmons et al.*, 2009). While this approach might be adequate in old, stable continental areas (*Chapman*, 1986; *Jagoutz and Mareschal*, 2010), their utility in regions characterized by recent and on-going tectonic activity is limited. Moreover, several issues undermine the reliability and applicability of temperature estimates from heat flow. For example, the local topographic and geological setting can diminish the measured heat flow at the surface because of the percolation of meteoric water, while fluid up-welling can increase heat flow. Moreover, borehole data are sparse and extremely shallow in some cases (reaching few hundreds meters depth), therefore their vertical and lateral representativeness is rather poor.

Both laboratory experiments and thermodynamic modeling(*Birch*, 2012; *Christensen and Mooney*, 1986; *Rudnick and Fountain*, 1995) show that temperature exerts a major control on the elastic behavior of rocks. Anomalies in seismic velocities can be therefore used for inferring temperature at depth. However, chemical composition, as well as water content and mineral association, also contributes to the bulk seismic properties of rocks. Thermodynamic modeling allows a more quantitative approach, by considering the simultaneous contribution of those variables and leading to more robust estimates of temperature. Employing thermodynamic modeling in our previous work (*Diaferia and Cammarano*, 2017), we have shown that a different chemical composition within the same crustal layers is not expected to produce a substantial change in seismic velocities. As a consequence, the more pronounced, first-order effect driven by temperature might justify overlooking chemical change for the sake of temperature inference at crustal depth. Based on this premise, we convert shear-wave velocities (V_S) into crustal temperature, obtaining the Moho thermal structure and thermal gradients across the Italian Peninsula. The Italian Apennines chain is a key tectonic site to understand the way the temperature field is depressed over a complex active margin. In fact, the style and mechanism of

convergence change dramatically along strike over few hundreds of kilometers. Beneath the Alps, we have a collision which is still active only in the Venetian-Friuli region. Beneath the northern Apennines, the Adria plate is slowly subducting/delaminating beneath the Tyrrhenian side. In the Central Apennines, subduction probably vanished a couple of million years ago and slab most probably broke off (*Wortel and Spakman*, 2000). Finally, beneath Calabria we have active oceanic subduction. All this lateral change provide different sources for a variation of the thermal field along strike.

Our analysis provides a new picture of the temperature field and geothermal gradient over the Apennines and the Alps. A particularly interesting result we anticipate is the high value of the Moho temperature, showing a rather uniform distribution with a value exceeding 800°C. Exceptions are limited to a small region on the Tyrrhenian side. This high value and the rather uniform Moho temperatures are due to the fact that in the regions with lower temperature gradient the Moho is deeper and vice-versa. Moreover, we identify anomalous zones in correspondence of recent/active volcanic activity, in the Molasse basin and we also identify a zone with anomalously high crustal temperatures below the Piedmont area (NW Italy).

2 Method

On the basis of thermodynamical modeling, we convert V_S at depth into temperature using non-linear relationships between the seismic properties of a mineralogical aggregate and the pressure-temperature conditions encountered at crustal depth. We implement the seismic model of *Molinari et al.* (2015), obtained through the inversion of phase and group velocities of Rayleigh waves from 1-years long recording of ambient noise that allows an optimal sensitivity for the whole crust. Ambient noise data are inverted with a Neighborhood Algorithm (*Sambridge*, 1999; *Wathelet*, 2008), covering almost the entire peninsula with a 0.25° x 0.25° grid spacing. Further details can be found in *Molinari et al.* (2015) and references therein.

We use thermodynamic modeling to predict the absolute temperatures at depth from seismic velocities. Predictions are made via `Perple_X` (*Connoly*, 2009), a code based on Gibbs Free energy minimization for the computation of the stable mineral association and its correspondent seismic properties, for any P-T condition. At each location the crust, whose thickness is retrieved form the model of *Molinari et al.* (2015), is subdivided in three layers (upper, middle, lower crust) of equal thickness. The chemical composition of these layers (required for thermodynamic modeling) is assumed as the global average proposed by *Rudnick and Gao* (2003) with the addition of 1 wt% H_2O.

The higher sensitivity of V_S to temperature rather than to chemical composition implies that the assumption of a single chemical composition does not translate into significant uncertainty when

inferring temperature from thermodynamic modeling (*Diaferia and Cammarano*, 2017). We correct the observed V_S to account for porosity, using the empirical formulas proposed by *Vitovtova et al.* (2014) and *Castagna et al.* (1985).

In agreement with previous findings (e.g. *Guerri et al.* (2015)), temperature estimates in the upper and middle crust are significantly higher than plausible temperatures. The reasons for this result are several. The applied porosity correction probably underestimates the actual porosity effects at these depths (*Diaferia and Cammarano*, 2017). In addition, it is likely that the shallow portion of the crust is in a metastable state and/or with chemical contamination by sedimentary compositions, causing V_S that are lower than those modeled with thermodynamics at these depths. On the other side, the temperatures inferred in the lower crust appear realistic and allow us to map the lateral temperature variations of the region. We infer temperatures through a robust, linear and weighted fit of the estimates made in the P-T plane for the lower crust. Though the characteristics of the lower crust are poorly constrained, it is reasonable to expect higher chemical homogeneity and limited porosity (as opposed to the shallower portion), a condition that resembles the pore-free, chemically homogeneous representation assumed with thermodynamic modeling.

3 Results and Discussion

In Figure 1 (left), we present the Moho depth according to the shear wave velocity model of *Molinari et al.* (2015). At these depths we calculate the temperature using thermodynamic modeling (Figure 1 (right)). As expected, we observe the highest Moho temperatures (>850°C) in the Alps and Apennines chains, where the Moho reaches depths >40 km. Such a hot Moho underneath the Apennines is consistent with the high temperature invoked by *Mele et al.* (1996) to explain the strong attenuation of Pn phases. Analogously to our findings, in the Western United States *Schutt et al.* (2018) found temperatures above 850°C at locations with a thick crust. A clear correlation between Moho depth and its temperature is evident in the scatter plot (Figure 1, upper side). The majority of data-points lies along the 21°C/km geotherm that can be considered, therefore, as an average geothermal gradient across the Italian peninsula.

3.1 Good correlation with existing data?

A small, yet relevant portion of the inferred Moho temperature does not correlate with depth, suggesting an anomalous hot Moho and thus higher geothermal gradients. In Figure 2 we plot the temperature anomaly at the Moho, calculated with respect to the reference thermal gradient of 21°C/km. The anomalous zones perfectly correlate with the well known Italian magmatic provinces.

The anomaly with the largest extent corresponds to the Tuscan magmatic province where both intrusive and extrusive events occurred in the past 8.5 Ma because of the subduction process in the Apennines (*Peccerillo and Frezzotti*, 2015). The area is characterized by a large heat flow (>100mW/m^2, *Della Vedova et al.* (2001)) and the presence of major, high enthalpy geothermal fields (Larderello, Travale-Radicondoli and Monte Amiata), which are used for electricity production (*Cataldi et al.*, 1995). The vigorous up-welling of steam and hot water is also documented in hundreds of exploration boreholes (ViDEPI - http://unmig.sviluppoeconomico.gov.it/videpi/videpi.asp, shown in Figure 2), and suggests the ongoing stagnation of melts within the shallow crust. The thermal anomaly we find at the Moho (> 250°C higher than reference temperature) suggests a deeper source for the heat, of which the stagnating partial melts within the upper crust are only the shallow expression. A Moho with relatively high temperature results in rather high geothermal gradients (see Figure 3), as high as 40-45°C/km in the whole province.

According to our results, the strongest thermal anomaly corresponds to the Southern Tyrrhenian Sea. Here the shallow Moho (10-15 km depth) exceeds 800°C, resulting in a geothermal gradient above 50°C/km. The Tyrrhenian basin opened due to the counter-clockwise rotation of the Apenninic com-

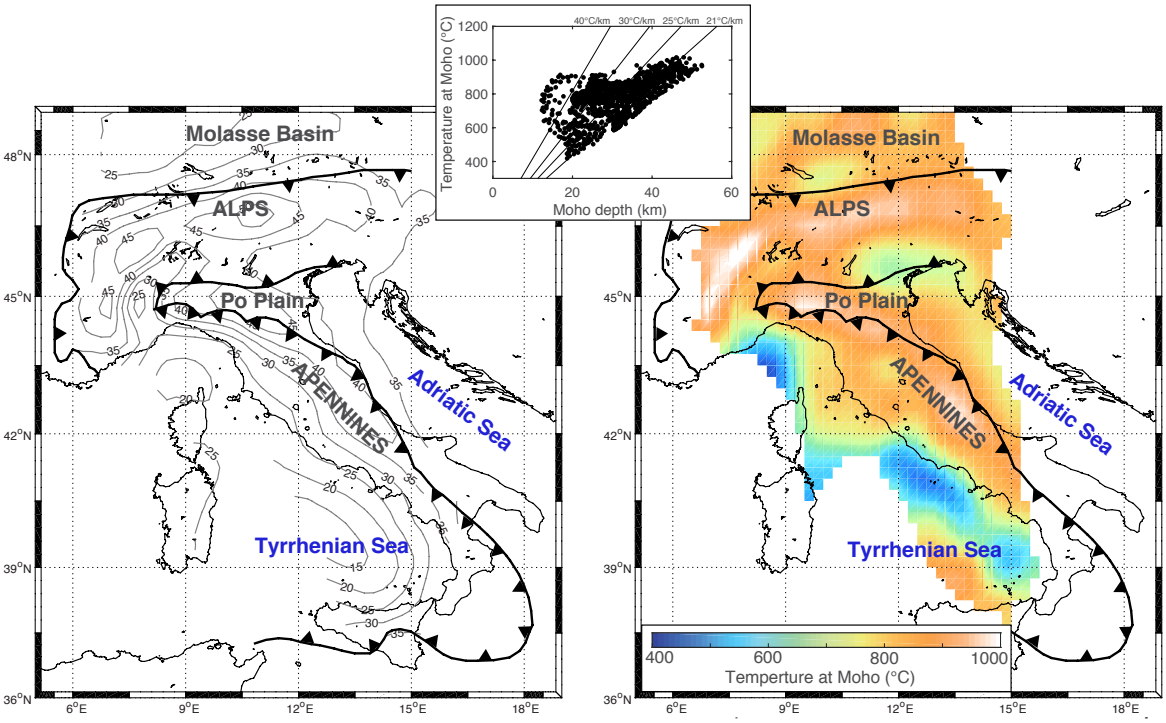

Figure 1: Left: Contour plot of Moho depths obtained from the shear-waves velocities model of *Molinari et al.* (2015). Right: Temperature at the Moho, obtained from the shear-wave velocities in the lower crust and thermodynamic modeling, assuming the chemical composition of *Rudnick and Gao* (2003). The highest temperatures (exceeding 900°C) correspond to thickenned portion of the crust along the Alpine and Apennine belts. In the upper side, the scatter plot of depth of the Moho vs. its temperature and its temperature shows that majority of the data are correlated and lies along the 21°C/km geotherm. Data-points with low correlation lay along hotter geotherms and depict an anomalously hot Moho.

pressive front in the past 15 Ma (e.g. *Carminati et al.* (1998, 2010) and *Faccenna et al.* (2001)). The moderate crustal thickness and high heat flow support the hypothesis of a relevant crustal thinning and extensive spreading (*Cataldi et al.*, 1995), followed by basaltic volcanism in the abyssal plain (e.g. Marsili and Vavilov seamounts) in addition to the calc-alkaline, subduction-related volcanism in the nearby Aeolian Arc. It is worth noting that the presence of a hot crust-mantle boundary has been suggested to explain the severe attenuation of Sn phases observed by *Mele et al.* (1997).

Another thermal anomaly is observed in the northern Alpine foreland, which corresponds to the Molasse basin. Here, the average geothermal gradient is estimated to be ∼32°C/km (*Agemar et al.*, 2012), which is compatible with the Moho temperature we obtain for this region (T∼800-900°C, for a Moho raging between 25-30 km depth). The area has the most promising geothermal potential in Germany (*Schellschmidt et al.*, 2010) because of the karstified, south-dipping Jurassic limestone aquifer underlying the whole basin (*Birn*, 2013). With a depth ranging between 1.5 and 5 km, the temperature of the aquifer ranges between 85-140°C and has permitted an extensive exploitation for heat and, recently, electricity generation (e.g. Unterhaching power plant, *Wolfgramm et al.* (2007)). Also in this case, the amount and the extent of the thermal anomaly indicate a deep source for such

geothermal area.

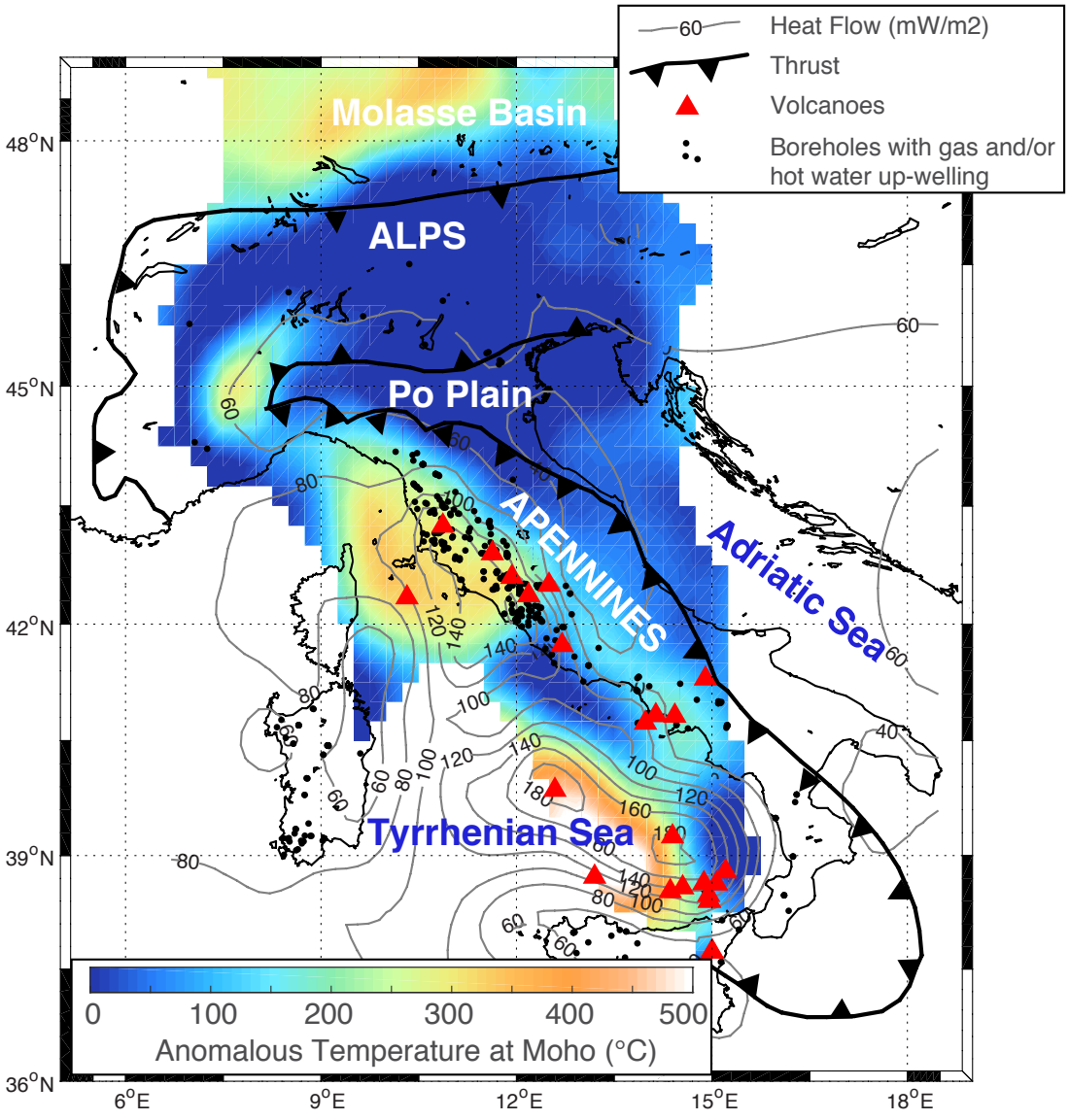

Figure 2: Absolute temperature anomaly of the Moho with respect to the a reference gradient of 21°C/km (see scatter plot in Figure 1). The areas showing an anomalously hot Moho represent well the magmatic Provinces of the Italian peninsula. Here, the highest values of heat flow are found, with diffuse past and current volcanism and evidences of hot water and gas in boreholes for geothermal exploration. Other areas with anomalous Moho temperature correspond to the Piedmont region, at the junction between the Apennines and southern Alps thrusts and to the Molasse basin.

3.2 A newly imaged thermal anomaly in NW Italy

The anomalies discussed so far well agree with the volcanism, heat flow anomalies, the tectonic and geodynamic setting of the Italian peninsula and neighboring regions. Interestingly, we also identify a new, unexpected minor anomaly in correspondence of north-western Italy (Piedmont region). Here, we obtain a Moho temperature exceeding 800°C at ~25 km depth. This region is sandwiched between

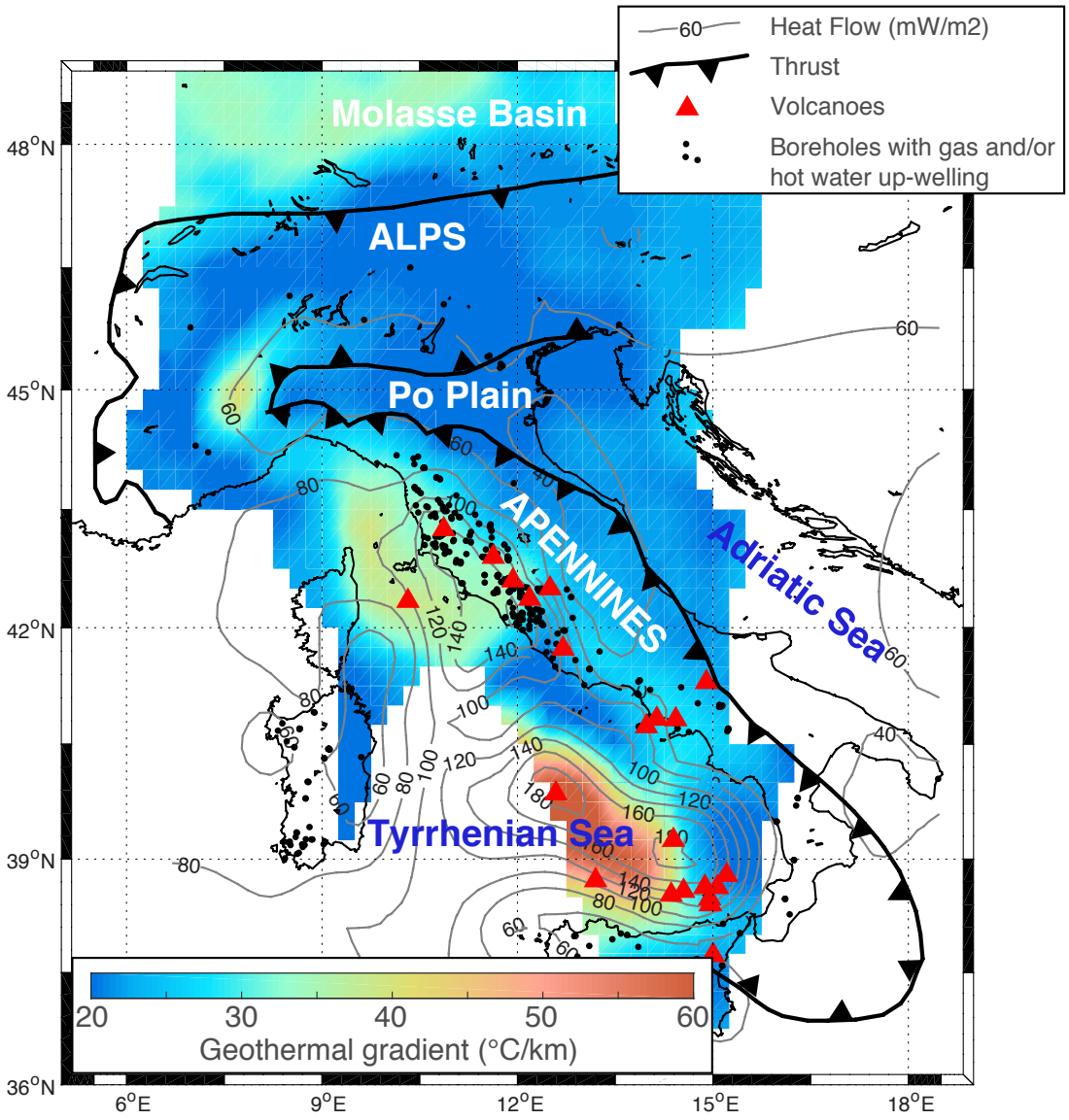

Figure 3: Map of geothermal gradient inferred from thermodynamic using shear wave velocities in the lower crust. High values (>40°C/km) are found in the Tuscan and Tyrrhenian magmatic provinces. Relatively hot gradients are also found in the Piedmont region, at the junction between the Apennines and southern Alps thrusts and to the Molasse basin.

the Alpine chain, to the west, and the Apennines in the eastern part, where the Moho rapidly deepens at >40 km depth at both sides. Surface heat flow is not anomalous and thus has not motivated any assessment of the geothermal potential of this area. Assuming a purely conductive heat transfer (*Chapman*, 1986), the average heat flow in the area (∼65 mW/m^2, see Figure 2) implies 680°C at the Moho, around 100°C lower than our estimates. We speculate that the reason for such discrepancy can be ascribed to the underestimated heat flow, obtained through an insufficient number of boreholes, that cannot capture the complexity of the area with its localized hot fluid ascents (*Dominco et al.*, 1980). It cannot be fully excluded that the low, crustal V_S that are recorded in the area might be caused by a possible seismic anisotropy rather than a high-temperature anomaly at depth. A better

seismic characterization would be beneficial for supporting one scenario over the other. The hydrogeological and geochemical characteristics of the localized thermal springs that are present in the area seem to support our observations. The hydrothermal system of Acqui Terme, with a water outlet of 9l/s at 70°C (*Dominco et al.*, 1980), is located on the southern border of the thermal anomaly we discovered. Geochemical evidence suggests that the fluid originates from a geothermal reservoir at 2-3 km depth and 130-140°, and, while ascending, mix and cool down with percolating meteoric water (*Marini et al.*, 2000). The reservoir is trapped underneath a sequence of tertiary marine sediments (comprising gypsum-bearing evaporites) that acts as an effective seal (*Marini et al.*, 2000). Sparse local springs (such as Acqui Terme) occur, therefore, only where permeability increases, i.e. along localized NW and W-trending, normal and strike-slip faults (*Piana et al.*, 1997) that cross the entire sedimentary overburden. Our observation agrees with the available data of the few boreholes drilled for oil and gas exploration (ViDEPI - http://unmig.sviluppoeconomico.gov.it/videpi/videpi.asp). Their bottom-hole temperatures indicate medium to high geothermal gradients that are compatible with our findings. For example, a temperature of 109°C at 3802 m is found through the "Sommariva del Bosco 001" borehole (gradient: 28°C/km). In "Valghera 001", at 732 m the registered temperature was 34°C. In conclusion, our findings appear to suggest the necessity of more in-depth studies of the area, for clarifying the origin of its thermal anomaly and its implication in the context of the transition from the Alpine to Apenninic orogen. *Vignaroli* (2008) propose that this area and the nearby Voltri Massif on its southern side have undergone a substantial extension during the counter-clockwise migration of the Apenninic front, favored by the toroidal flow of the asthenospheric mantle during the roll-back of the Adriatic slab.

A compositional rather than a thermal anomaly causing the low V_S in the Piedmont area cannot be fully excluded. *Speranza et al.* (2016) imaged a large magnetic anomaly (>50 nT) that is explained with the presence of a large serpentinized body at shallow depth. Since V_S and V_P decrease with the degree of serpentinization (*Christensen*, 2004), such methamorphism can explain the low velocities seen in this area by *Molinari et al.* (2015) and in *Zhao et al.* (2015). Coincidentally, the latter interpret such low velocities as indicative of a serpentinized Adriatic mantle ("Ivrea Body", *Closs and Labrouste* (1963)) reaching crustal depth, above the subducting continental slab of the European plate. In this scenario, the role of temperature can still be relevant, though of second order. In fact *Speranza et al.* (2016), after filtering out the magnetic effect induced by the shallow serpentized body, retrieved Curie temperature (∼550°C) at shallow depths that implies high geothermal gradients (>40°C/km), comparable to those we obtain from seismic velocities and thermodynamics. Such temperatures can be explained with the upraised geotherms due to the emplacement of the Adriatic mantle at crustal depth. Concluding, the existing geophysical evidence and our finding are not contradictory and suggests a

mixed contribution of lithological and temperature driven effect in generating low seismic velocities in the Piedmont region owing its peculiar position in the contest of the Alpine-Apennine transition.

3.3 Varying thermal structure along strike: the case of the Apennine orogen

With the envisioned thermal structure across the Apennine chain, several observations can be made in the context of the geodynamic evolution of the area. The transition from the Central to Northern Apennine (slightly above the 44° parallel) is accompanied by a decrease in Moho temperature (around 100°C), whilst its depth remains basically the same ($\sim$ 40 km) along the orogen front. Consequently, the geothermal gradient decreases northwards by 3-4°C/km, reaching values as low as 19°C/km within the Po Plain, where the front of the thrust is underneath a thick sedimentary cover (*Molinari et al.*, 2015). This is the only part of the Apennine system where the subduction of the Adriatic slab is ongoing, as suggested by geological evidence and the compressive seismicity (*Doglioni et al.*, 1999; *Minelli and Faccenna*, 2010; *Chiarabba et al.*, 2005; *Bennet et al.*, 2012), with an overall convergence rate in the order of mm/year (*Picotti and Pazzaglia*, 2008). *Faccenna et al.* (2001) have shown that the entire Apennine subduction system must have decreased its convergent velocity from a peak of few cm/year, when the oceanic crust was entirely consumed and more buoyant continental crust started to be subducted. Such low convergent rate must enhance the role of heat conduction through the lithosphere, rebalancing the isotherms (depressed due to the subduction of the cold slab (*Peacock*, 1996)) and gradually increases the geothermal gradient. This scenario is coherent with the geothermal gradients we observe, that are substantially higher than those inferred for the initial, fast-convergent stage of the Apennine subduction.

What is the fate of a vanishing subduction, when the positively buoyant continental crust can be no longer subducted? The answer can be found southward, in the Central Apennine, where we find higher crustal temperature and hotter geothermal gradients. The current seismicity suggests an extensional regime juxtaposed to the uplift of the entire area. Slab break-off might have occurred, or subduction might have culminated in the delamination of cold lithospheric material (*Wortel and Spakman*, 2000; *Gvirtzman and Nur*, 2001). The higher geothermal gradients that we observe along strike seem to favor the latter scenario. Indeed, the foundering of the cold, gravitationally unstable lower lithosphere might have led to the upwards and eastwards migration of hot asthenospheric material, increasing temperature underneath the orogen and explaining the thermal anomaly at the Moho (>100°C). Regarding temperature-driven gravitational instability, *Jagoutz and Behn* (2013) and *Jull and Kelemen*

(2001) showed that if the temperature at Moho is >900°C, a density contrast ≤300 kg/m^3 can lead to the foundering of 1-10 km of lower crust in a 1-10 Ma time window, due to the activation of vertical viscous flow. This implies that a hot orogen might be affected by the delamination of dense portion of the deep crust into a more buoyant upper mantle, contributing to the differentiation of the crust. This process might be particularly evident in the thickest portion of the Apennine orogen where the Moho exceed 45-50 km depth and density at lower crust reached the highest values (>3000 g/cm^3, according to our thermodynamic calculation) and thus the strongest density contrast with the underlying hot mantle.

A mantle wedge that is more towards the chain than expected has been recently pointed out by *Piana Agostinetti and Faccenna* (2018) through the analysis of active/passive seismic data. However, while the role of asthenosphere in contributing to the thermal structure and uplift of the Central Apennine might remain speculative, the extent and characteristics of the nearby Tuscan Magmatic province must invoke a deep source of heat. As a matter of fact, the strong attenuation (*Mele et al.*, 1996), low V_P (*Di Stefano et al.*, 2009), large heat flow(*Della Vedova et al.*, 2001) and the relevant thermal anomaly we observe suggest an up-welling of hot asthenosphere (reaching depth as shallow as ∼50 km), the same that might pervade eastward, intrude and replace the delaminated portion of the lower crust underneath the Central Apennine orogen.

4 Conclusions

We used shear-wave velocities and thermodynamics to retrieve the thermal structure of the crust, that we have presented in terms of temperature at the Moho. Our methodology remedies to the data scarcity and overall limitations of temperature extrapolation from heat flow measurements.

The highest Moho temperatures are found at the base of the thick crust along the Alps and Apennines, a scenario that reconciles with the attenuation of refracted Pn phases observed in other studies.

Using the average ∼21°C/km geotherm as a reference, we have imaged the zones of anomalously high-temperature at the Moho. These regions correspond to the well known magmatic Italian provinces, namely the Tuscan area and the Tyrrhenian basin. We also highlight a thermal anomaly at the base of the crust in the Molasse basin (Southern Germany), known for its relevant geothermal potential.

We find the smallest, yet relevant, anomaly in the Piedmont region (NW Italy), at the transition between the Alpine and Apennine belts. This zone is not regarded as a potentially interesting location for geothermal exploitation. However, well documented hot fluid up-welling and hydrogeological evidence indicate a geothermal gradient that is higher than the average for the Italian peninsula. The hypothesis of a thermal anomaly does not contradict the possible presence of a shallow serpentinized

upper mantle that, beside the high crustal temperature, might contribute in explaining the low seismic velocities.

Crustal temperature increase moving southward along the Apennine chain. This can be an evidence of the ceased convergence along the Central Apennine, as opposed to the northern Apennine where the cold slab is still slowly subducting. In spite of the apparently strong assumption of a chemically homogeneous lower crust for the thermodynamic calculation, our approach has shown the capability of imaging the deep crustal thermal structure of the Italian peninsula. In view of the geologic and tectonic complexity of the studied area, we foresee that our methodology can be applied also to other regions. This approach can bypass the limitations and scarcity of heat flow measurement, and contribute to a better understanding of crustal behavior, evolution and relation with the mantle underneath and neighboring plates.

APPENDIX A: Thermodynamic modeling and conversion of seismic velocities to temperature

Given a certain chemical composition, the stable mineral association can be obtained by imposing the minimization of the Gibbs Free Energy of the system. Following this criterion, the code `Perple_X` (*Connoly*, 2009) solves iteratively the thermodynamics equation of state in any given range of pressure and temperature, assessing which minerals are stable in such condition and their amount. For each of the minerals constituting the modeled bulk rock, the V_P and V_S are function of the adiabatic bulk modulus (K) and density (ρ), both related to the derivatives of the Gibbs Free Energy with respect to pressure and temperature. More specifically:

$$K = -\frac{\partial G}{\partial P}\left\{\frac{\partial^2 T}{\partial G^2}\left[\frac{\partial^2 G}{\partial P^2} + \left(\frac{\partial}{\partial P}\frac{\partial G}{\partial T}\right)^2\right]\right\}^{-1} \tag{1}$$

$$\rho = N\frac{\partial P}{\partial G} \tag{2}$$

where G is the Gibbs Free energy and N is the molar weight. Regarding the shear modulus μ:

$$\mu = \mu_0 + T\frac{\partial \mu}{\partial T} + P\frac{\partial \mu}{\partial P} \tag{3}$$

where μ_0, $\frac{\partial \mu}{\partial T}$ and $\frac{\partial \mu}{\partial P}$ are constants evaluated through laboratory experiments. Known the compressional and shear wave velocities of each mineral composing the modeled rock, its bulk seismic properties are calculated through Voigt-Ross-Hill (*Hill*, 1952) averaging scheme. For our specific ap-

plication to crustal domain, we implement the thermodynamic database from *Holland and Powell* (1998), augmented with the experimentally constrained shear moduli provided by *Hacker and Abers* (2004), including the experiments from *Ohno et al.* (2006) regarding the pecualiar behavior of quartz at its transition from the α to β form around 580°C. By matching the observed V_S profiles with the modeled velocities in the P-T space, seismic velocities are finally converted into temperature that are compatible with such observation. The thermal gradients are obtained by fitting the inferred temperatures with a robust linear equation and a data weighting (inverse of the uncertainty of each temperature estimation on the P-T space).

Bibliography

Agemar, T., Schellschmidt, R., & Schulz, R. (2012). Subsurface temperature distribution in Germany. *Geothermics, 44*, 65-77.

Bennett, R. A., Serpelloni, E., Hreinsdòttir, S., Brandon, M. T., Buble, G., Basic, T., & Minelli, G. (2012). Syn-convergent extension observed using the RETREAT GPS network, northern Apennines, Italy. *Journal of Geophysical Research: Solid Earth, 117*(B4).

Birch, F. (1961). The velocity of compressional waves in rocks to 10 kilobars: 2. *Journal of Geophysical Research, 66*(7), 2199-2224. `https://doi.org/10.1029/JZ066i007p02199`

Bird, P. (1979). Continental delamination and the Colorado Plateau. *Journal of Geophysical Research: Solid Earth, 84*(B13), 7561-7571.

Birner, J. (2013). Hydrogeologisches Modell des Malmaquifers im Sddeutschen Molassebecken (Doctoral dissertation, Freie Universitat Berlin).

Carminati, E., Wortel, M.J.R., Spakman, W. & Sabadini, R. 1998. The role of slab detachment in the opening of the western-central Mediterranean basins: Some geological and geophysical evidence. *Earth and Planetary Science Letters, 160*, 651-665.

Carminati, E., Lustrino, M., Cuffaro, M., & Doglioni, C. (2010). Tectonics, magmatism and geodynamics of Italy: what we know and what we imagine. textitJournal of the Virtual Explorer, 36(8).

Castagna, J. P., Batzle, M. L., & Eastwood, R. L. (1985). Relationships between compressional-wave and shear-wave velocities in clastic silicate rocks*Geophysics, 50*(4), 571-581.

Cataldi, R., Mongelli, F., Squarci, P., Taffi, L., Zito, G., & Calore, C. (1995). Geothermal ranking of Italian territory. *Geothermics, 1*(24), 115-129.

Chapman, D. S. (1986). Thermal gradients in the continental crust. *Geological Society, London, Special Publications, 24*(1), 63-70.

Chiarabba, C., Jovane, L., Di Stefano, R., 2005. A new view of the Italian seismicity using 20 years of instrumental recordings. *Tectonophysics 395*, 251-268.

Christensen, N. I., & Mooney, W. D. (1995). Seismic velocity structure and composition of the continental crust: A global view. *Journal of Geophysical Research, 100*(B6), 9761-9788. `https://doi.org/10.1029/95JB00259`

Christensen, N. I. (2004). Serpentinites, peridotites, and seismology. *International Geology Review, 46*(9), 795-816.

Closs, H., and Labrouste, Y., 1963, Recherches sÃ©ismologiques dans les Alpes Occidentales au moyen des grandes explosions en 1956, 1958 et 1960: *AnnÃ©e GÃ©ophysique Internationale, XII, 2*: Paris, Centre National de la Recherche Scientifique, 241

Connolly, J. A. D. (2009). The geodynamic equation of state: what and how. *Geochemistry, Geophysics, Geosystems, 10*(10).

Currie, C. A., & Hyndman, R. D. (2006). The thermal structure of subduction zone back arcs. *Journal of Geophysical Research: Solid Earth, 111*(B8).

Della Vedova, B., Bellani, S., Pellis, G., & Squarci, P. (2001). Deep temperatures and surface heat flow distribution. In *Anatomy of an orogen: the Apennines and adjacent Mediterranean basins* (pp. 65-76). Springer, Dordrecht.

Diaferia, G., & Cammarano, F. (2017). Seismic signature of the continental crust: What thermodynamics says. An example from the Italian peninsula. *Tectonics*, 36, 3192-3208. https://doi.org/10.1002/2016TC004405

Di Stefano, R., Kissling, E., Chiarabba, C., Amato, A., & Giardini, D. (2009). Shallow subduction beneath Italy: Three-dimensional images of the Adriatic-European-Tyrrhenian lithosphere system based on high-quality P wave arrival times. *Journal of Geophysical Research: Solid Earth, 114*(B5).

Doglioni, C., Merlini, S., & Cantarella, G. (1999). Foredeep geometries at the front of the Apennines in the Ionian Sea (central Mediterranean). *Earth and Planetary Science Letters, 168*(3-4), 243-254.

Dominco, E., Giraudi, C., Zanella, E., Fancelli, R., Noto, P., Nuti, S., 1980. Le Sorgenti Termali del Piemonte. Regione Piemonte, Assessorato alle Acque Minerali e Termali, Torino.

Faccenna, C., Becker, T.W., Lucente, F.P., Jolivet, L. & Rossetti, F. 2001. History of subduction and back-arc extension in the Central Mediterranean. *Geophysical Journal International, 145*, 809-820.

Fullea, J., Afonso, J. C., Connolly, J. A. D., Fernandez, M., GarcÃa-Castellanos, D., & Zeyen, H. (2009). LitMod3D: An interactive 3-D software to model the thermal, compositional, density, seismological, and rheological structure of the lithosphere and sublithospheric upper mantle. *Geochemistry, Geophysics, Geosystems, 10*(8).

Guerri, M., Cammarano, F., & Connolly, J. A. (2015). Effects of chemical composition, water and temperature on physical properties of continental crust. *Geochemistry, Geophysics, Geosystems, 16*(7), 2431-2449. https://doi.org/10.1002/2015GC005819

Gvirtzman, Z., & Nur, A. (2001). Residual topography, lithospheric structure and sunken slabs in the central Mediterranean. *Earth and Planetary Science Letters, 187*(1-2), 117-130.

Hacker, B. R., & Abers, G. A. (2004). Subduction factory 3: An Excel worksheet and macro for calculating the densities, seismic wave speeds, and H2O contents of minerals and rocks at pressure and temperature. *Geochemistry, Geophysics, Geosystems, 5*, Q01005. https://doi.org/10.1029/2003GC000614

Hacker, B. R., Kelemen, P. B., & Behn, M. D. (2015). Continental lower crust. *Annual Review of Earth and Planetary Sciences, 43*, 167-205.

Holland, T. J. B., & Powell, R. (1998). An internally consistent thermodynamic data set for phases of petrological interest. *Journal of Metamorphic Geology, 16*(3), 309-343.https://doi.org/10.1111/j.1525-1314.1998.00140.x

Hill, R. (1952). The elastic behaviour of a crystalline aggregate. *Proceedings of the Physical Society. Section A, 65*(5), 349-354. https://doi.org/10.1088/0370-1298/65/5/307

Jagoutz, O., & Behn, M. D. (2013). Foundering of lower island-arc crust as an explanation for the origin of the continental Moho. *Nature, 504*(7478), 131.

Jaupart, C., & Mareschal, J. C. (2010). Heat generation and transport in the Earth. Cambridge university press.

Jull, M., & Kelemen, P. (2001). On the conditions for lower crustal convective instability. *Journal of Geophysical Research: Solid Earth, 106*(B4), 6423-6446.

Kincaid, C., & Griffiths, R. W. (2003). Laboratory models of the thermal evolution of the mantle during rollback subduction. *Nature, 425*(6953), 58.

Lachenbruch, A. H., & Morgan, P. (1990). Continental extension, magmatism and elevation; formal relations and rules of thumb. *Tectonophysics, 174*(1-2), 39-62.

Marini, L., Bonaria, V., Guidi, M., Hunziker, J. C., Ottonello, G., & Zuccolini, M. V. (2000). Fluid geochemistry of the Acqui Terme-Visone geothermal area (Piemonte, Italy). *Applied Geochemistry, 15*(7), 917-935.

Mele, G., Rovelli, A., Seber, D., & Barazangi, M. (1996). Lateral variations of Pn propagation in Italy: Evidence for a high attenuation zone beneath the Apennines. *Geophysical research letters, 23*(7), 709-712.

Mele, G., Rovelli, A., Seber, D., & Barazangi, M. (1997). Shear wave attenuation in the lithosphere beneath Italy and surrounding regions: tectonic implications. *Journal of Geophysical Research: Solid Earth, 102*(B6), 11863-11875.

Minelli, L., & Faccenna, C. (2010). *Evolution of the Calabrian accretionary wedge (central Mediterranean). Tectonics, 29*(4).

Molinari, I., Verbeke, J., Boschi, L., Kissling, E., & Morelli, A. (2015). Italian and Alpine three-dimensional crustal structure imaged by ambient-noise surface-wave dispersion. *Geochemistry, Geophysics, Geosystems, 16*(12), 4405-4421.

Molinari, I., Argnani, A., Morelli, A., & Basini, P. (2015). Development and testing of a 3D seismic velocity model of the Po Plain sedimentary basin, Italy. *Bulletin of the Seismological Society of America, 105*(2A), 753-764.

Ohno, I., Harada, K., & Yoshitomi, C. (2006). Temperature variation of elastic constants of quartz across the alpha-beta transition. *Physics and Chemistry of Minerals, 33*(1), 1-9. `https://doi.org/10.1007/s00269-005-0008-3`

Peacock, S. M. (1996). Thermal and petrologic structure of subduction zones. *Subduction: top to bottom, 96*, 119-133.

Peccerillo, A., & Frezzotti, M. L. (2015). Magmatism, mantle evolution and geodynamics at the converging plate margins of Italy. *Journal of the Geological Society, 172*(4), 407-427.

Piana, F., D'Atri, A. R., & Orione, P. (1997). The Visone Formation, a marker of the Early Miocene tectonics in the Alto Monferrato domain (Tertiary Piemonte Basin, NW Italy). *Memorie di Scienze Geologiche, 49*, 145-162.

Piana Agostinetti, N., & Faccenna, C. (2018). Deep structure of Northern Apennines subduction orogen (Italy) as revealed by a joint interpretation of passive and active seismic data. *Geophysical Research Letters, 45*(9), 4017-4024.

Picotti, V., & Pazzaglia, F. J. (2008). A new active tectonic model for the construction of the Northern Apennines mountain front near Bologna (Italy). *Journal of Geophysical Research, 113*, B08412. https://doi.org/10.1029/2007JB005307

Rudnick, R. L., & Fountain, D. M. (1995). Nature and composition of the continental crust: A lower crustal perspective. *Reviews of Geophysics, 33*(3), 267-309. https://doi.org/10.1029/95RG01302

Rudnick, R. L., & Gao, S. (2003). Composition of the continental crust. *Treatise on geochemistry, 3*, 659.

Sambridge, M. (1999b), Geophysical inversion with a Neighbourhood Algorithm-II. Appraising the ensemble, *Geophysical Journal International, 138*(2), 727-746.

Schellschmidt, R., Sanner, B., Pester, S., & Schulz, R. (2010). Geothermal energy use in Germany. In *Proceedings World geothermal congress,152*, 19).

Schutt, D. L., Lowry, A. R., & Buehler, J. S. (2018). Moho temperature and mobility of lower crust in the western United States. *Geology, 46*(3), 219-222.

Simmons, N. A., Forte, A. M., & Grand, S. P. (2009). Joint seismic, geodynamic and mineral physical constraints on three-dimensional mantle heterogeneity: Implications for the relative importance of thermal versus compositional heterogeneity. *Geophysical Journal International, 177*(3), 1284-1304.

Speranza, F., Minelli, L., Pignatelli, A., & Gilardi, M. (2016). Curie temperature depths in the Alps and the Po Plain (northern Italy): Comparison with heat flow and seismic tomography data. *Journal of Geodynamics, 98*, 19-30.

Sobolev, S. V., Zeyen, H., Granet, M., Achauer, U., Bauer, C., Werling, F., & Fuchs, K. (1997). Upper mantle temperatures and lithosphere-asthenosphere system beneath the French Massif Central constrained by seismic, gravity, petrologic and thermal observations. *Tectonophysics, 275(*1-3), 143-164.

Vignaroli, G., Faccenna, C., Jolivet, L., Piromallo, C., & Rossetti, F. (2008). Subduction polarity reversal at the junction between the Western Alps and the Northern Apennines, Italy. *Tectonophysics, 450*(1-4), 34-50.

Vitovtova, V. M., Shmonov, V. M., & Zharikov, A. V. (2014). The porosity trend and pore sizes of the rocks in the continental crust of the earth: Evidence from experimental data on permeability. Izvestiya, *Physics of the Solid Earth, 50*(5), 593-602.

Wathelet, M. (2008), An improved neighborhood algorithm: Parameter conditions and dynamic scaling, *Geophysical Research Letters, 35* .

Wolfgramm, M., Bartels, J., Hoffmann, F., Kittl, G., Lenz, G., Seibt, P., & Unger, H. J. (2007). Unterhaching geothermal well doublet: structural and hydrodynamic reservoir characteristic; Bavaria (Germany). In *European Geothermal Congress*

Wortel, M. J. R., & Spakman, W. (2000). Subduction and slab detachment in the Mediterranean-Carpathian region. *Science, 290*(5498), 1910-1917.

Zeyen, H., & Fernàndez, M. (1994). Integrated lithospheric modeling combining thermal, gravity, and local isostasy analysis: Application to the NE Spanish Geotransect. *Journal of Geophysical Research: Solid Earth, 99*(B9), 18089-18102.

Zhao, L., Paul, A., Guillot, S., Solarino, S., Malusà, M. G., Zheng, T., & Zhu, R. (2015). First seismic evidence for continental subduction beneath the Western Alps. *Geology, 43*(9), 815-818.